Enhancing the oncolytic efficacy of vaccinia virus by mutagenic augmentation of EEV production

By:

Aimée Nicole Laporte

Supervisor: Dr. John Bell

A thesis submitted to the Faculty of Graduate and Postdoctoral Studies
in partial fulfilment of the requirements for the degree of
Master of Science

Department of Biochemistry, Microbiology and Immunology
Specialization Human and Molecular Genetics

University of Ottawa
Faculty of Medicine
Ottawa, Ontario, Canada
(July 2012)

ABSTRACT

Oncolytic viruses are currently under investigation as anti-cancer therapies due to their innate ability to selectively infect and destroy cancer cells. Major barriers to this anti-tumour effect include inefficient viral spread and immune-mediated neutralization. This study aims to overcome these limitations by taking advantage of the life cycle of the oncolytic clinical candidate known as vaccinia virus (VACV). Naturally, a small proportion (<1%) of VACV progeny are released from infected cells with a cell-derived membrane and become known as extra-cellular enveloped virus (EEV). Due to this additional membrane, EEV can be shielded from many anti-viral immune factors, allowing it to travel further and largely avoid host-mediated neutralization. This form of VACV is important for long range virus dissemination as well as sustained infection. Though the exact mechanism remains to be elucidated, it has been demonstrated that EEV release can be influenced by Abl tyrosine kinase (Abl TK) function. Specific point mutations in viral envelope proteins are known to bring about enhanced viral release, resulting in an elevated proportion of produced EEV. In this study, we investigate the effect of EEV enhancing modifications within various oncolytic VACV strains. Our data reveals that this augmentation of EEV production through the A34R L151E mutation within the Copenhagen (Cop) backbone can enhance the oncolytic potential of VACV *in vivo* through enhanced spread and immunoevasion.

ACKNOWLEDGMENTS

I would foremost like to thank Dr. John Bell for allowing me the opportunity to work on this project within his lab, for his enthusiasm and for his unique and exceptional ideas. I would also very much like to thank every member of the Bell/Atkins/Auer lab, it was an extremely enriching and supportive environment and an enjoyable group to be a part of. To the Jennerex team, Dr. Jiahu Wang and Dr. Chris Storbeck, thank you for all your work in creating the recombinants, for your helpful input in the virus production process and for aiding in troubleshooting every wall I ran into. To Dr. Carolina Ilkow and Dr. Caroline Breitbech, my conference call teammates, thank you so much for your ideas and inputs as well as for always being so positive and encouraging, you were amazing. To my TAC committee, Dr. Christina Addison and Dr. Ken Dimock, thank you for taking the time to meet with me and for all your helpful ideas and insights.

To Laura Evgin, you were an immense help with this project. Thank you so much for answering my many questions and for being a western blot master, I really appreciate all the time you gave me. To the immunology gods, Dr. Julia Rintoul, Dr. Chantal Lemay and Dr. Lee-Hwa Tai, thank you for all you did in helping me figure out the flow machine and in deciphering the results. To Dr. Fabrice Le Boeuf, thank you so much for all your help in experimental design and for your sustained excitement for the project. To Theresa Falls and Christiano Tanese de Souza, the animal wranglers, thank you for helping me with all the *in vivo* work and for creating an engaging work environment. You were irreplaceable. To Monica Komar, you taught me everything I know, you always have an answer to any question and I greatly appreciate all your help. To Dr. Rozanne Arulanandam and Dr. Kelly Parato, thank you so much for your helpful ideas and interest in this project. To Naomi De

Silva, Dom Roy, Michelle Becker, Corey Batenchuk, Anu Ananth and all of the other students that came and went, thank you for always being around to help, and even more so to have a laugh, you made the lab a great place to be.

To my friends and family, thanks for listening to my elated banter or grimacing complaints about my latest experimental results. You in all likelihood had no idea what I was talking about, but the sympathetic nods and support were always appreciated.

This project was funded by CIHR and the government of Ontario with the Ontario Graduate Scholarship.

Table of Contents

List of Abbreviations

5-FC	5-fluorocytosine
5-FU	5-fluorouracile
Abl TK	Abl tyrosine kinase
APC	Antigen presenting cell
Cop	Copenhagen vaccinia virus
CEV	Cell-associated enveloped virus
CF	Cell fraction
DAMP	Danger/Damage Associated Molecular Pattern
DNA	Deoxyribonucleic acid
dpi	Days post injection
dsDNA	Double-stranded deoxyribonucleic acid
EGF	Epidermal growth factor
EGFR	Epidermal growth factor receptor
EEV	Extra-cellular enveloped virus
GM-CSF	Granulocyte Monocyte/Macrophage-Colony Stimulating Factor
Gleevec	Imatinib mesylate
HSV	Herpes Simplex Virus
hGM-CSF	Human Granulocyte Monocyte/Macrophage-Colony Stimulating Factor
hpi	Hours post infection
met	Metastases
MOI	Multiplicity of infection
NK	Natural killer cell
IEV	Intra-cellular enveloped virus
IFN	Interferon

IHD-J	International Health Department-J vaccinia virus
IMV	Intracellular mature virus
IN	Intranasal
IP	Intraperitoneal
IT	Intratumoural
IV	Intravenous
JX	Jennerex Biotherapeutics Inc.
MVA	Modified Vaccinia Ankara vaccinia virus
NYVAC	New York Vaccinia virus
OV	Oncolytic virus
PBS	Phosphate buffered saline
PAMP	Pathogen Associated Molecular Pattern
PVE	Post-vaccination encephalitis
pfu	Plaque forming unit
SN	Supernatant
Src TK	Src tyrosine kinase
SQ	Subcutaneous
TAA	Tumour associated antigen
T_C cell	Cytotoxic T cell (CD8+)
TGN	*trans*-Golgi network
T_H cell	Helper T cell (CD4+)
TK	Thymidine kinase
U	International units
VACV	Vaccinia virus
VGF	Vaccinia growth factor

VIG	Vaccinia Immunoglobulin
vvDD	Vaccinia virus double-deleted
WI	Western Reserve expressing IHD-J A34R recombinant vaccinia virus
WR	Western Reserve vaccinia virus
wt	wildtype
Wy	Wyeth vaccinia virus
yCD	Yeast cytosine deaminase

List of Figures

1. INTRODUCTION

1.1 ONCOLYTIC VIRUSES

1.1.1 CANCER AND THE NECESSITY FOR NOVEL THERAPIES

Every day, an average of 200 Canadians die from cancer and another 500 are newly diagnosed (1). This disease type has established itself as one of the leading causes of death worldwide, demanding the attention of modern society. Cancer is characterized by uncontrolled cellular growth with the capacity to spread, invade tissues and impede vital bodily functions, causing death. Normal cell growth is controlled on a number of levels, and ultimately is thrown off course by changes, known as mutations, to the DNA sequence. As such, the numerous and convoluted mutagenic sources that bring about these changes have made this disease type incredibly difficult to decipher. Furthermore, the more than two hundred neoplastic subtypes each have unique and complicated characteristics, wherein the attributes typical of disease progression make treatment a delicate and often risky process (16).

Current treatment protocols largely enlist severe, cytotoxic methods of attack, aimed at destroying cells dividing at a higher rate. Chemotherapeutics and radiation therapy destroy cancer cells and aid in preventing disease progression, but in their wake these methods also annihilate cells that naturally divide quickly. Components of the bone marrow and the gastrointestinal tract are destroyed during treatment, eliciting severely compromising side effects (48). The body is damaged and the immune system is impaired, leaving the patient susceptible to infection and vastly impeding the healing process (32). Life-threatening complications therefore often arise from the toxic effects of these aggressive treatment protocols (32, 48). Furthermore, the nature of the rapidly dividing cancer cell is to

retaliate and mutate further, often bringing about resistance to utilized treatment protocols and requiring the use of a subsequent panel of toxic compounds (67). Consequently, the need for innovative, more highly discriminating and sophisticated treatment strategies is obvious.

1.1.2 Potential for Targeted Viral Therapy Platforms

Novel anti-cancer therapies are currently under investigation for enhanced selectivity and efficacy in reducing tumour burden without provoking the same toxic implications brought about by the current standard. At the forefront of this investigative endeavour is the field of oncolytic virotherapy. This approach encompasses an intricate and multifaceted biotherapeutic tactic wherein malignant cell subtypes are selectively infected and destroyed while normal tissue is left unharmed (47). Oncolytic viruses (OV) are immunomodulatory, self-propagating, easily genetically manipulated, efficient gene therapy vectors and importantly, they are highly selective for lytic replication in cancer cells (34, 47). Thus, oncolytic viruses have emerged as an exceedingly attractive anti-cancer therapy platform.

The ability of OVs to specifically target and destroy a wide range of cancer cells vastly sets this therapy apart from current strategies. This selectivity is attained on a molecular level, where the virus has the capacity to specifically exploit the genetic defects found in malignant neoplastic cells. The cancer cell's high rate of division causes it to accumulate mutations that bring about chromosomal instability, providing growth advantages at the cost of normal cellular defense mechanisms (14, 86). A number of viral species have shown a high natural tropism for tumour cells due to enhanced cellular growth factors promoting viral replication, inhibited interferon (IFN) pathways preventing the cell from mounting an anti-viral campaign as well as due to aspects of the tumour microenvironment promoting preferential infection (40, 86). On top of this, many genetic

modifications to the viral genomes have been observed to confer higher infection specificity and conditional replication in cancer cells by further exploitation of neoplastic growth, promoting a higher degree of safety and tumour selectivity (30, 86).

1.2 Vaccinia Virus (VACV)

1.2.1 Oncolytic VACV Overview

VACV, a member of the poxvirus family, has made significant progress as an oncolytic candidate in recent years. Historically, VACV was used worldwide as the highly immunogenic vaccine against smallpox, leading to the complete eradication of the disease by 1971 (6). VACV is characterized by a large double-stranded (ds) DNA genome encoding more than 200 genes, a vast mammalian cell host-range, the ability to effectively spread systemically and a rapid lytic replication cycle occurring entirely within the host cell cytoplasm with little pathogenicity in humans (6, 31, 93). These features have proven to be highly favourable within an oncolytic candidate platform.

Its history of use in humans has allowed for long-term clinical observation of safety, toxicity and immunogenicity, as well as extensive investigation of VACV biology (75). This experience has demonstrated a superior safety profile as well as firmly established manipulation and study protocols. Additionally, the inherent immunogenicity of the virus elicits an adaptive response with the potential to be harnessed and used to prime the immune system against the tumour microenvironment (31, 57, 66). The large dsDNA genome can accommodate up to 25 kb of foreign DNA, making VACV a proficient gene therapy vector capable of expressing large transgenes for enhancing therapeutic potential (78). Furthermore, the vast range of infectable mammalian cell subtypes makes VACV suitable for effective study in animal models as well as for use in human cancer cell populations (54).

The cytoplasmic replication cycle ensures the virus genome does not enter the

nucleus, eliminating the possibility of mutagenic chromosomal integration, further solidifying an enhanced safety profile, in comparison with products that replicate within the nucleus (31, 75). The cytoplasmic replication is also rapid, allowing for quick action, efficient lysis and cell-to-cell spread as well as more highly streamlined manufacturing protocols (54, 75). Poxviruses have also evolved mechanisms for immune evasion and efficient systemic spread through the blood, facilitating overall treatment efficacy and providing an advantage over other viral species of oncolytic products (73). Finally, VACV has little toxicity in humans and largely induces only minor side effects. However, if uncontrolled replication were to occur, a number of anti-viral compounds have been approved to counteract the VACV infection. These include immunotherapy tactics such as vaccinia immunoglobulin (VIG) and the viral DNA polymerase inhibitor cidofovir, further elevating the therapeutic safety profile (18, 31, 94). Overall, VACV possesses several qualities that make it an ideal species for oncolytic virotherapy development.

1.2.2 Oncolytic Mechanism of Action

The inherent oncolytic potential of VACV has been demonstrated to be the result of three diverse mechanisms of action (41). Primarily, direct infection, replication and lysis of the cancer cell occurs, leading to its destruction by necrosis and/or apoptosis. From here, the virus is propagated and spreads to neighbouring cells, undertaking an initial tumour-debulking process (31, 41). Secondarily, the initial infection and cell destruction releases immune mediators, including damage/danger associated molecular patterns (DAMP), viral pathogen associated molecular patterns (PAMP) as well as tumour associated antigens (TAA), that together trigger a response to the site (71, 96). This action recruits an innate immune-mediated attack against the tumour site and the release of TAAs seems to have the potential to elicit an adaptive response against the tumour itself (41). Harnessing the power

of the immune system against the tumour greatly augments the efficiency of this therapeutic platform.

Finally, VACV functions in facilitating tumour vascular collapse (46). The infection elicits the release of a variety of chemokines and cytokines that establish the recruitment of innate immune cells to the tumour site. Here, neutrophils take on a rigid phenotype and can functionally block the tumour microvasculature, creating a thrombosis and starving the cancer cells, promoting necrosis (11). It has also been demonstrated that VACV has the capacity to directly infect the rapidly dividing tumour-associated endothelial cells, furthering the vascular shut down mechanism and promoting overall tumour destruction (42). Ultimately, these diverse points of attack greatly strengthen this therapeutic approach against the highly heterogeneous nature of the tumour microenvironment.

1.3 VACV Strains and Oncolytic Potential

VACV exists in several different strain subtypes, each with variable virulence and oncolytic capabilities. Strains Modified Vaccinia Ankara (MVA) and New York Vaccinia (NYVAC) are not able to replicate in mammalian cells but are highly immunogenic, making them suitable as potential vaccine vectors but not in an oncolytic capacity (31, 41). The Tian Tan strain was used extensively in China as a vaccine during the smallpox eradication, but has not been investigated as an oncolytic agent (41). The Lister strain was used as a vaccine in the United Kingdom and has been investigated as an oncolytic candidate as it possesses some inherent tumour selectivity (83). Finally, strains Wyeth (Wy), Western Reserve (WR) and Copenhagen (Cop) have displayed significant, yet variable, innate oncolytic potency as well as inherent tumour specificity, bringing them to the foreground in the investigation of VACV therapeutic potential (41, 83).

1.3.1 Wyeth (Wy) VACV

Wy was utilized as the smallpox vaccine in North America and as such is the most common VACV strain clinically used in humans, resulting in a wealth of data generated on its action within the human body (39, 41). Wy is the least virulent of the oncolytic strains in that, based on historic data, approximately 1.4 cases of a severe complication to VACV vaccination, known as post-vaccination encephalitis (PVE) as well as 2.9 deaths in 1 million vaccinations, will occur. This is in contrast to 26.2 cases of PVE and 2.5 deaths in 1 million vaccinations occurring with the Lister strain (44). Wy has displayed minimal inherent tumour selectivity when compared with other VACV strains, but can be engineered into a successful oncolytic candidate (41).

1.3.2 WESTERN RESERVE (WR) VACV

The WR strain is a laboratory-derived virus, created from Wy after serial passaging through mouse brain tissues (12, 36). It is highly tumour selective, as demonstrated by an enhanced replication in cancer cell lines, and has demonstrated a strong oncolytic profile, but WR has had minimal use in humans and therefore possesses a shorter clinical history (41, 83). WR is highly adapted to murine models, replicating to a very high extent in the brain as well as the nose, lungs, ovaries and skin of mouse species (36, 90). The WR strain has also been engineered into a successful oncolytic candidate (83) .

1.3.3 COPENHAGEN (COP) VACV

Cop was the Northern European vaccine strain during the smallpox eradication campaign, but it was withdrawn due to high levels of toxicity (41). It is estimated to induce approximately 33.3 cases of PVE and 31.2 deaths per 1 million vaccinations, making it the most virulent oncolytic strain used clinically in humans (44). Cop has been demonstrated to possess inherent *in vitro* tumour selectivity and an attenuated version has been used successfully in mouse models as a gene therapy vector for a pro-drug converting enzyme

within a colorectal tumour model (28). Cop has yet to be investigated as a clinical oncolytic candidate, due to its history of toxicity in humans and overall higher anticipated degree of virulence.

1.4 Engineered Selectivity and Enhancing Modifications

For use on an oncolytic therapy platform, a number of specific mutations to the viral genome have been investigated in order to enhance the inherent tumour selectivity and anti-tumour action of VACV, thereby reinforcing the overall targeted approach and safety profile. A number of gene deletions have been noted to strengthen infection selectivity in cancer cells by exploiting the innate differences between neoplastic and normal cell types. The alterations that bring about uncontrolled cell growth also allow for their engineered targeting by viruses, from a variety of angles. Some of the more widely used examples of these selectivity modifications include deletions or alterations of viral thymidine kinase (*TK*), vaccinia growth factor (*VGF*) and *B18R* genes. Together with selectivity enhancements, immunostimulatory and chemo-targeted mechanisms are also under investigation for their potential to initiate anti-tumour action. These avenues include immunomodulatory molecules designed to harness and utilize the power of the immune system as well as pro-drug converting enzymes designed for a synergistic approach with specific chemotherapeutics for ideal anti-tumour clinical candidate production (41).

1.4.1 Thymidine Kinase (TK) Deletion

The most highly utilized means of attenuating VACV is the deletion of its viral TK enzyme. VACV encoded TK is utilized for the synthesis of the thymidine nucleotide, required for viral DNA synthesis and ultimately for viral replication (31, 75). Dividing cells also transiently express TK in order to produce the components required for division during the synthesis phase of the cell cycle (33). As such, the majority of rapidly dividing cancer

cells constitutively express TK and the pool of nucleotides is consistently high (12, 33). Therefore, in deleting the viral TK gene from the VACV genome, tumour selectivity is enhanced by forcing the virus to rely on the cellular TK, most highly expressed in cancer cells, for replication and sustained infection. It has been demonstrated that TK deleted (TK-) VACV is highly attenuated in normal cell lines and is less pathogenic in mice than wildtype (wt) VACV, while it is still able to replicate in transformed cell lines (12). Furthermore, TK- VACV has exhibited preferential infection in tumours *in vivo* in several different tumour-bearing mouse models (31, 65).

1.4.2 VACV GROWTH FACTOR (VGF) DELETION

A secondary deletion has further been established as an effective selectivity enhancing method. VACV encodes VGF, a human epidermal growth factor (EGF) homologue that is secreted to functionally stimulate cellular mitosis (85). This action induces a higher than normal rate of host cell proliferation, enhancing the virus' replicative potential and allowing for sustained viral infection and spread. When deleted, VGF- VACV has been demonstrated to replicate less efficiently in normal cell lines as well as be significantly less pathogenic in mice than is wt VACV, establishing the importance of VGF to VACV virulence (13, 52).

By inhibiting VGF action, the virus is more likely to preferentially infect cells already replicating to a higher degree, making the VGF- VACV mutant more tumour-selective than the wt (31). A VACV mutant known as double deleted VACV (vvDD) has been engineered from the WR strain backbone with deletions of both the *TK* and *VGF* genes. This double mutant has been shown to be highly selective for replication in cancer cell lines with an activated EGF receptor (EGFR) pathway and to be significantly tumour selective in

murine models, while at the same time is highly attenuated in non-dividing cell lines *in vitro* (41, 52).

1.4.3 B18R TRUNCATION

Another means of enhancing the selectivity of VACV for tumour cells is to counteract the virus' innate immunoevasive mechanisms. Wt VACV infection attempts to outmaneuver the host's immune system by encoding B18R, a soluble IFN-receptor mimetic that sequesters IFN at the cell surface, thereby preventing the cell from mounting an anti-viral campaign (3). This function attributes to VACV strains, such as WR, an evasive quality that facilitates sustained infection (19). It has been demonstrated that when deleted, B18R- VACV is cleared from normal tissues more rapidly than the wt VACV but maintains its infection in tumours, due to the disabled IFN pathways inherent to cancer cells (42). This is suggestive of heightened tumour selectivity. The Wy strain of VACV naturally encodes a truncated version of B18R that binds IFN with a lower affinity (3). Clinical candidates of the Wy backbone are therefore inherently more likely to have a heightened safety profile due to the weakened anti-IFN mechanism (49).

1.4.4 HSV TK

A final potential approach by which VACV can be engineered for the enhancement of its clinical safety profile is to include the herpes simplex virus (HSV) *TK* gene, in place of VACV TK (61). HSV TK confers a sensitivity to the anti-viral drug acyclovir, allowing for a back-up safety switch to clear uncontrolled viral replication, were it to occur (64). Acyclovir is a purine nucleoside analog that lacks a 3' hydroxyl group, normally required for DNA elongation during the replication process. When incorporated by HSV DNA polymerase, acyclovir induces DNA chain-termination and prevents viral replication, effectively halting infection (26). This process is highly specific for HSV species, as HSV

TK is able to phosphorylate acyclovir, a requirement for integration into the viral DNA replication cycle, while other viral and cellular TK do not (29). Acyclovir has demonstrated low order toxicity in animal models and in uninfected cells, correlating to its selectivity for HSV TK (84). This is in contrast to the inherently higher toxicity levels of the current anti-VACV drug cidofovir (20). This mechanism could provide an extra level of safety for clinical use of the more virulent strains of VACV.

1.4.5 hGM-CSF Transgene Inclusion

In addition, transgene inclusions into the viral genome have also been investigated for their capacity to equip oncolytic candidates with enhancing anti-cancer attributes. Currently, one of the most successful methods of improving the VACV backbone for optimal oncolytic action was undertaken in the addition of human granulocyte monocyte-colony stimulating factor (hGM-CSF), a potent immunostimulatory cytokine (21). GM-CSF functionally stimulates the recruitment and maturation of many innate cell subtypes, including natural killer (NK) cells, monocytes, basophils and granulocytes, amplifying the immune response exponentially (45). It has been demonstrated that when expressed, GM-CSF induces long lasting and specific anti-tumour immunity in animal models, conceivably through the augmented triggering of antigen-presenting cells (APC) and ultimate initiation of anti-tumour cytotoxic T lymphocyte (T_c cell) populations (22, 23, 45).

1.4.6 Pro-drug Converting Enzyme Inclusion

A subsequent means by which oncolytic candidates can be armed for tumour destruction is through the inclusion of transgenes designed to aid in targeted chemotherapy. When expressed at the tumour site, pro-drug converting enzymes are able to transform non-toxic pro-drug compounds into cytotoxic anti-cancer drugs within the tumour (41). This allows for a more selective chemotherapeutic approach and enhances the overall anti-tumour

effect of the treatment. A successful example of this approach is the inclusion of the enzyme yeast cytosine deaminase (yCD), a hydrolase that deaminates cytosine, which functionally converts the pro-drug 5'fluorocytosine (5-FC) into 5-fluorouracile (5-FU), a DNA synthesis inhibitor and potent chemotherapeutic (51). It has been demonstrated that inclusion of the yCD transgene in combination with 5-FC treatment resulted in longer survival for virus-treated tumour-bearing mice (15). A number of pro-drug converting enzymes have the potential to be integrated for a wide range, tumour-type specific efficacy.

Together, combinations of these safety enhancing, immunostimulatory and anti-tumour mechanisms can be utilized to ensure the selectivity as well as potency of an oncolytic candidate. This combinatorial approach allows for an efficacious yet discriminating systemic treatment protocol. With these methods, successful oncolytic candidates have been developed for clinical use and in a number of ways these have demonstrated the great power behind the oncolytic virus platform. Subsequently, these candidates have also elucidated limitations to the treatment scheme that necessitate novel research and development perspectives.

1.5 CURRENT ONCOLYTIC PRODUCTS

1.5.1 JX-963

Jennerex Biotherapeutics Inc. has developed prototypic oncolytic candidates based on enhanced tumour selectivity and anti-tumour immunomodulation within VACV backbones. JX-963 was developed from the WR backbone, chosen based on its inherent tumour selectivity as well as its advanced potency of replication in transformed cell lines (83). It was engineered have deletions of both the *TK* and *VGF* genes, allowing for enhanced tumour selectivity and *hGM-CSF* was included in order to enhance anti-tumour immunity.

In preclinical trials with tumour bearing animal models, it has been demonstrated that

JX-963 exhibits highly potent and selective tumour clearing capabilities when compared with wt WR, TK- Wy and oncolytic adenovirus Onyx-015 (83). JX-963 has also demonstrated systemic efficacy, with IV dosing shown to clear primary and metastatic tumours in animal models. In order to verify the impact of hGM-CSF on treatment outcome a rabbit model was utilized as, due to species differences, the hGM-CSF molecule is inefficient in murine models (45, 74). It was demonstrated that hGM-CSF was expressed and secreted into the blood in tumour bearing rabbits, but not in naïve animals, effectively demonstrating tumour replicative selectivity as well as successful transgene expression. The JX-963 treatment and hGM-CSF expression also correlated pre-clinically with increases in innate leukocyte concentrations as well as tumour-specific T_C cell stimulation (45).

1.5.2 JX-929

JX-929 was built on the same fundamental properties as JX-963, in that it is derived from the WR backbone and lacks functional *TK* and *VGF*, but the transgene inclusion was altered. JX-929 includes yCD for 5'FU targeted chemotherapy at the tumour site (41). JX-929 is currently under investigation in Phase I clinical trials by intratumoural (IT) as well as intravenous (IV) dosing in pancreatic, breast, melanoma and colorectal cancers (2, 41) . The JX-929 platform is demonstrating intratumoural replication, anti-tumour efficacy and an effective safety profile (2).

1.5.3 JX-594

JX-594 is the most highly characterized of the candidates, having been included in a greater number of trials. It was created from the Wy backbone, based on its inherent safety profile and natural *B18R* truncation. In JX-594, the viral *TK* gene is disrupted and *hGM-CSF* has been included for enhanced specificity and anti-tumour potency (39). JX-594 expression of the hGM-CSF was also described in a pre-clinical rabbit model, demonstrating the

transgene's proficient biological activity in the activation of tumour infiltrating T_C cells, in addition to tumour specific viral replication (39). JX-594 has been highly investigated in phase I and II clinical trials in liver, colon, kidney, lung and melanoma cancer types where it has exhibited selective tumour infection and replication bringing about significant decreases in tumour size and inducing tumour necrosis (2). Recently, the IV delivery of JX-594 during clinical trials has been described and shown to be highly efficacious in selective tumour infection, replication and hGM-CSF expression at the tumour site (10).

1.6 Limitations of Current VACV Oncolytic Candidates

1.6.1 Immune-Mediated Barriers

Though current oncolytic products are demonstrating great anti-tumour potential in clinical trials, significant hurdles to optimal therapy protocols remain. Upon systemic administration, oncolytic VACV runs into obstacles implemented by the immune system, in the form of anti-viral neutralizing antibodies, the complement cascade and circulating leukocytes, that can prevent the virus from reaching the tumour site for replication (17, 62).

These virus-clearing mechanisms are especially heightened in a significant proportion of the population due to pre-existing immunity brought about by the widespread smallpox vaccination campaign. Vaccinated individuals have established antibody titres that react against the therapeutic, potentially clearing it before the virus is able to reach the tumour site (62). Furthermore, in this way, antibody production against the oncolytic product after an initial dose can hinder subsequent dosing protocols, limiting the overall treatment potential as multiple dosing regimens are most likely required to produce optimal effects (41).

1.6.2 Immunoevasive Strategies

In order to overcome these immune specific limitations, a number of tactics have been suggested to shield VACV from the immune system, in order to allow viral

dissemination in the face of neutralizing antibodies and to initiate infection at distant tumour sides. Investigated tactics have included carrier cell and adjuvant cloaking devices, undertaken to mask the viral antigens from the immune system and allow therapeutic administration, though these avenues have presented hurdles in successful tumour targeting (62). A means by which this antigen-shrouding and immunoevasion can be subsequently attempted is in the manipulation of the innate life cycle of VACV. VACV has naturally evolved a stealth viral form to promote long range viral dissemination, known as extra-cellular enveloped virus (EEV) (73, 77). Ultimately, enhancing the immunoevasive and spreading capabilities of VACV could aid in improving the overall efficacy of the current clinical candidates.

1.7 The VACV Life Cycle

1.7.1 Infection and Replication

Initial infection by VACV occurs by direct fusion with the cell membrane or by receptor mediated endocytosis, leading the viral core along microtubules into the cell cytoplasm (59). VACV replication then occurs entirely within the cytoplasm of the host cell, at points of replication called viral factories (Fig. 1.1) (69). Initial replication relies on the viral DNA-dependent RNA polymerase to initiate the transcription of early gene products required for the viral replication cycle. dsDNA replication is undertaken, bringing about the transcription of viral proteins. Immature virions are then assembled and processed at this site.

1.7.2 Egress and Release

When complete, replication within the viral factories results in the production of intracellular mature virus (IMV), a fully infectious form of VACV that, upon cell lysis, goes on to infect neighbouring cells and continue the cycle of infection. However, early on in the

Figure 1.1 VACV life cycle. 1. Binding and entry (fusion/endocytosis) 2. Viral core transport on microtubules 3. Uncoating, DNA replication, transcription and IMV formation 4. Some IMV is transported to the TGN for wrapping to become IEV 5. IEV is transported to the cell surface on microtubules 6. The outermost IEV membrane fuses with the cell membrane to expose CEV 7. Actin tail formation drives CEV towards neighboring cell 8. CEV is released as EEV with immunoevasive and long range dissemination qualities (<1% of total progeny). *Figure by A.N. Laporte adapted from Roberts & Smith, 2008.*

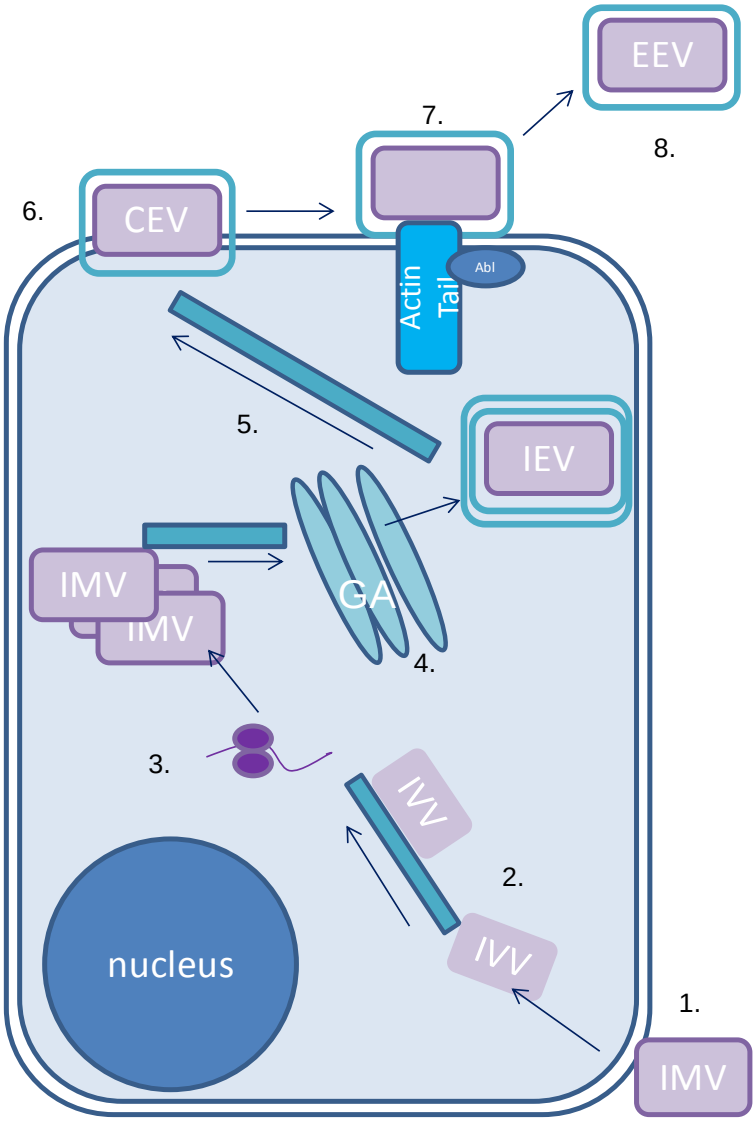
EEV
7.
8.
6.
CEV
Actin Tail
Abl
5.
IEV
IMV
IMV
GA
4.
3.
IVV
2.
nucleus
IVV
1.
IMV

infection cycle, a certain percentage of IMV are transported within the cytoplasm to the *trans*-Golgi network (TGN), where they are wrapped in a cell-derived lipid bilayer to become intra-cellular enveloped virus (IEV) (69, 80). From here, IEV is transported by microtubules to the cell membrane where the outer layer of the envelope fuses and the virion is pushed to the outer cell surface. At this site, the majority of the virions are tethered as cell-associated enveloped virus (CEV) (80). CEV can be driven into neighbouring cells by actin tail formation from within the infected cell, constituting cell-to-cell spread, or CEV can be released from the cell surface as EEV, allowing for long range dissemination of the virus (5, 72). During replication of most VACV strains, less than 1% of the total viral progeny is released as EEV (9).

1.7.3 Tyrosine Kinase (TK) Action

Though the exact mechanism remains to be elucidated, it has been observed that CEV recruits cellular actin tail polymerization for propulsion into neighbouring cells. The VACV IMV protein known as A36R has been shown to be phosphorylated by locally activated Src tyrosine kinases (Src TK), initiating a signal cascade toward the induction of actin tail mobilization (60). Furthermore, Abl tyrosine kinase (Abl TK) has been demonstrated to be recruited to VACV-induced actin tails and can also phosphorylate A36R *in vitro* (60, 68). The means by which EEV is released from the cell surface is another currently ambiguous point, but it has been shown that when treated with the Abl TK inhibitor imatinib mesylate (Gleevec), EEV release was blocked while actin tail formation was not, indicating a role for Abl TK action in EEV liberation (53, 68).

1.8 Extra-cellular Enveloped Virus (EEV)

1.8.1 Envelope Proteins

The EEV form of VACV derives its envelope from the TGN within the host cell.

Within this membrane are incorporated viral proteins, known as envelope proteins, as well as a number of host-derived peptides. The major viral envelope proteins are known as A33R, a 23-28 kDa glycoprotein (70), A34R, the heterotrimer of glycoproteins gp22-gp24 (25), A56R, virus hemaglutinin gp86 (76), B5R, the 42 kDa glycoprotein gp42 (27) and F13L, a 42 kDa unglycosylated, palmitylated protein (Fig 1.2) (35). It has been demonstrated that F13L and B5R are important for facilitating the IMV wrapping process for CEV/EEV production (8, 27, 35). All envelope proteins have also been demonstrated to be important for optimal virus infection, as when individually deleted plaque size is highly reduced in all cases while IMV production remains normal (70, 79). It has further been demonstrated that actin tail formation does not occur during infection of viruses deleted of *A33R, A34R, B5R* and *F13L*, illustrating the importance of envelope proteins in initiating actin tail motility (79, 91). Generally, VACV envelope proteins are highly important for efficient viral infection early on in the replication cycle and their lack of function is highly attenuating.

1.8.2 Enhanced Infection Efficiency and Spread

Due to the cell-derived membrane, EEV possess a number of favourable, immunoevasive qualities lacked by the naked IMV. Primarily, EEV has been observed to be more efficient in infection than IMV. It has been shown *in vitro* as well as *in vivo* that EEV are released early on in the infection cycle and mediate long-range spread of infection (63, 80). It has also been demonstrated that EEV have a higher rate of infectivity, as measured by a lower particle to plaque forming unit (pfu) ratio when compared to IMV infection (87). This is likely due to variability in route of entry, as EEV is believed to infect by direct fusion with the cell membrane whereas IMV have been observed to enter by the less efficient means of receptor-mediated endocytosis (59, 69, 89). It has been demonstrated that IMV and EEV bind distinct cell receptors, though further characterization is required.

Figure 1.2. Virion structure and potential EEV enhancing mutations. Three envelope associated proteins (A34R, A33R, and B5R) have been shown to be involved in actin tail formation and EEV release. Specific mutations within each of these proteins have been shown to enhance EEV release during the VACV replication cycle. *Figure by A.N. Laporte.*

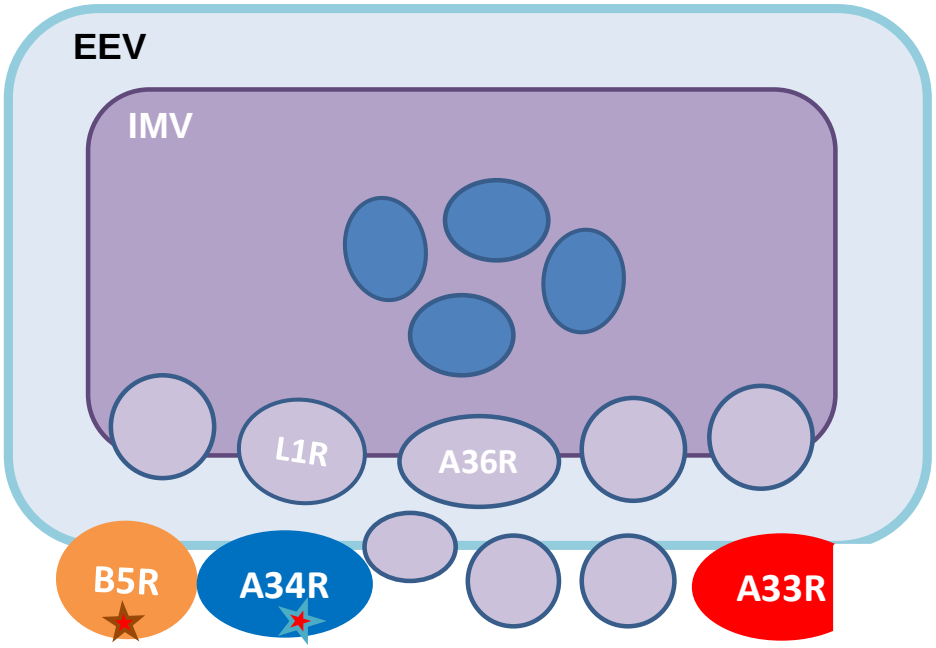
EEV
IMV
L1R
A36R
B5R
A34R
A33R

1.8.3 IMMUNOEVASIVE MECHANISMS

VACV in its EEV form possess a number of characteristics that confer immunoevasive qualities that aid in viral spread and sustained infection (5, 63). EEV has been shown to be resistant to complement mediated neutralization due to the incorporation of proteins CD46, CD55 and CD59 from the host cell membrane into the EEV envelope (80, 88). These cellular proteins are known to down-regulate the complement cascade at various points of action, and upon incorporation into the envelope, seem to allow EEV escape (88). Furthermore, the antigenic profile of EEV also varies greatly from that of IMV, as few viral proteins are expressed on the outer surface. It has been observed that B5R is the only surface antigen that is a target for neutralizing antibodies (4, 7, 24). This is indicative that the shrouding effect of the envelope confers incredible resistance to antibody neutralization when compared to the inherent immunogenicity of IMV.

Overall, when compared with IMV, the EEV form of VACV is produced faster, able to spread farther, infects more efficiently and is highly resistant to complement as well as antibody mediated neutralization. These qualities could aid in overcoming the current limitations of the oncolytic therapeutic platform in the side-stepping of immune neutralization and potentially allow for the treatment of vaccinated individuals, effective serial administration protocols and efficient spread to distant metastatic tumour sites. Means of enhancing EEV release could therefore be incredibly favourable for therapeutic purposes.

1.9 EEV RELEASE AUGMENTATION

EEV release from infected cells has been shown to be possible through the deletion of viral envelope proteins, due to actin tail motility inhibition and the resulting prevention of cell-to-cell spread (70, 79) . This loss of actin action promotes CEV to be released as EEV to a much greater extent, but it is also significantly attenuating. When deleted of *A34R*, EEV

release is enhanced by up to 25 times (55, 79, 95), of *B5R* by up to 10 times (50) and of *A33R* by 2-3 times (70, 79). Though EEV release is enhanced, overall viral production in each case was severely inhibited, due to the lack of cell-cell spread and resultant loss of infection efficiency, as measured by significant decreases in viral plaque sizes as well as decreased virulence and prolonged survival *in vivo* (55, 72).

1.9.1 A34R L151E

While most VACV strains naturally produce less than 1% EEV, one strain from the International Health Department known as IHD-J has been observed to naturally produce up to 30% of its progeny as EEV (63). The evolved proportional difference in viral subtype production illuminates the possibility that EEV release can be effectively enhanced within an efficiently replicating virus. Despite the enhanced EEV production, IHD-J has been shown to possess a similar level of infectivity to that of the WR strain (55) and is still able to induce actin tail formation (72). IHD-J has also been shown to produce enhanced levels of IEV when compared to WR and MVA, indicating it may be more efficient in wrapping IMV at the TGN site (56). Upon sequence analysis and comparison with WR, it was demonstrated that the enhanced EEV releasing phenotype was the result of a single nucleotide substitution within the *A34R* gene, which caused the lysine residue at position 151 to become glutamic acid (L151E) within the putative carbohydrate binding domain (9).

When the IHD-J *A34R* gene was introduced into WR in the place of wt *A34R*, producing the recombinant virus WI, the EEV enhancing phenotype was conferred, as demonstrated by comet-like plaque formation (9, 55). The WI recombinant has been investigated on an oncolytic platform wherein it was demonstrated to spread more efficiently between a primary tumour and distant metastases, as well as elicit enhanced survival when

compared to wt WR in a tumour-bearing, immunocompetent mouse model (43). It was also shown that WI could spread effectively after VIG administration while wt WR infection was significantly limited (43).

1.9.2 B5R P189S AND A33R C-TERMINUS TRUNCATION

Specific, spontaneously induced mutations to the B5R and the A33R proteins have also been shown to be able to enhance EEV release. After investigating plaque formation by VACV deleted of A36R, it was noted that a proportion of the plaques began to demonstrate an enhanced EEV phenotype, as measured by comet-like plaque formation (38). This novel phenotype was hypothesized to be due to spontaneous compensatory mutations to enhance viral spread in the face of inactivated actin tail production. In order to investigate this, the envelope proteins were sequenced, and it was demonstrated that one EEV enhanced isolate contained an amino acid substitution in the *B5R* gene, changing the proline residue at position 189 to a serine residue (P189S), while a second isolate had an induced frame-shift mutation that brought about a truncation of the c-terminus of *A33R* (37, 38).

It was demonstrated that these envelope specific mutations both resulted in enhanced EEV release as well as significantly inhibited actin tail formation (37). It was shown *in vivo* that both mutations were attenuating in that they decreased viral virulence, as measured by mouse weight after intranasal (IN) dosing. The A33R mutation was more highly attenuating, while the B5R mutant virus was mildly less virulent. This was most highly observed at lower IN doses in comparison with the wt WR infection, while at higher doses no significant differences in the virulence of the experimental viruses were observed. It was concluded that A33R and B5R are likely to be highly involved in actin tail formation and subsequent cell-to-cell spread and that the enhanced EEV release could not fully compensate *in vivo* for this loss of actin tail action.

1.10 Hypothesis Rationale

The enhanced dissemination and immunoevasive capabilities brought about by EEV release make it a desirable trait for an oncolytic candidate. Three specific mutations have been uncovered that enhance EEV production from VACV. Investigating the impact of each of these mutations in an oncolytic setting within the candidate strains could demonstrate optimized therapeutic efficacy due to the enhanced EEV release.

1.11 Hypothesis

Introducing specific EEV enhancing mutations into the viral envelope proteins of VACV will enhance its oncolytic potential *in vivo* through enhanced spread and immunoevasion.

1.12 Experimental Objectives

I – To engineer *A34R* L151E, *B5R* P189S and *A33R* c-terminus truncation into oncolytic VACV strains Cop, Wy and WR in order to determine if one specific backbone and one mutation combination is superior in EEV production.

II – To investigate the impact of each mutation on the growth and infection capabilities of the virus, as well as to assess potential attenuations due to the mutations in each backbone.

III – To develop *in vitro* assays for the investigation of enhanced EEV production as a result of the specific mutations.

IV – To develop *in vivo* models for the investigation of enhanced viral spread and immunoevasion as a result of the specific mutations.

V – To investigate variability in immunostimulation *in vivo* due to the specific mutations.

VI – To assess implications of Abl TK action on EEV release.

2. Materials and Methods

2.1 Cell Lines

CT-26-lacZ (murine colon adenocarcinoma expressing the β-galactosidase (lacZ) reporter gene), HeLa (human cervical carcinoma), U2-OS (human osteosarcoma), SW-620 (human colorectal adenocarcinoma), MRC-5 (normal human fibroblast), U-87 (human glioblastoma), MDA-MB-231 (human breast adenocarcinoma), MCF-7 (human breast adenocarcinoma) and BSC-40 (African green monkey kidney cells) were obtained from the American Type Cell Collection (ATCC; Manassas, VA). Each cell line was maintained in Dulbecco's modified Eagle's medium (DMEM; HyClone, Logan, UT) supplemented with 10% fetal bovine serum (FBS; HyClone, Logan, UT) and was grown at 37°C and 5% CO_2.

2.2 Viruses

Wildtype Wyeth (wt Wy) and Western Reserve (wt WR) VACV strains were obtained from the ATCC (Manassas, VA). Copenhagen (wt Cop) VACV was received courtesy of G. McFadden (University of Florida, Gainesville, FL). JX-594 was received courtesy of Jennerex Biotherapeutics Inc. (San Francisco, CA). All recombinant viruses were created from these backbones (see below). VACV-LCMV-gpG2 was received courtesy of J. Bramson (McMaster University, Hamilton, ON). Virus stocks were propagated in confluent HeLa cells (ATCC, Manassas, VA) infected at a multiplicity of infection (MOI) of 0.01 for 48-72 hours. The cell fractions (CF) were collected, pelleted and freeze/thawed. Virus was purified on a sucrose cushion by ultracentrifugation and titre in pfu/mL was determined by titration.

2.3 Virus Titration

Virus stocks and samples were titred on U2-OS and BSC-40 cell lines. Samples were

freeze/thawed 3 times prior to titration. Full or half log serial dilutions were performed. 150 µL of each dilution was plated on confluent cells and incubated for 1 hour at 37°C and 5% CO_2. Inoculum was then removed and replaced with an overlay of 3% carboxymethycellulose (CMC; Sigma-Aldrich, Oakville, ON) and 2x DMEM+ 20% FBS at a 1:1 ratio. Plaques were developed with 0.1% crystal violet in 80% methanol (CV) at 48-72 hours post infection (hpi). Plaque number was counted and pfu/mL was calculated.

2.4 Recombinant Virus Production

2.4.1 Plasmid Construction

Plasmids for recombinant site-directed mutagenesis were ordered from GeneArt (Life Technologies, Burlington, ON). Plasmids were designed with the kanamycin resistance gene, a multiple cloning site and one of the *A34R* L151E AAA→GAG substitution, the *B5R* P189S GGC→CTC substitution or with the *A33R* frameshift mutation and resulting c-terminus truncation, LYDYV→LAHstop. The YFP/GPT (yellow fluorescence protein/ guanine phosphoribosyltransferase) selection cassette was inserted into each plasmid at the multiple cloning site. Plasmids were linearized by restriction enzyme digestion overnight at 37°C and were purified by gel electrophoresis and DNA extraction using the illustra GFX PCR DNA and Gel Band Purification Kit (GE Healthcare, Piscataway, NJ).

2.4.2 Infection/Transfection Recombination

Confluent U2-OS cells were infected with wt Cop, wt WR, wt Wy or JX-594 at an MOI of 0.01 for 1 hour. Linearized plasmid DNA was incubated with Lipofectamine 2000 transfection reagent (Invitrogen, Burlington, ON) at a ratio of 0.4 µg:1µL for 20 minutes at room temperature (RT). Transfection inoculum was then added into infected wells and incubated at 37°C and 5% CO_2 for 4-6 hours. Inoculum was removed and replaced with DMEM+10% FBS for 48 hours. YFP positive wells were collected and freeze/thawed three

times.

2.4.3 Recombinant Clone Rescue and Purification

Recombinant viruses were positively selected for based on YFP expression as well as negativity selected for using the GPT substrate, mycophenolic acid treatment. Virus was plaque purified on BSC-40 cells. Recombinants were filtered through a 0.65 µM pore to eliminate aggregates with wt virus. Plaque purification was continued until all plaques were YFP positive. DNA was extracted from infected cells using the DNeasy Blood and Tissue Kit (Quiagen, Missassagua, ON). The mutated genes, *A34R, B5R* or *A33R* were amplified with site specific primers by PCR and isolated using the illustra GFX PCR DNA and Gel Band Purification Kit. Genes were then sequenced by the StemCore sequencing facility (Ottawa Hospital Research Institute, Ottawa, ON) in order to assess successful recombination (Fig. I.1- I.3).

2.4.4 Recombinant Virus Nomenclature

Recombinant viruses were designated based on the backbone and the introduced envelope protein mutation. Backbones Cop, WR, Wy and JX-594 were utilized. Within the recombinants, the *A34R* L151E mutation is referred to as A34R, the *B5R* P189S mutation is referred to as B5R and the *A33R* c-terminus truncation is referred to as A33R.

2.5 Neutralizing Antibody Western Blot

Relative neutralizing antibody concentrations in plasma samples were assessed utilizing a western mini-blot protocol. 1e7 pfu of wt Cop was denatured at 100°C for 5 minutes in loading buffer with reducing agent dithiothreitol (DTT). The protein was separated on a 2 lane gel and transferred onto a nitrocellulose membrane. The membrane was then blocked overnight with skim milk at 4°C with agitation. The membrane was

inserted into the mini-blot apparatus, creating 20 lanes. Lanes were incubated with agitation in 1% mouse plasma in skim milk for 4 hours at 4°C. Membranes were washed 3 times in TBS-T for 10 minutes, then incubated with a 1/3000 dilution of secondary antibody goat anti-mouse IgG-HRP (horseradish peroxidase conjugate) (Jackson ImmunoResearch Laboratories, Inc., West Grove, PA) in skim milk for 1 hour at room temperature with agitation. Membranes were washed 3 times in TBS-T for 10 minutes, developed using the SuperSignal West Pico Chemiluminescent Substrate (Thermo Scientific, Ottawa, ON) and exposed on film for a short time (30 seconds – 5 minutes).

2.6 MICROSCOPY

Fluorescent microscopy was utilized for the detection of YFP expression with the Zeiss Axiovert s100 microscope. Pictures were taken at 5x magnification for comet visualization.

2.7 PHYLOGENETIC ANALYSIS

Phylogenetic trees to assess evolutionary relationships between VACV strains were created. The maximum-likelihood method was utilized with the Tamura-Nei model of nucleotide substitution using Mega5 (Molecular Evolutionary Genetics Analysis) software (82).

2.8 *IN VITRO* ASSAYS

2.8.1 COMET ASSAY

Comet formation is an indication of enhanced EEV release, as virus released into the supernatant (SN) follows the constant convection current present within the media and falls on a new site along the current path, creating a 'comet' shaped plaque. Comet assays must be incubated in a location where they will not be disturbed, as any motion or vibration will alter the convection current path and prevent comets from forming properly. Virus was

plated on confluent BSC-40 cells, as well as cancer cell lines U2-OS and HeLa at an MOI of 0.1 and serially diluted 10-fold, 6 times. Inoculum was incubated with cells for 1 hour at 37°C and 5% CO_2. Inoculum was then removed and replaced with a liquid overlay of DMEM+10% FBS. Plates were incubated at 37°C and 5% CO_2 for at 48-96 hpi in a place where they would not be moved or disrupted. Comets were developed with 0.1% CV.

MRC-5 cells were treated for 16 hours with 100 or 1000 international units (U) of IFN-β (Bayer, Montville, NJ), or were left untreated. Virus was then plated on confluent MRC-5 cells, from the treated and untreated conditions, at an MOI of 0.01. Plates were incubated at 37°C and 5% CO_2 for 96 hours in a place where they would not be moved or disrupted. Comets were developed with 0.1% CV.

2.8.2 Neutralizing Comet Assay

Confluent BSC-40 cells were infected at an MOI of 0.01 in a low volume for 1 hour at 37°C and 5% CO_2. Inoculum was then replaced with DMEM+10% FBS including increasing concentrations of monoclonal antibody anti-B5R (BEI Resources, Manassas, VA). Plates were incubated for 48 hours in a place where they would not be moved or disrupted. Comets were developed with 0.1% CV.

2.8.3 Virus Release Assay

Confluent cells were infected at an MOI of 0.01 in a low volume for 1 hour at 37°C and 5% CO_2. Inoculum was then removed and replaced with DMEM+10% FBS and incubated for 16 or 24 hours. SN were then collected and titred. CF were harvested in 1 mL serum-free media (SFM), freeze/thawed 3 times and titred. Each condition was assessed in triplicate.

2.8.4 Multi-Step Growth Curve

Confluent HeLa cells were infected at an MOI of 0.01 in a low volume for 1 hour at

37°C and 5% CO_2. Inoculum was then removed and replaced with DMEM+10% FBS. Total well contents (SN and CF) were collected at 0, 4, 8, 12, 24, 48, 72, 96, 120 and/or 144 hpi. Each condition was performed in triplicate and samples were titred for virus concentration.

2.8.5 EEV Freeze/Thaw Analysis

EEV particles were collected from the SN of cells infected at an MOI of 0.01 with Cop A34R. Particles were freeze/thawed in 50 µL, 0-6 times. Samples were then either left untreated or treated for 1 hour with anti-IMV antibody L1R. Samples were titred and percent change due to freeze/thaw cycle number was assessed. Each condition was assessed in triplicate.

2.9 *In vivo* Assays

2.9.1 Animals

Female, 6-8 week old Balb/c (immunocompetent), C57Bl/6 (immunocompetent) and CD-1 nude (immunodeficient) mice were supplied by Charles River Canada (St. Constant, QC). Mice were housed in a biocontainment level-2 facility at the University of Ottawa Animal Care and Veterinary Services (ACVS).

2.9.2 Biodistributions

CD-1 nude, SW-620 tumour bearing mice were treated with a single IV dose of 5e6 pfu of wt Cop, wt Wy or wt WR (n=15/group). Five mice per group were euthanized at days 1, 5 and 14. The tumour, brain, lungs, liver, spleen, heart, kidney and ovaries were excised from each animal. All samples were weighed. Tissues were then homogenized in 1 mL of phosphate buffered saline (PBS) and freeze/thawed 3 times. Tissue samples were titred for virus concentration.

Balb/c mice were treated with a single IV dose of 1e7 pfu of wt Cop or Cop A34R

(n=12/group). Three mice per group were euthanized at 1, 3, 5 and 7 dpi. The brain, lungs, liver, spleen, heart, kidney and ovaries were excised from each animal. Spleen mass was measured to assess degree of splenomegaly. Samples were processed as described above.

2.9.3 Suboptimal Lung Metastasis Model

Balb/c mice received 1e5 CT-26-lacZ cells IV for lung metastasis (met) seeding. Five days later, mice were treated with a suboptimal IV dose of 5e6 pfu wt Cop, 5e6 pfu Cop A34R, 5e6 pfu Cop B5R or 100 µL PBS (n=6/group). At 7 dpi, mice were euthanized and the spleen and lungs were excised. Spleen mass was measured to assess degree of splenomegaly. Lung mets were visualized by staining for LacZ expression with x-gal (synthetic galactose substrate). Lungs were fixed with formalin and lobes were dissected. Mets were counted using a light microscope.

2.9.4 Suboptimal Lung Metastasis Vaccination Model

Balb/c mice were either left unvaccinated (naïve; n=20) or were vaccinated by intraperitoneal (IP) administration of 1e7 pfu wt Cop during week 1 and week 3 (n=20). Vaccinations were performed 2 weeks apart, followed by a 2 week time point before the treatment protocol was initiated. Saphenous bleeds were performed on day 27 and blood plasma was and utilized for a pre-treatment neutralizing antibody western blot. Mice then received 1e5 CT-26-lacZ cells IV for lung met seeding. Five days later, mice were treated with a suboptimal IV dose of 5e6 pfu wt Cop, 5e6 pfu Cop A34R, 5e6 pfu Cop B5R or 100 µL PBS (n=5/group, vaccinated and unvaccinated). At 7 dpi, mice were euthanized, cardiac punctures were performed and the spleen and lungs were excised. Blood plasma was separated and used for assessing post-treatment neutralizing antibody concentrations by western blot. Spleen mass was measured to assess degree of splenomegaly. Lung mets were visualized by staining for LacZ expression with x-gal. Lungs were fixed with formalin and

lobes were dissected. Mets were counted using a light microscope.

2.9.5 Distant Tumour Model

CD-1 nude mice were implanted with bilateral flank tumours by subcutaneous (SQ) injection of 1e6 U-87 cells. Fourteen days later, mice were treated IT (right flank) with 100 µL PBS, 5e7 pfu wt Cop or 5e7 pfu Cop A34R. On day 17 (3 days post treatment), mice were euthanized. The right and left flank tumours were excised, homogenized in 1 mL of PBS, freeze/thawed 3 times and titred.

2.10 Flow Cytometry

Balb/c or C57Bl/6 mice were treated IV with 1e7 pfu wt Cop or Cop A34R (n=6/group). Four dpi, mice were euthanized, the spleens were excised and cardiac punctures were performed. Spleens were homogenized through a 100 µm cell strainer (Fisher Scientific, Toronto, ON). The splenocyte WBC populations were isolated from erythrocytes using ACK lysing buffer (0.15 mol/l NH_4Cl, 10 mmol/l $KHCO_3$, 0.1 mmol/l Na_2EDTA) and total number was determined utilizing the vi-Cell cell counter (Beckman-Coulter Inc., Brea, CA).

The cells were then stained for population-defining epitopes using the following antibodies: Panel 1 - B-cells: B220-FITC, CD19-PC5. Panel 2 -T cells: CD122-PE, CD8a-AF700, CD3-PerCP. Panel 3 - Innate cells: GR-1-FITC, F4/80-PC5, CD11b-PE. Panel 4 – dendritic cells (DC): CD11c-PC7, 440c-PE (BD Biosciences, Mississauga, ON, eBioscience, San Diego, CA). Cell populations were defined as follows: B cells (CD19+B220+), T_c cells (CD3+CD8+), T cells (CD3+CD8-), NKT cells (CD3+CD122+), NK cells (CD3-CD122+), Granulocytes (GR-1+CD11b+), Macrophages (F4/80+CD11b+), DC (CD11c+C440+, CD11c+CD8+). Experiments were performed on a Beckman Coulter CyAn flow cytometer

and data was analyzed using Kaluza software (version 1.1; Beckman Coulter).

2.11 Abl Over-Expression Transfection

Plasmids for the constitutive expression of Abl TK (*v-Abl*: Ableson mutation and *Bcr/Abl*: chromosomal translocation) were ordered from AddGene (Cambridge, MA). Plasmids were transfected into U2-OS and HeLa cell lines using the Lipofectamine 2000 reagent (Invitrogen). Expression was assessed by YFP expression levels in the control plasmid wells. Twenty-four to 30 hours post transfection, cells were infected at an MOI of 0.01 and the virus release assay was performed. Each condition was assessed in triplicate.

2.12 Statistical Analysis

All statistical analyses were performed using GraphPad Prism 5.0 (GraphPad Software, La Jolla, CA). Error bars signify standard error of mean (SEM). Significance was assessed by p-values, using unpaired, two-tailed T-test analysis with Welch's correction.

3. RESULTS

3.1 COP VACV IS EFFICIENT BUT NOT EXCESSIVELY VIRULENT IN MICE

In order to demonstrate the variation in the virulence of the wt VACV backbones, wt Cop, wt Wy and wt WR, a biodistribution was undertaken in tumour-bearing CD-1 nude mice (Fig 3.1). After a 5e6 IV dose, mice were euthanized at 1, 5 and 14 dpi. The wt WR day 14 group reached endpoint early, at day 6. One mouse in the wt Wy group reached endpoint at day 14. Wt WR was significantly more virulent in this model, as was expected due to its adaptation to infection in mice. It was demonstrated that wt Cop was more highly dispersed and had the highest brain tissue tropism initially, representative of a higher rate of virulence in early infection. As seen previously, wt Wy was much less tumour tropic than the other two VACV strains, as demonstrated by a lack of tumour infection at day 1. Wt Cop was not significantly more virulent than wt Wy in long term infection or tissue distribution.

3.2 COP VACV IS MORE HIGHLY RELATED TO IHD-J THAN WR AND WY

A phylogenetic analysis of the *A34R* gene was undertaken to demonstrate the evolutionary relationships between the various VACV strains (Fig 3.2). It was shown that the Cop and IHD-J strains are more closely related to each other than to the Wy, WR or MVA strains. Lister is intermediately situated.

3.3 RECOMBINANT DEVELOPMENT

Recombinant cloning was successfully completed for the A34R and B5R mutations within the Cop, Wy, WR and JX-594 backbones and the A33R mutation was introduced into Cop and Wy (Fig. I.1, I.2, I.3). The A33R mutation cloning within the WR backbone was not attained, as the recombinant was not viable. After 3 plaque purification cycles, the YFP expression was lost from WR A33R, indicating it was not stably introduced into the WR

Figure 3.1. Wt VACV strain comparison. A biodistribution in CD-1 nude mice (n=5/group) established that wt WR was the most virulent strain in this model. Wt Cop initiated a more widespread infection initially than wt Wy, indicating a higher rate if virulence in early infection. Wt Cop also infected the tumour site to a higher degree than wt Wy early on. No significant difference was observed in late stage infection. The day 14 wt WR group end-pointed at day 6.

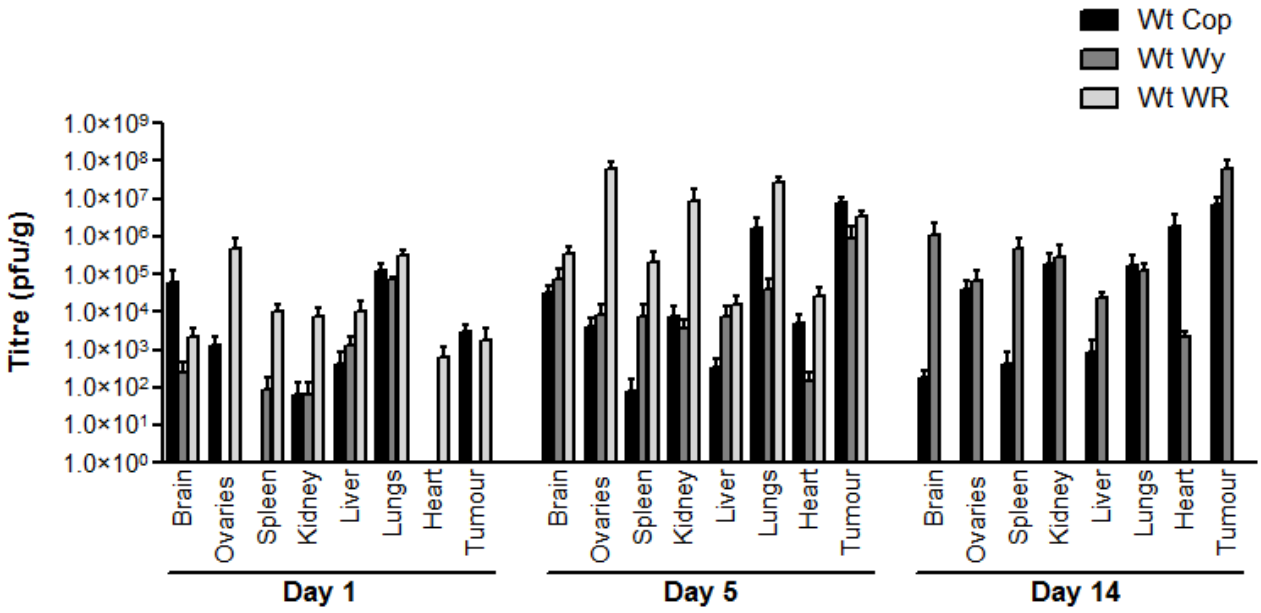
Wt Cop
Wt Wy
Wt WR
Titre (pfu/g)
1.0×10⁹
1.0×10⁸
1.0×10⁷
1.0×10⁶
1.0×10⁵
1.0×10⁴
1.0×10³
1.0×10²
1.0×10¹
1.0×10⁰
Brain
Ovaries
Spleen
Kidney
Liver
Lungs
Heart
Tumour
Day 1
Day 5
Day 14

Figure 3.2. VACV phylogenetic analysis based on the *A34R* gene. Phylogenetic analysis revealed that the Cop and IHD-J strains are more closely related than the Wy or WR strains. The maximum-likelihood method was used with the Tamura-Nei model of nucleotide substitution with Mega5 software.

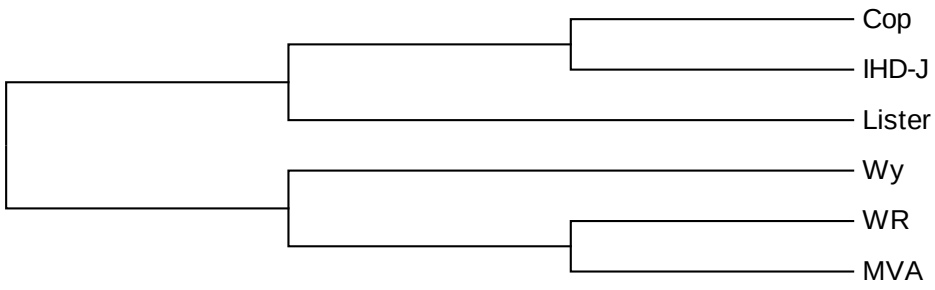
Cop
IHD-J
Lister
Wy
WR
MVA

backbone. The A33R mutation was not inserted into JX-594, due to its lack of enhanced EEV productivity as demonstrated by the lack of comet formation from the Cop and Wy A33R recombinants.

3.4 COP A34R AND B5R RECOMBINANTS DISPLAY ENHANCED EEV RELEASE FROM BSC-40 CELLS

At 72 hpi, comet formation is visible by Cop A34R and Cop B5R recombinants, indicating enhanced EEV release (Fig. 3.3). The wt Cop backbone displayed a slight propensity to enhanced EEV release, but not to the same degree as the A34R and B5R recombinants. No other virus displayed comet formation at this time point. The Cop backbone seems to have the highest propensity towards enhanced EEV release and the most efficient viral spread, resulting in further infection within this cell line.

The comet phenotype results in smaller plaque comet head followed by a long tail, resultant of virus spread within the supernatant. The Cop A34R comets were relatively larger, while the Cop B5R comets were consistently smaller. Plaque phenotypes varied for the subsequent recombinants as well. The A34R and B5R mutations consistently resulted in smaller plaques in the WR, Wy and JX-594 backbones, with the greatest decrease in size consistently seen as a result of the B5R mutation (Fig. 3.3-3.3.7).

Comet formation was then assessed at various time points after 1 passage through BSC-40 cells, in order to demonstrate if enhanced EEV production was possible from the recombinants of each backbone (Fig 3.4). Cop A34R and Cop B5R recombinants displayed comet formation at 48 hpi. Wy A34R and Wy B5R displayed comet formation at 92 hpi. The A33R recombinants did not display comet formation at any time point measured and plaque phenotype was similar to the wt backbones, indicating that this mutation does not enhance EEV release. WR A34R and WR B5R displayed small comet formation at 92 hpi. JX-594

Figure 3.3. Comet assay on BSC-40 cells, 72 hpi. Comet formation is an indication of enhanced EEV release. At this time point, comet formation is visible by Cop A34R and Cop B5R.

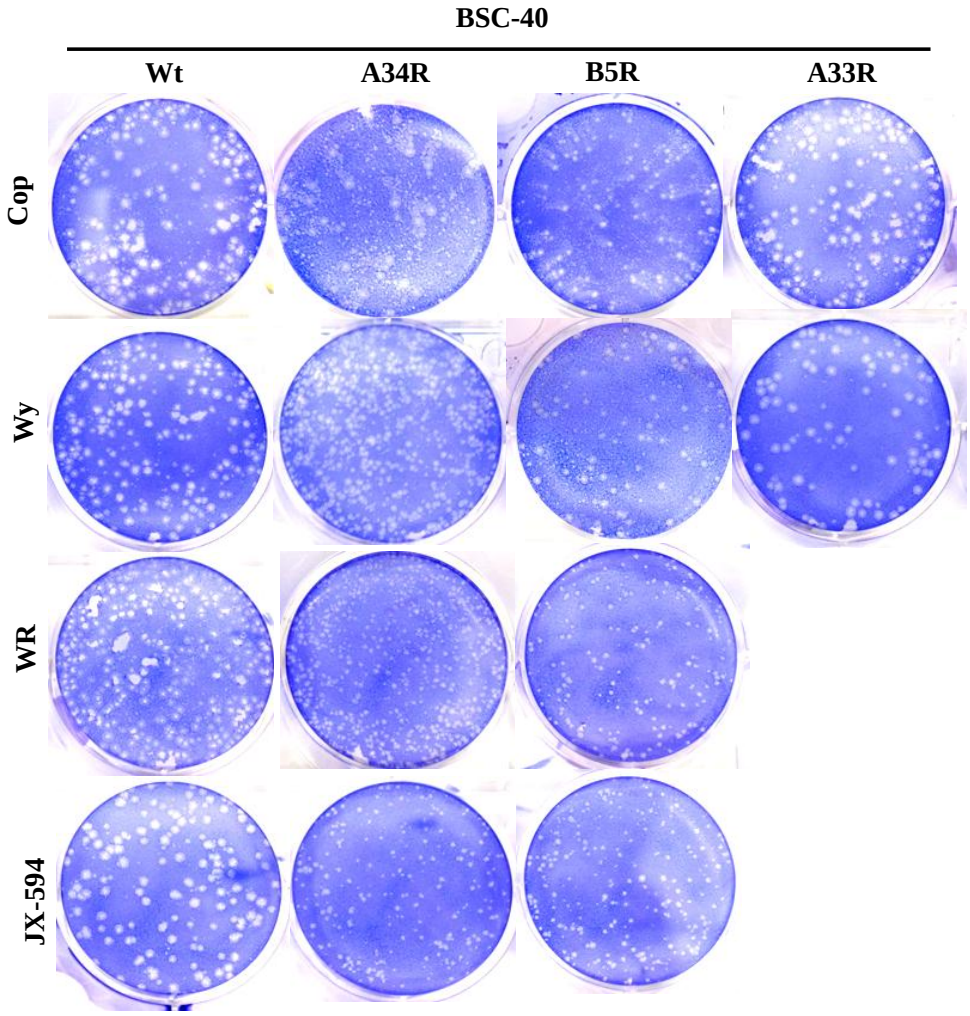
BSC-40
Wt
A34R
B5R
A33R
Cop
Wy
WR
JX-594

Figure 3.4. Comet assay on BSC-40 cells, variable incubation times. Comet formation was assessed at various time points. a) Cop A34R and Cop B5R recombinants displayed comet formation at 48 hpi. b) Wy A34R and Wy B5R displayed comet formation at 92 hpi. c) WR A34R and WR B5R displayed small comet formation at 92 hpi. d) JX-594 A34R and B5R recombinants did not display comet formation at time points up to 96 hpi (96 hpi shown here).

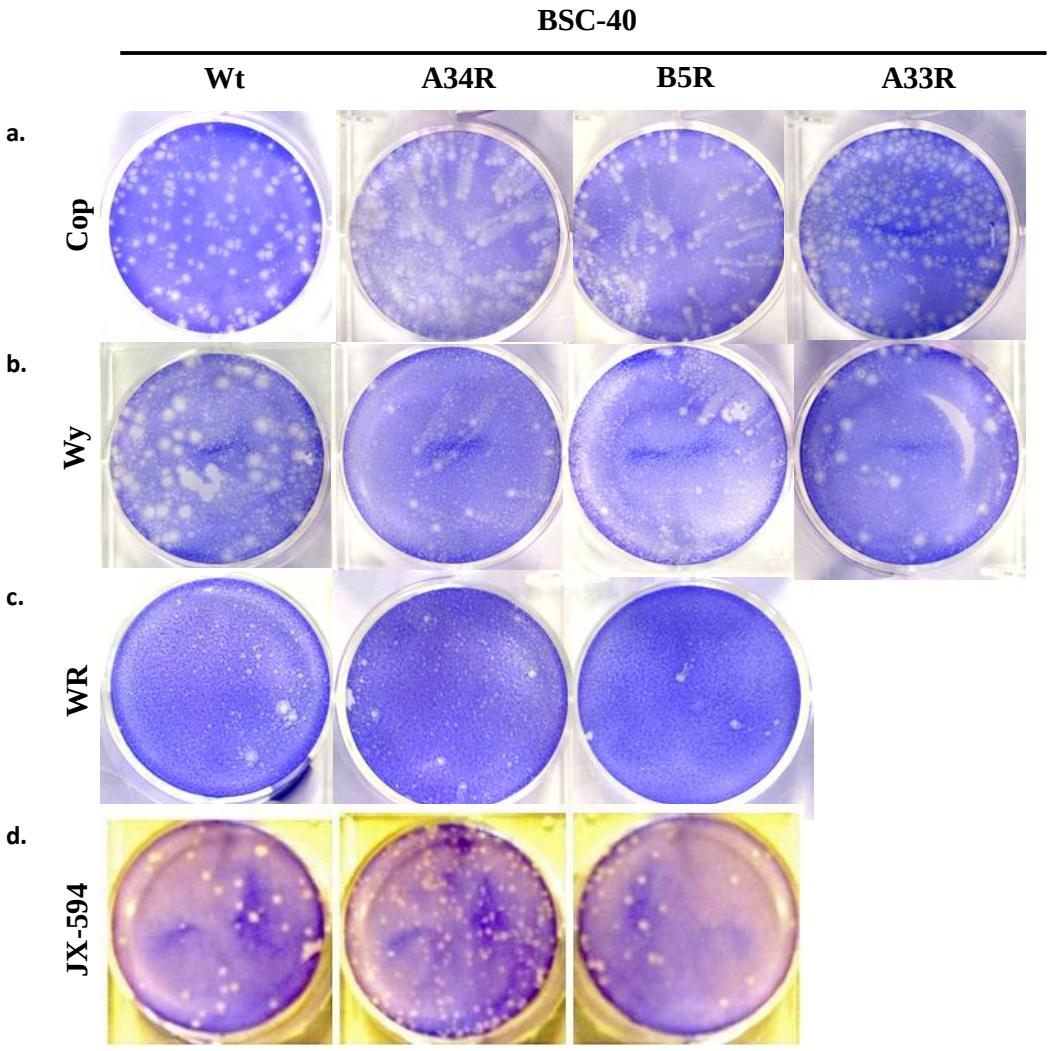
BSC-40
Wt
A34R
B5R
A33R
a.
Cop
b.
Wy
c.
WR
d.
JX-594

A34R and B5R recombinants did not display comet formation at time points up to 96 hpi. JX-594 is a more highly attenuated virus due to the TK inactivation. With a greater timeframe, the JX-594 recombinants may have been able to display comet formation but this was out of the range of the assay's capabilities due to cell overgrowth. It was demonstrated that Cop A34R and Cop B5R brought about the most efficient EEV release. Again, Cop A34R production was shown to be the greatest, as observed by the larger size of comet, while Cop B5R seemed to be slightly attenuated as demonstrated by the smaller comet phenotype.

This same relationship was observed when measuring comet formation by YFP expression. Comet production was visualized at 48 hpi (Fig. 3.5). The wt strains do not express YFP but plaque size was observed for comparative purposes. Cop A34R and Cop B5R displayed significantly larger comet formation than any other isolate. The Cop A33R recombinant did display some small comet-like plaques, but this likely to be similar to the wt production. Overall, Cop A34R and Cop B5R are the most successful and efficient in comet formation on BSC-40 cells.

3.5 COP A34R AND B5R RECOMBINANTS DISPLAY ENHANCED EEV RELEASE FROM HUMAN CANCER CELL LINES

Comet formation was then assessed on human cancer cell lines to demonstrate if EEV release can be enhanced for oncolytic purposes. At 72 hpi, comet formation is visible by the Cop A34R and Cop B5R recombinants on both the U2-OS (Fig. 3.6, II.1) and HeLa cell lines (Fig. 3.7). Cop A34R comets were consistently the largest in comparison with the B5R recombinant. Wt Cop infections had a propensity toward a small comet-like plaque phenotype within the cancer cell lines. The Wy, WR and JX-594 recombinants did not produce comets on either line at this time point.

Figure 3.5. Comet assay on BSC-40 cells, YFP expression. Comet formation was assessed at 48 hpi. The largest comets formed were demonstrated by the Cop recombinants, Cop A34R and Cop B5R. Images were taken at a magnification of 5x.

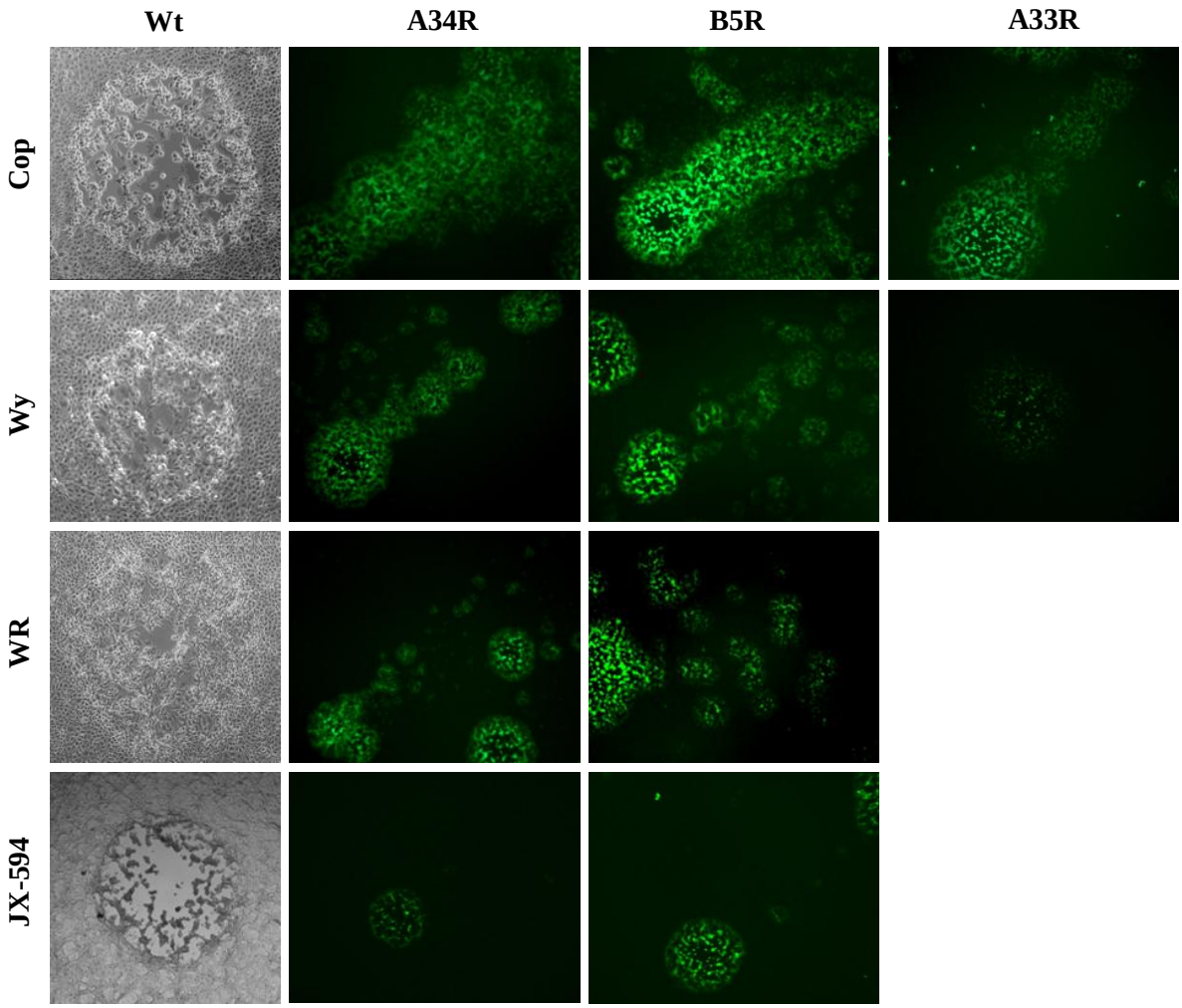
Wt
A34R
B5R
A33R
Cop
Wy
WR
JX-594

Figure 3.6. Comet assay on U2-OS human cancer cells, 72 hpi. Comet formation was assessed at 72 hpi. Comet formation is visible by Cop A34R and Cop B5R infections.

.

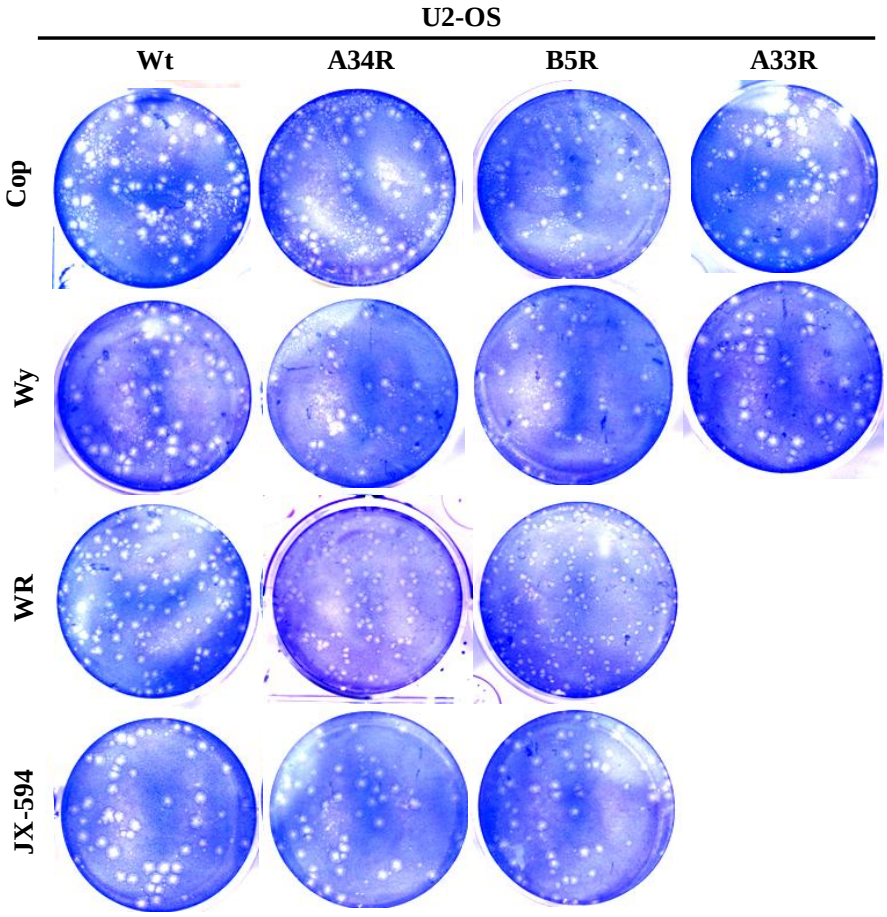
U2-OS
Wt
A34R
B5R
A33R
Cop
Wy
WR
JX-594

Figure 3.7. Comet assay on HeLa human cancer cells, 72 hpi. Comet formation was assessed at 72 hpi. Comet formation is visible by Cop A34R infection.

.

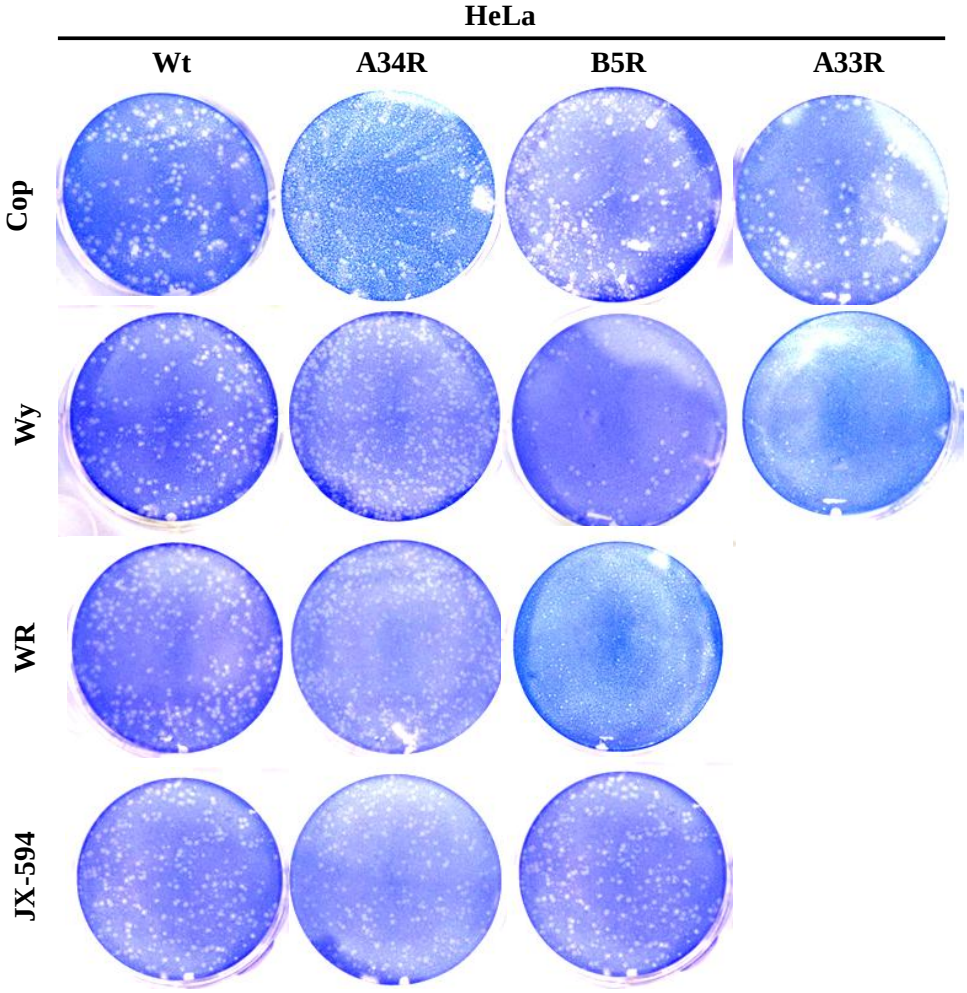
HeLa
Wt
A34R
B5R
A33R
Cop
Wy
WR
JX-594

3.6 COP B5R COMETS ARE NEUTRALIZED BY ANTI-B5R ANTIBODY

Comet formation was assessed on BSC-40 cells in the presence of anti-B5R antibodies (Fig. 3.8). When treated with 25µg/mL anti-B5R antibody, EEV production from Cop B5R is highly neutralized as demonstrated by a loss of comet formation. This is indicative that comet formation is due to EEV release and that the EEV B5R antigen is a target for neutralization, as previously described (4). This neutralization of EEV production from Cop B5R by the anti-B5R antibody occurs in a dose-dependent manner. The comet formation of the Cop A34R mutant is not inhibited by the anti-B5R antibody, but in contrast the antibody treatment seems to be enhancing the releasing process. This is also evident in the wt Cop group, as at the highest treatment doses small comets begin to form.

3.7 EEV SPREAD/INFECTION IS NEUTRALIZED BY IFN ACTION IN NORMAL CELLS

Comet formation was conducted on MRC-5 normal cells to assess safety. MRC-5 cells were either untreated or received either 100U or 1000U of IFN-β at 16 hours pre infection. Comets were created by Cop A34R in the untreated condition and infection appears more widespread than that of the wt Cop condition, as demonstrated by a higher degree of cell death and a comet-like pattern of infection (Fig. 3.9). When treated with IFN-β, plaque size was greatly reduced in both the wt Cop and Cop A34R conditions. Plaque size was smaller in the Cop A34R infection when compared with wt Cop, indicating EEV infection of normal cells may be neutralized by IFN action.

3.8 COP A34R DEMONSTRATES THE MOST SIGNIFICANTLY ENHANCED VIRUS RELEASE FROM BSC-40 AND U2-OS CELLS

Enhanced virus release was assessed from each recombinant in comparison with the wt virus. The A34R and B5R recombinants in each backbone released the most virus from BSC-40 cells at 16 or 24 hpi. (Fig. 3.10a). The Cop recombinants released the greatest

Figure 3.8. Neutralizing comet assay. Comet formation was assessed on BSC-40 cells in the presence of anti-B5R antibodies. When treated with anti-B5R antibody, EEV production from Cop B5R is highly neutralized as demonstrated by a loss of comet formation. The comet formation of the Cop A34R mutant is not inhibited by the anti-B5R antibody. Comet formation seems to be enhanced in the Cop A34R and wt Cop groups at the highest doses of anti-B5R antibody treatment.

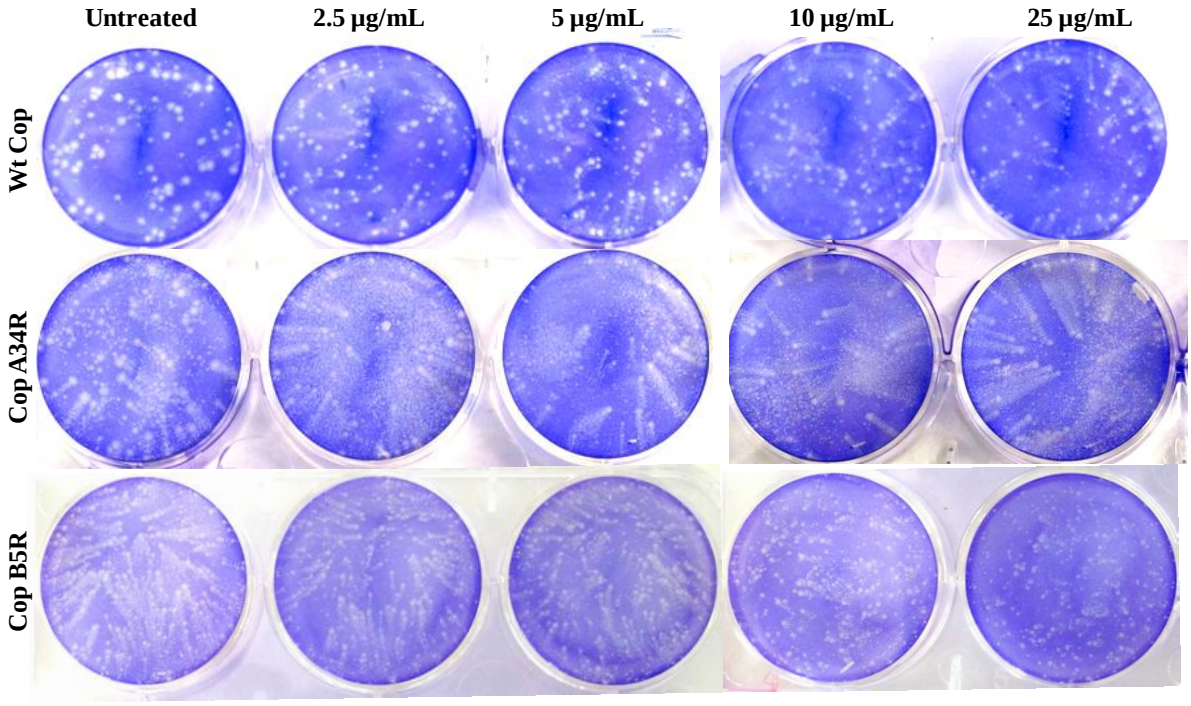
Untreated
2.5 µg/mL
5 µg/mL
10 µg/mL
25 µg/mL
Wt Cop
Cop A34R
Cop B5R

Figure 3.9. Normal cell comet assay. Comet formation was conducted on MRC-5 normal cells. MRC-5 cells were either untreated or received either 100U or 1000U of IFN-β. Sixteen hours later, cells were infected at an MOI of 0.01 and comet formation was assessed at 96 hpi. Comets were created by Cop A34R in the untreated condition. When treated with IFN-β, plaque size was greatly reduced in both the wt Cop and Cop A34R conditions. Plaque size was smaller in the Cop A34R infection when compared with Wt Cop, indicating EEV infection may be neutralized by IFN action.

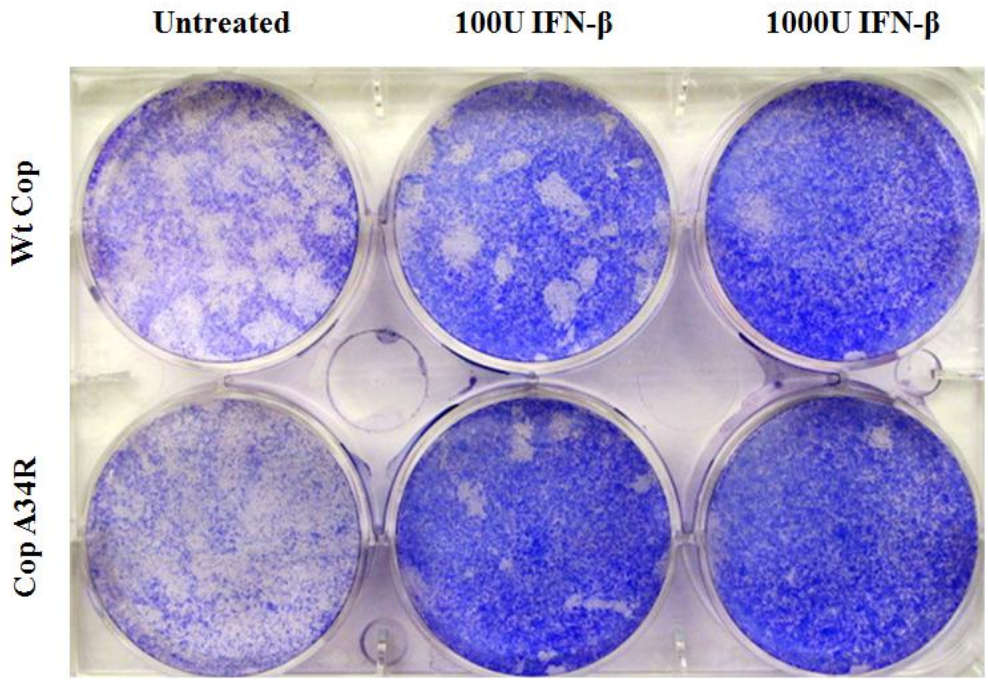
Untreated
100U IFN-β
1000U IFN-β
Wt Cop
Cop A34R

Figure 3.10. Virus release assay, BSC-40 cells. Enhanced virus release was assessed from each recombinant in comparison with the wt virus strains. a) Virus release into the supernatant (SN) was quantified and plotted on a log scale to demonstrate the difference between the recombinants and the wt virus. The A34R and B5R mutants released the most virus at 16 and 24 hpi when compared to the wt virus strains. b) Virus release was plotted on a linear scale to demonstrate the differences between the viral strains. The Cop recombinants produced the greatest quantity of EEV. c) Total virus production was assessed in looking at both the SN and cell fraction (CF) titres (total pfu) Virus production was consistent between the wt and recombinants within each strain, while Cop A34R and Cop B5R infections resulted in heightened levels of virus in the SN. The Cop backbone produced the most virus in both fractions and the Cop A34R had the greatest quantity of virus released. d) The Wy A34R had the greatest percent of total released.

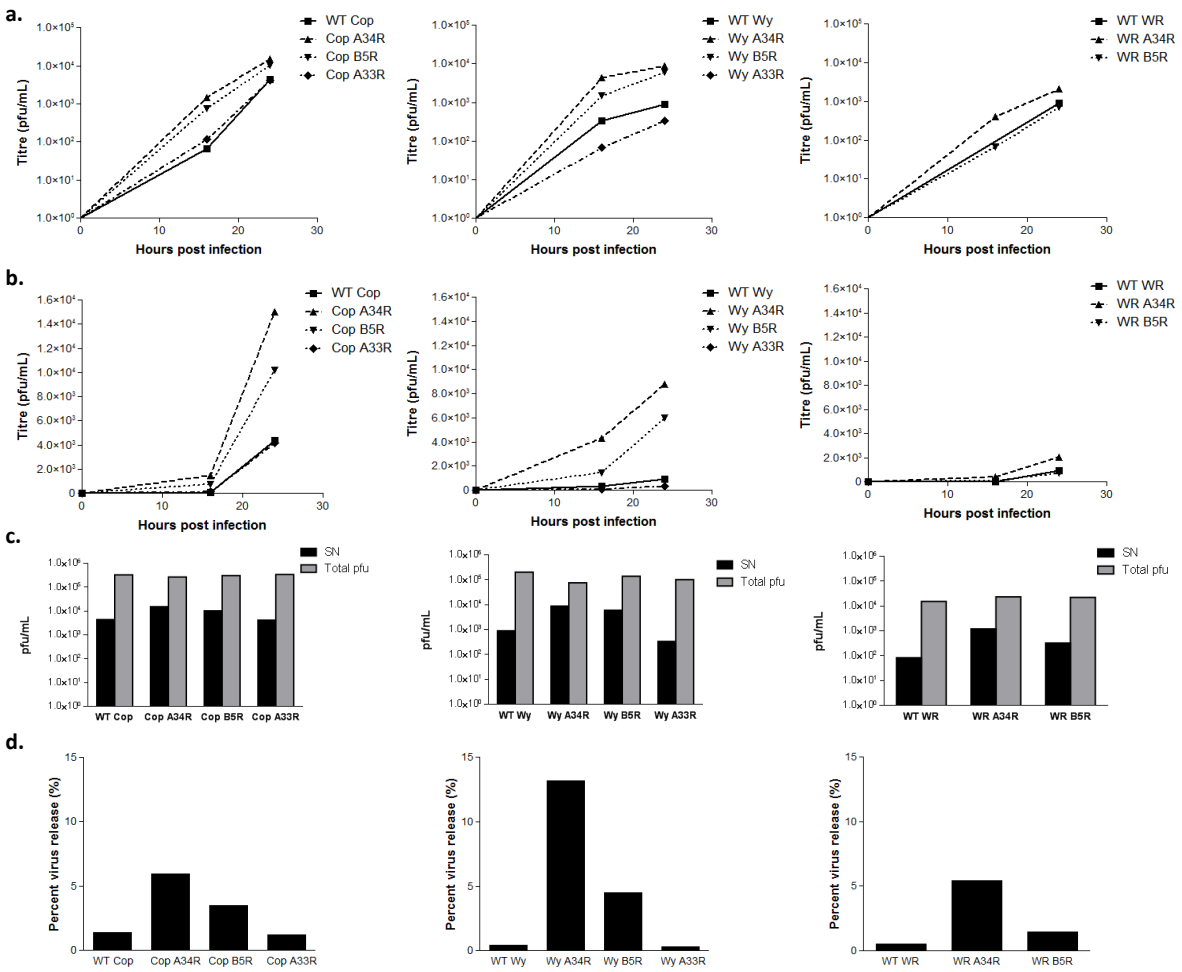
a.
WT Cop
Cop A34R
Cop B5R
Cop A33R
WT Wy
Wy A34R
Wy B5R
Wy A33R
WT WR
WR A34R
WR B5R
Titre (pfu/mL)
Hours post infection
b.
c.
SN
Total pfu
pfu/mL
WT Cop
Cop A34R
Cop B5R
Cop A33R
WT Wy
Wy A34R
Wy B5R
Wy A33R
WT WR
WR A34R
WR B5R
d.
Percent virus release (%)

quantity of virus into the SN when compared to the other backbones (Fig. 3.10b). Total virus production was also assessed in looking at both the SN and CF titres. Virus production was consistent between the wt and recombinants within each strain while Cop A34R and Cop B5R infections resulted in heightened levels of virus in the SN (Fig. 3.10c). The Cop recombinants produced the most virus in both fractions and the Cop A34R had the greatest quantity of virus released. Percent virus release was assessed and it was observed that the Wy A34R had the greatest percent of total virus released (Fig. 3.10d), though the overall highest output was seen from Cop A34R.

Enhanced virus release was then assessed on the U2-OS cell line (Fig. 3.11). A similar relationship to the BSC-40 assay was observed. Virus release was most significantly enhanced in the Cop A34R recombinant group (Fig. 3.11a, c). In addition, the Wy backbone recombinants released a significant amount of virus (Fig. 3.11a, d). The Cop and Wy backbones released virus more quickly than that of the WR and JX-594 backbone recombinants (Fig. 3.11a, b).

3.9 THE COP A34R MUTANT IS THE ONLY A34R RECOMBINANT NOT TO BE ATTENUATED BY THE L151E MUTATION

A growth curve was conducted over a period of 144 hours with all wt virus strains and A34R recombinants in order to assess if viral growth and replication was impeded by the introduced mutation (Fig. 3.12a). The growth rates of each wt strain were not significantly different in HeLa cells over this timeframe (Fig. 3.12b). It was demonstrated that Cop A34R was the only recombinant not attenuated by the mutation during replication in this cancer cell lines (Fig. 3.12c). Cop A34R grew to significantly higher titers when compared to the other A34R recombinants at time points 96, 120 and 144 hpi.

Figure 3.11. Virus release assay, U2-OS human cancer cells. Enhanced virus release was demonstrated from each recombinant in comparison with the wt virus strains. a) Virus release into the SN was quantified and plotted on a log scale to demonstrate the difference between the recombinants and the wt virus. The A34R and B5R mutants released the most virus at 16 hpi within the Cop and Wy strains and 24 hpi within the WR and JX-594 strains. Total virus production was assessed in looking at both the supernatant (SN) and cell fraction (CF) titres (total pfu) at b) 16 hpi and c) 24 hpi. Virus production was consistent between the wt and recombinants in the Cop and Wy strains and slightly attenuated in the recombinant WR and JX-594 strains. Overall, Cop A34R and Cop B5R infections resulted in heightened levels of virus in the SN. The Cop backbone produced the most virus in both fractions and the Cop A34Rinfection resulted in greatest quantity of virus released. d) The Wy A34R had the greatest percent of total virus released. Error bars signify standard error of mean (SEM), p-values were measured by unpaired, two-tailed T-test analysis.

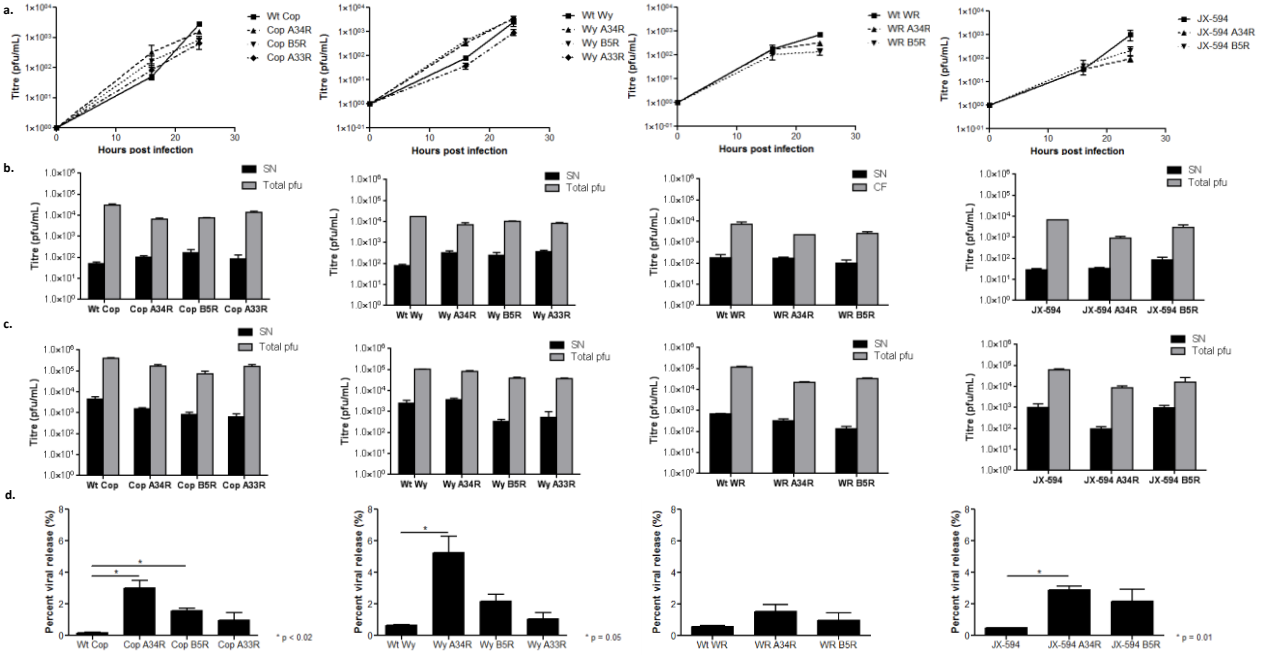
a.
Wt Cop
Cop A34R
Cop B5R
Cop A33R
Wt Wy
Wy A34R
Wy B5R
Wy A33R
Wt WR
WR A34R
WR B5R
JX-594
JX-594 A34R
JX-594 B5R
Titre (pfu/mL)
Hours post infection
b.
c.
SN
Total pfu
CF
Wt Cop
Cop A34R
Cop B5R
Cop A33R
Wt Wy
Wy A34R
Wy B5R
Wy A33R
Wt WR
WR A34R
WR B5R
JX-594
JX-594 A34R
JX-594 B5R
d.
Percent viral release (%)
* p < 0.02
* p = 0.05
* p = 0.01

Figure 3.12. Multi-step growth curve, HeLa cells. a) A growth curve was conducted over a period of 144 hours with all virus strains and A34R recombinants. b) The wt virus growth rates were not significantly different in HeLa cells over this time frame. c) It was demonstrated that Cop A34R was the only recombinant not attenuated by the mutation during replication in cancer cells. Cop A34R grew to significantly higher titers when compared to the other A34R recombinants at time points 96, 120 and 144 hpi. Error bars signify standard error of mean (SEM), p-values were measured by unpaired, two-tailed T-test analysis.

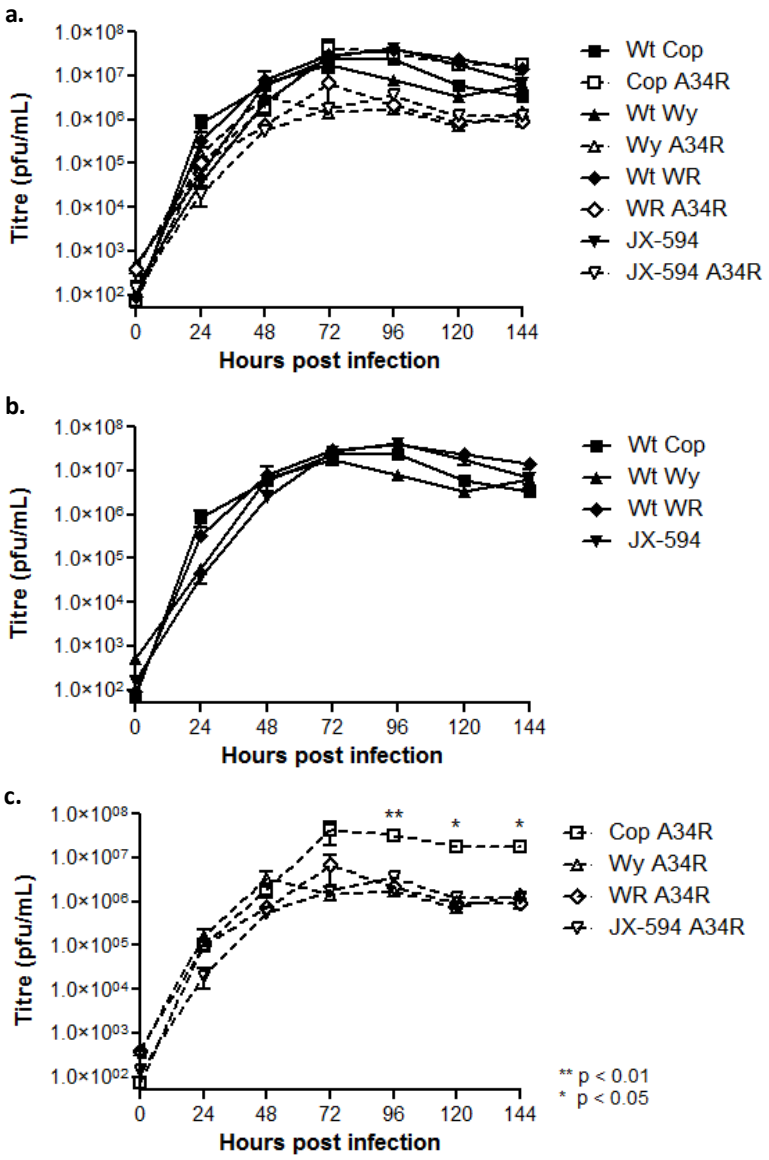
a.
Titre (pfu/mL)
1.0×10⁸
1.0×10⁷
1.0×10⁶
1.0×10⁵
1.0×10⁴
1.0×10³
1.0×10²
0
24
48
72
96
120
144
Hours post infection
Wt Cop
Cop A34R
Wt Wy
Wy A34R
Wt WR
WR A34R
JX-594
JX-594 A34R
b.
Titre (pfu/mL)
Hours post infection
Wt Cop
Wt Wy
Wt WR
JX-594
c.
Titre (pfu/mL)
1.0×10⁰⁸
1.0×10⁰⁷
1.0×10⁰⁶
1.0×10⁰⁵
1.0×10⁰⁴
1.0×10⁰³
1.0×10⁰²
**
*
*
Hours post infection
Cop A34R
Wy A34R
WR A34R
JX-594 A34R
** p < 0.01
* p < 0.05

3.10 THE COP A34R AND B5R MUTANTS ARE NOT SIGNIFICANTLY ATTENUATED BUT POSSESS VARIATIONS IN VIRAL GROWTH

A growth curve was conducted for EEV releasing recombinant comparison over period of 120 hours with wt Cop and recombinants Cop A34R and Cop B5R, to further assess any potential attenuation brought about by the EEV enhancing mutations. There was no significant attenuation in viral production brought about by the mutations visible on the single step growth curve (Fig. 3.13a) or on the multistep growth curve (Fig. 3.13b) in HeLa cells. On a linear scale, it is evident that the Cop A34R and Cop B5R reach the viral production peak at a later time point than that of wt Cop, indicating a potentially slower growth rate (Fig. 3.13c). Cop B5R has been observed to grow slower in the manufacturing processes, requiring an extra day for replication to reach maximum titres (data not shown). Cop A34R reached an overall higher titre than Cop B5R after 72 hours. Viral release into the SN was also measured over the time period. While the release kinetics were variable, Cop A34R and wt Cop titres were not significantly different while Cop B5R production was significantly inhibited, indicating inhibited viral growth (Fig. 3.13d).

3.11 COP A34R IS NOT SIGNIFICANTLY ATTENUATED OR MORE VIRULENT THAN WT COP *IN VIVO*

A biodistribution for the comparison of the enhanced EEV mutant with wt Cop in tissue distribution was undertaken (Fig. 3.14a). On day 1, viral distribution was more widespread in the wt Cop group, while titres in the lungs were higher in the Cop A34R group (Fig. 3.14b). On day 3, replication in the ovaries was much greater in the Cop A34R group. By day 7, both viruses were cleared below detectable levels. No significant enhancement to virulence or significant attenuation *in vivo* was observed as a result of the A34R mutation. Significant splenomegaly was demonstrated in the wt Cop group over the 7 day period when

Figure 3.13. Growth curves for recombinant comparison, HeLa cells. A growth curve was conducted over a period of 120 hours with wt Cop and recombinants Cop A34R and Cop B5R to assess any potential attenuation brought about by the EEV enhancing mutations. a) There was no significant attenuation in viral production brought about by the mutations visible on the single step growth curve or b) on the multistep growth curve in HeLa cells. c) On a linear scale, it is evident that the Cop A34R and Cop B5R reach the viral production peak at a later time point than that of wt Cop, indicating a potentially slower growth rate. Cop A34R reached a higher titre than Cop B5R. d) Viral release into the SN was measured over the time period. Cop A34R and wt Cop were not significantly different, while Cop B5R production was significantly inhibited, indicating inhibited viral growth. Error bars signify SEM, p-values were measured by unpaired, two-tailed T-test analysis.

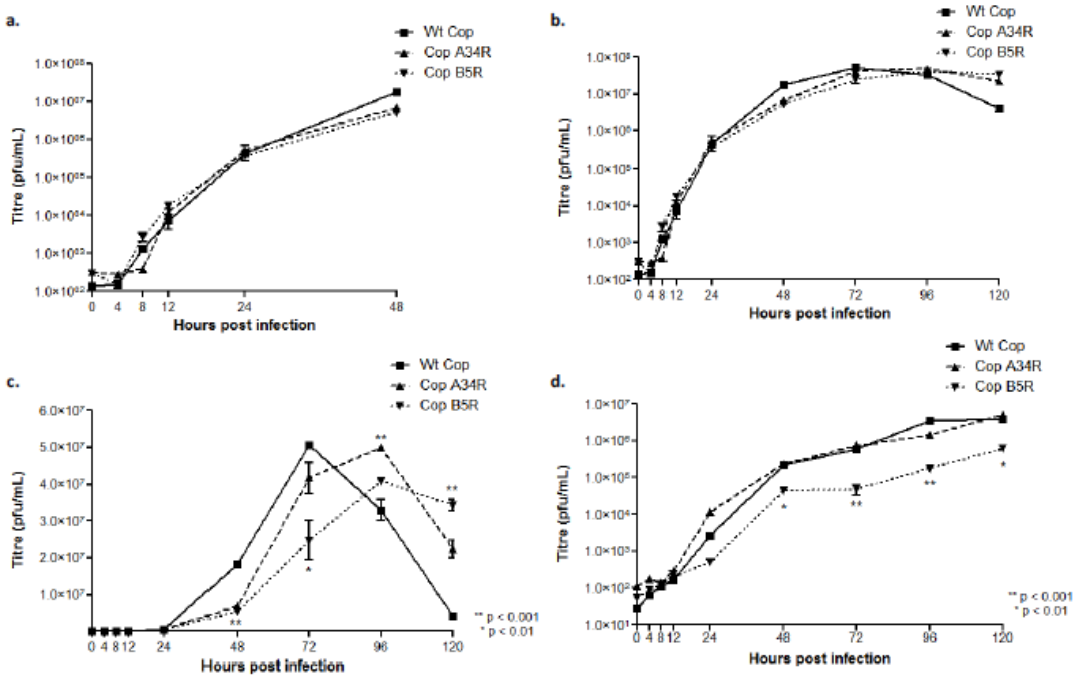
a.
Wt Cop
Cop A34R
Cop B5R
Titre (pfu/mL)
Hours post infection
b.
Wt Cop
Cop A34R
Cop B5R
Titre (pfu/mL)
Hours post infection
c.
Wt Cop
Cop A34R
Cop B5R
Titre (pfu/mL)
Hours post infection
** p < 0.001
* p < 0.01
d.
Wt Cop
Cop A34R
Cop B5R
Titre (pfu/mL)
Hours post infection
** p < 0.001
* p < 0.01

Figure 3.14. Biodistribution for wt Cop and A34R tissue distribution comparison. a) Balb/c mice were injected IV with 1e7 pfu wt Cop or Cop A34R. The brain, ovaries, spleen, kidney, liver, lungs and heart were excised at 1, 3, 5, and 7 dpi. Tissues were homogenized and titred. b) On day 1, viral distribution was greater in the wt Cop group. Delivery to the lungs was higher in the Cop A34R group. On day 3, replication in the ovaries was greater in the Cop A34R group. By day 7, both viruses were cleared below detectable levels. No enhancement to virulence or significant attenuation *in vivo* was observed as a result of the A34R mutation. c) Significant splenomegaly was demonstrated in the wt Cop group over the 7 day period indicating potential variability in immunostimulation. The dotted line signifies normal spleen mass. Error bars signify SEM, p-values were measured by unpaired, two-tailed T-test analysis.

a.

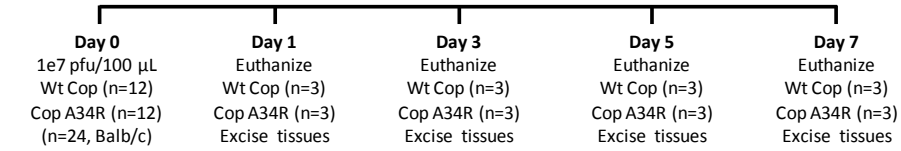
Day 0
1e7 pfu/100 µL
Wt Cop (n=12)
Cop A34R (n=12)
(n=24, Balb/c)
Day 1
Euthanize
Wt Cop (n=3)
Cop A34R (n=3)
Excise tissues
Day 3
Euthanize
Wt Cop (n=3)
Cop A34R (n=3)
Excise tissues
Day 5
Euthanize
Wt Cop (n=3)
Cop A34R (n=3)
Excise tissues
Day 7
Euthanize
Wt Cop (n=3)
Cop A34R (n=3)
Excise tissues

b.

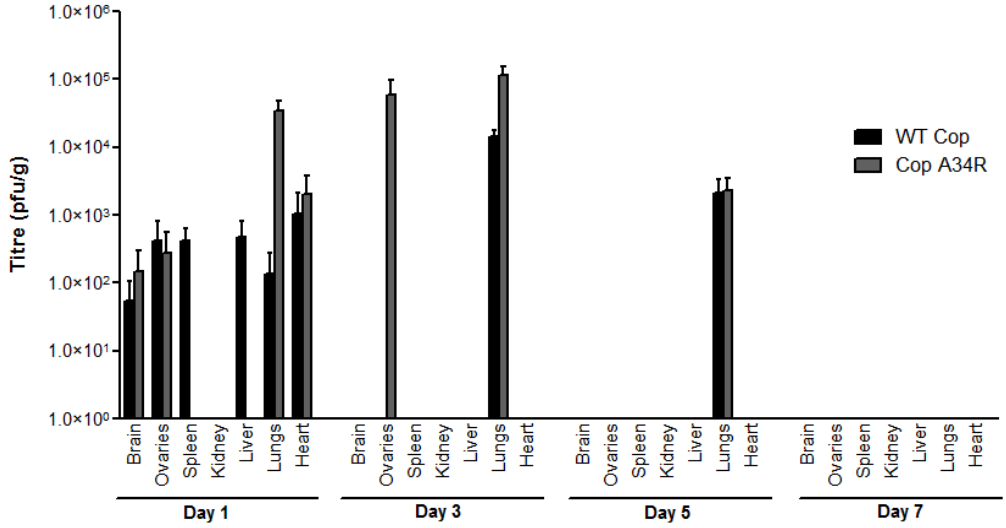
Titre (pfu/g)
1.0×10⁶
1.0×10⁵
1.0×10⁴
1.0×10³
1.0×10²
1.0×10¹
1.0×10⁰
WT Cop
Cop A34R
Brain
Ovaries
Spleen
Kidney
Liver
Lungs
Heart
Day 1
Day 3
Day 5
Day 7

c.

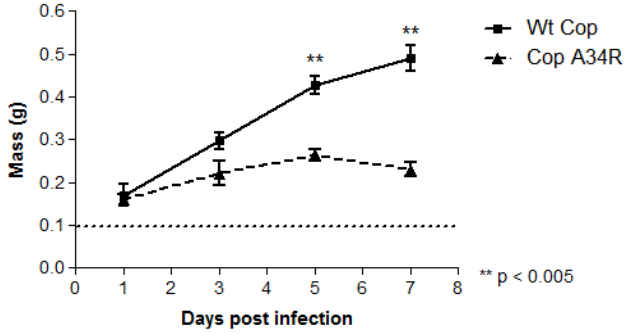
Mass (g)
0.0
0.1
0.2
0.3
0.4
0.5
0.6
0 1 2 3 4 5 6 7 8
Days post infection
Wt Cop
Cop A34R
**
**
** p < 0.005

compared with the only minor increases in spleen size seen in the Cop A34R group, indicating potential variability in immunostimulation profiles (Fig. 3.14c).

3.12 COP A34R DECREASES TUMOUR BURDEN TO A GREATER DEGREE THAN WT COP OR COP B5R

Virus release was assessed from CT-26-lacZ cells. Percent virus release was significantly enhanced in the Cop A34R infection when compared to the wt Cop and Cop B5R recombinant in this cell line (Fig. 3.15a). Total virus production was not significantly different between the viruses while the Cop A34R infection resulted in heightened levels of virus in the SN. (Fig. 3.15b). CT-26-lacZ cells were introduced IV into Balb/c mice for lung met seeding. On day 5, mice were treated IV with a suboptimal dose of virus (Fig 3.15c). Lung met count was significantly lower in the Cop A34R group, indicating enhanced spread between the mets due to EEV release (Fig 3.15d). All virus treatments brought about a significant decrease in met count compared to the PBS control. Spleen mass was used to assess degree of splenomegaly in each treatment condition. Wt Cop treatment induced a significantly higher increase in spleen size than the recombinant EEV enhanced viruses (Fig. 3.15e).

3.13 ENHANCED EEV SPREAD OCCURS IN THE FACE OF NEUTRALIZING ANTIBODIES

Balb/c mice were immunized with wt Cop IP twice over a four week period. CT-26-lacZ cells were then introduced for lung met seeding (Fig 3.16a). Neutralizing antibody level was assessed by western blot and it was demonstrated that before treatment the vaccinated group produced anti-wt Cop antibodies while the naïve group did not (Fig 3.16b). In the naïve group, lung met count was shown to be significantly decreased by the Cop A34R treatment when compared with the wt Cop group. The same pattern was demonstrated in the vaccinated group, but the difference between the wt Cop and Cop production was slightly

Figure 3.15. Suboptimal lung metastasis model. a) Virus release was assessed from CT-26-lacZ cells. Percent virus release was significantly enhanced in the Cop A34R condition when compared to the wt Cop and Cop B5R recombinant in this cell line. b) Total virus production was not significantly different between the viruses, while the Cop A34R infection resulted in heightened levels of virus in the SN. c) CT-26-lacZ cells were introduced IV into Balb/c mice for lung met seeding. On day 5, mice were treated IV with a suboptimal IV dose of virus. On day 13, lung mets were counted and spleen size was assessed. d) Met count was significantly lower in the Cop A34R group, indicating enhanced spread between the mets due to EEV release. All virus treatments brought about a significant decrease in met count compared to the PBS control. e) Spleen mass was used to assess degree of splenomegaly in each treatment condition. Wt Cop treatment induced a significantly higher increase in spleen size than the EEV enhanced viruses. Error bars signify SEM, p-values were measured by unpaired, two-tailed T-test analysis.

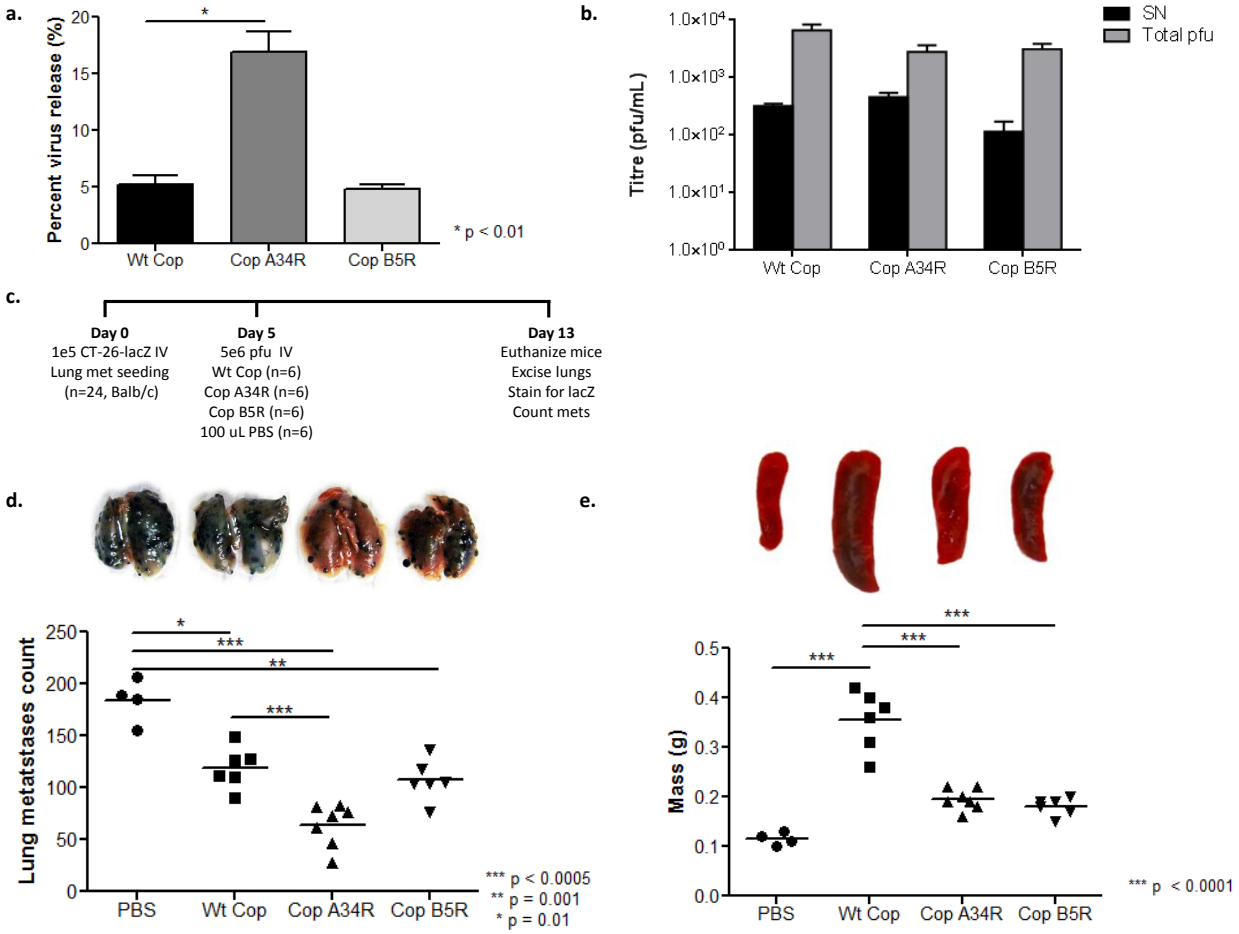
a.
Percent virus release (%)
20
15
10
5
0
*
Wt Cop
Cop A34R
Cop B5R
* p < 0.01
b.
Titre (pfu/mL)
1.0×10⁴
1.0×10³
1.0×10²
1.0×10¹
1.0×10⁰
SN
Total pfu
Wt Cop
Cop A34R
Cop B5R
c.
Day 0
1e5 CT-26-lacZ IV
Lung met seeding
(n=24, Balb/c)
Day 5
5e6 pfu IV
Wt Cop (n=6)
Cop A34R (n=6)
Cop B5R (n=6)
100 uL PBS (n=6)
Day 13
Euthanize mice
Excise lungs
Stain for lacZ
Count mets
d.
Lung metatstases count
250
200
150
100
50
0
*
***
**
***
PBS
Wt Cop
Cop A34R
Cop B5R
*** p < 0.0005
** p = 0.001
* p = 0.01
e.
Mass (g)
0.5
0.4
0.3
0.2
0.1
0.0
***
***
***
PBS
Wt Cop
Cop A34R
Cop B5R
*** p < 0.0001

Figure 3.16. Suboptimal vaccinated lung metastasis model. a) Balb/c mice were left naïve or were immunized with 1e7 pfu wt Cop IP, and boosted 2 weeks later. Two weeks post-vaccination, CT-26-lacZ cells were introduced for lung met seeding. b) Saphenous bleeds were taken on day 27 and a neutralizing antibody western blot was undertaken to demonstrate the presence of anti-VACV antibodies from the vaccinated group in comparison with the naïve group, pre-treatment. c) Lung met count was significantly decreased in the Cop A34R treated group when compared with the wt Cop group, indicating EEV spread in the face of anti-VACV antibodies. d) Spleen mass was measured to assess splenomegaly. Spleen size was significantly enhanced in the naïve group and was highest in the wt Cop treatment group. The same splenomegaly was not observed in the vaccinated group. p-values were measured by unpaired, two-tailed T-test analysis. Post-treatment antibody concentrations demonstrated e) slight production in the naïve wt Cop and Cop B5R groups and f) significant production in all virus treated animals of the vaccinated group. The wt Cop and Cop B5R appear to have more diverse antibody production as demonstrated by a greater number of bands.

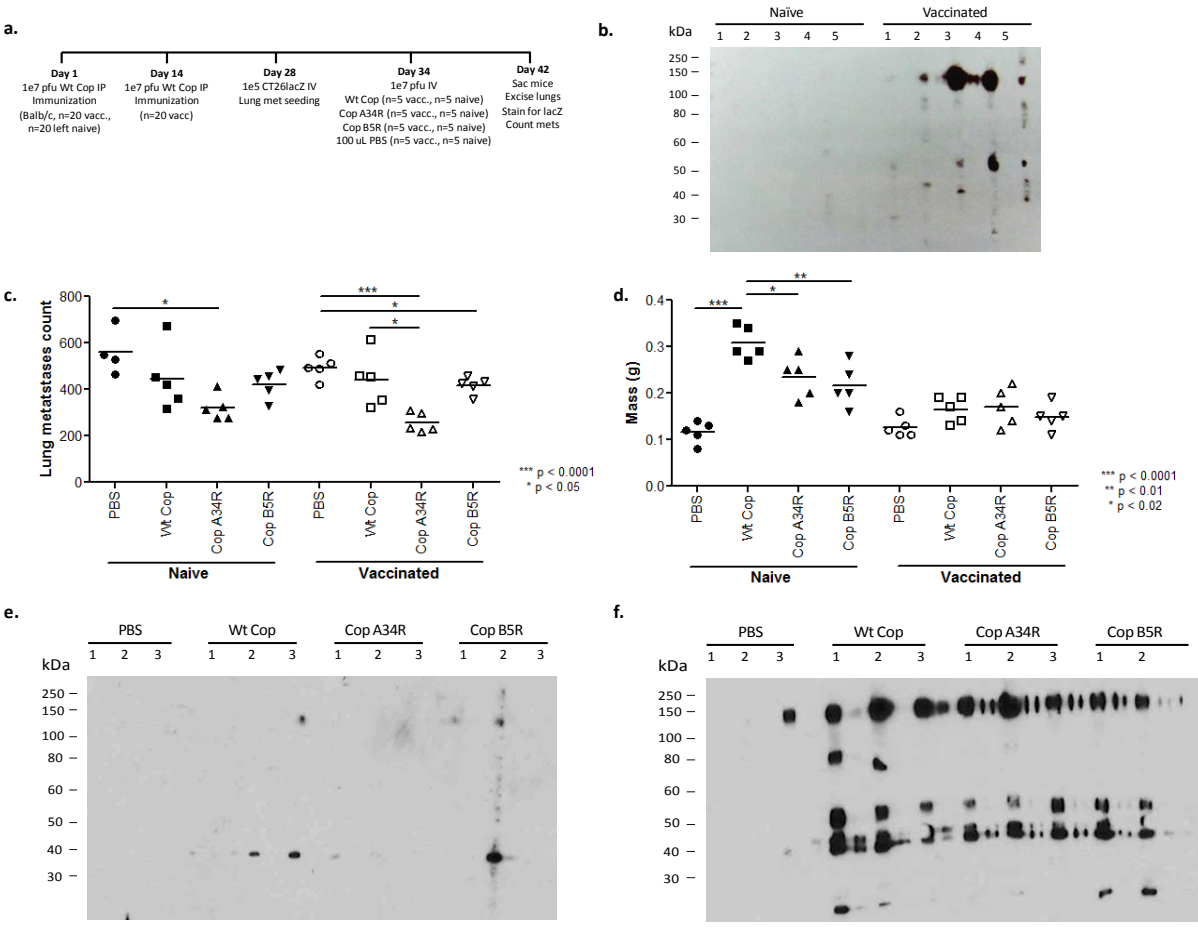
a.
Day 1
1e7 pfu Wt Cop IP
Immunization
(Balb/c, n=20 vacc., n=20 left naive)
Day 14
1e7 pfu Wt Cop IP
Immunization
(n=20 vacc)
Day 28
1e5 CT26lacZ IV
Lung met seeding
Day 34
1e7 pfu IV
Wt Cop (n=5 vacc., n=5 naive)
Cop A34R (n=5 vacc., n=5 naive)
Cop B5R (n=5 vacc., n=5 naive)
100 uL PBS (n=5 vacc., n=5 naive)
Day 42
Sac mice
Excise lungs
Stain for lacZ
Count mets
b.
Naïve
Vaccinated
kDa
1 2 3 4 5 1 2 3 4 5
250
150
100
80
60
50
40
30
c.
Lung metatstases count
800
600
400
200
0
PBS
Wt Cop
Cop A34R
Cop B5R
Naive
Vaccinated
*** p < 0.0001
* p < 0.05
d.
Mass (g)
0.4
0.3
0.2
0.1
0.0
*** p < 0.0001
** p < 0.01
* p < 0.02
e.
PBS
Wt Cop
Cop A34R
Cop B5R
kDa
1 2 3
250
150
100
80
60
50
40
30
f.
PBS
Wt Cop
Cop A34R
Cop B5R
kDa
250
150
100
80
60
50
40
30

larger and the wt Cop was more similar to the PBS group (Fig. 3.16c).

Spleen size was significantly enhanced in the naïve group and was highest in the wt Cop treatment group. The same splenomegaly was not observed in the vaccinated group. (Fig. 3.16d). Post-treatment antibody concentrations demonstrated slight production in the naïve wt Cop and Cop B5R groups and significant production in all virus treated animals in the vaccinated group (Fig. 3.16 e, f). The wt Cop and Cop B5R appear to have more diverse antibody production in the vaccinated group as demonstrated by a greater number of bands, at approximately 80 and 20 kDa for wt Cop and 20 kDa for Cop B5R (Fig 3.16f).

3.14 Cop A34R displayed enhanced spread in a preliminary distant xenograft tumour model

Virus release was assessed from U-87 cells. Percent virus release was significantly enhanced in the Cop A34R condition when compared to the wt Cop and Cop B5R recombinant in this cell line (Fig.3.17a). The total virus production was not significantly different between the viruses while the Cop A34R infection resulted in heightened levels of virus in the SN (Fig 3.17b). U-87 cells were introduced SQ into CD-1 nude mice for bilateral flank tumour seeding. On day 14, mice were treated IT with 5e7 pfu of wt Cop or Cop A34R (Fig 3.17c). Three dpi, both tumours were excised and titred. There were 2 logs more virus present in the uninjected tumour in the Cop A34R treated group than in the wt Cop treated group (Fig.3.17d).

3.15 Wt Cop infection results in significant immune recruitment to the spleen while Cop A34R infection results in greater WBC populations in the blood stream

In order to investigate the increased splenomegaly demonstrated in the wt Cop group when compared with the EEV mutants, Balb/c and C57Bl/6 mice were treated IV with 1e7

Figure 3.17. Preliminary distant tumour, xenograft model. a) Virus release was assessed from U-87 cells. Percent virus release was significantly enhanced from the Cop A34R infection when compared to the wt Cop and Cop B5R recombinant in this cell line. b) Total virus production was not significantly different between the viruses, while the Cop A34R infection resulted in heightened levels of virus in the SN. c) U-87 cells were introduced SQ into CD-1 nude mice for bilateral flank tumour seeding. On day 14, mice were treated IT with 5e7 pfu of Wt Cop or Cop A34R. On day 17, tumours were excised and titred. d) There were 2 logs more virus in the uninjected tumour of the Cop A34R treated group.

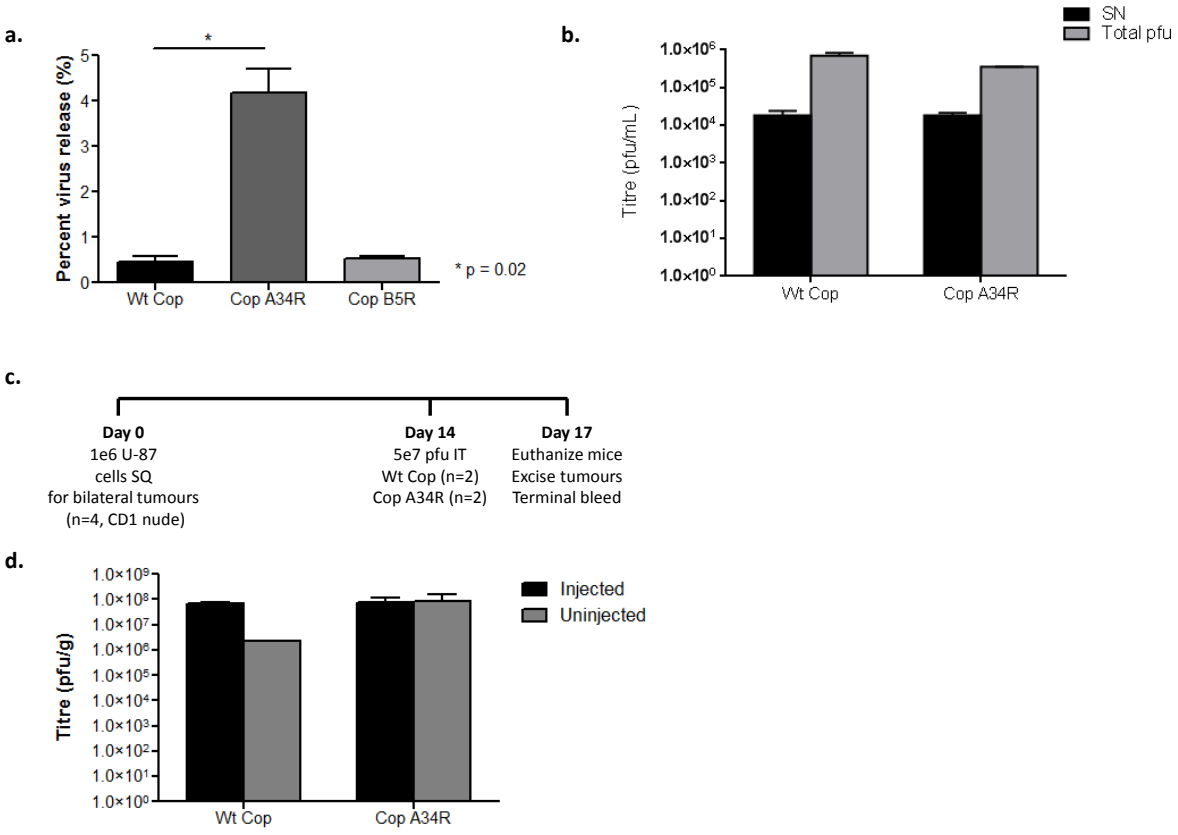
a.
Percent virus release (%)
0
1
2
3
4
5
*
* p = 0.02
Wt Cop
Cop A34R
Cop B5R
b.
SN
Total pfu
Titre (pfu/mL)
1.0×10⁰
1.0×10¹
1.0×10²
1.0×10³
1.0×10⁴
1.0×10⁵
1.0×10⁶
Wt Cop
Cop A34R
c.
Day 0
1e6 U-87
cells SQ
for bilateral tumours
(n=4, CD1 nude)
Day 14
5e7 pfu IT
Wt Cop (n=2)
Cop A34R (n=2)
Day 17
Euthanize mice
Excise tumours
Terminal bleed
d.
Titre (pfu/g)
1.0×10⁰
1.0×10¹
1.0×10²
1.0×10³
1.0×10⁴
1.0×10⁵
1.0×10⁶
1.0×10⁷
1.0×10⁸
1.0×10⁹
Injected
Uninjected
Wt Cop
Cop A34R

pfu wt Cop or Cop A34R (Fig. 3.18a, 3.19a). Both mouse species were investigated as each displays slightly different immunological profiles. The C57Bl/6 model has been demonstrated as having a more significant humoral response to infection while the Balb/c have been shown to induce a greater cellular response (58). In both models, spleen mass was shown to be increased in the wt Cop group (Fig. 3.18b, 3.19c) and total splenocyte white blood cell (WBC) count was significantly increased when compared with the Cop A34R treatment (Fig. 3.18c, 3.19d). WBC populations within the spleen were assessed by flow cytometry.

Splenocyte adaptive and innate population analysis demonstrated a trending increase in B-cell and innate populations in the Wt Cop treatment group (Fig. 3.18d,e 3.19e,f). Blood analysis demonstrated a trending increase in B-cell and NK cell populations as well as macrophages, granulocytes and DC cells in the Cop A34R treatment group (Fig. 3.18f,g, 3.19g,h). Virus delivery was assessed in the C57Bl/6 model by titration of the lungs and it was demonstrated that virus titre was similar between the two groups, indicating comparable dosing (Fig. 3.19b).

3.16 VACV-LCMV-GPG2 HAS THE EEV ENHANCED PHENOTYPE DERIVED FROM A SPONTANEOUS L151E MUTATION IN THE *A34R* GENE

The VACV recombinant, VACV-LCMV-gpG2, was created with the insertion of the glycoprotein gpG2 of the arenavirus lymphocytic choriomeningitis virus (LCMV) into the TK locus of the WR VACV backbone (92). It was created in 1988 and has been utilized for the immunostimulatory characterisation of LCMV glycoprotein epitopes. In this study, it was shown that VACV-LCMV-gpG2 spontaneously began forming comets on BSC-40 and U2-OS cells (Fig. 3.20a). Sequence analysis demonstrated a spontaneous mutation to the *A34R* gene, bringing about the L151E substitution and thereby conferring the enhanced EEV

Figure 3.18. Immunostimulatory analysis, Balb/c model. a) Balb/c mice were treated IV with 1e7 pfu wt Cop or Cop A34R and 4 dpi the spleens were excised and a cardiac puncture was conducted. b) Spleen mass was increased in the wt group and c) total splenocyte white blood cell (WBC) count was significantly increased when compared with the Cop A34R treatment. WBC populations within the spleen were assessed by flow cytometry. d) Splenocyte adaptive and c) innate population analysis demonstrated a trending increase in B-cell and innate populations in the wt Cop treatment group. f) Blood analysis demonstrated a trending increase in B-cell populations as well as g) macrophages and DC cells in the Cop A34R treated group. Cell populations were defined as follows: B cells (CD19+B220+), T_c cells (CD3+CD8+), T cells (CD3+CD8-), NKT cells (CD3+CD122+), NK cells (CD3-CD122+), Granulocytes (GR-1+CD11b+), Macrophages (F4/80+CD11b+), DC (CD11c+C440+, CD11c+CD8+). Error bars signify SEM, p-values were measured by unpaired, two-tailed T-test analysis.

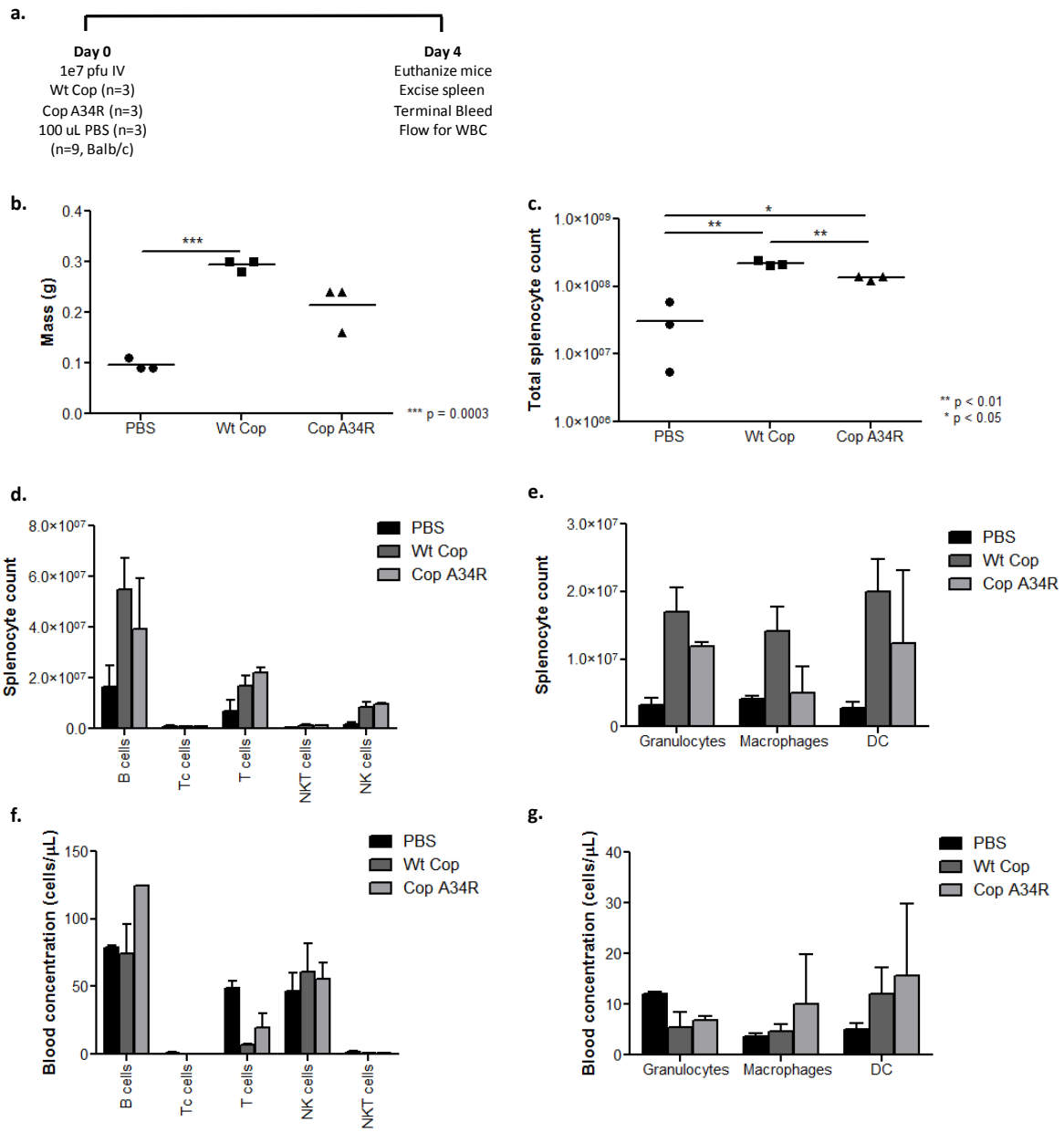
a.
Day 0
1e7 pfu IV
Wt Cop (n=3)
Cop A34R (n=3)
100 uL PBS (n=3)
(n=9, Balb/c)
Day 4
Euthanize mice
Excise spleen
Terminal Bleed
Flow for WBC
b.
Mass (g)
0.4
0.3
0.2
0.1
0.0
***
PBS
Wt Cop
Cop A34R
*** p = 0.0003
c.
Total splenocyte count
1.0×10^09
1.0×10^08
1.0×10^07
1.0×10^06
*
**
**
PBS
Wt Cop
Cop A34R
** p < 0.01
* p < 0.05
d.
Splenocyte count
8.0×10^07
6.0×10^07
4.0×10^07
2.0×10^07
0.0
PBS
Wt Cop
Cop A34R
B cells
Tc cells
T cells
NKT cells
NK cells
e.
Splenocyte count
3.0×10^7
2.0×10^7
1.0×10^7
0
PBS
Wt Cop
Cop A34R
Granulocytes
Macrophages
DC
f.
Blood concentration (cells/μL)
150
100
50
0
PBS
Wt Cop
Cop A34R
B cells
Tc cells
T cells
NK cells
NKT cells
g.
Blood concentration (cells/μL)
40
30
20
10
0
PBS
Wt Cop
Cop A34R
Granulocytes
Macrophages
DC

Figure 3.19. Immunostimulatory analysis, C57Bl/6 model. a) C57Bl/6 mice were treated IV with 1e7 pfu wt Cop or Cop A34R and 4 dpi the spleens were excised and cardiac punctures were conducted. b) The lungs were titred to assess delivery consistency and it was demonstrated that a comparable dose of virus was received by each group. c) Spleen mass was significantly increased in the wt group and c) total splenocyte WBC count was significantly increased when compared with the Cop A34R treatment. WBC populations within the spleen were assessed by flow cytometry. d) Splenocyte adaptive and c) innate population analysis demonstrated a significant increase in B-cell and macrophage populations in the wt Cop treatment group. f) Blood analysis demonstrated a trending increase in B-cell and NK cell populations as well as g) granulocytes in the Cop A34R treatment group. DC cells populations were assessed but were below detectable levels in this model (not shown). Cell populations were defined as follows: B cells (CD19+B220+), T_c cells (CD3+CD8+), T cells (CD3+CD8-), NKT cells (CD3+CD122+), NK cells (CD3-CD122+), Granulocytes (GR-1+CD11b+), Macrophages (F4/80+CD11b+), DC (CD11c+C440+, CD11c+CD8+). Error bars signify SEM, p-values were measured by unpaired, two-tailed T-test analysis.

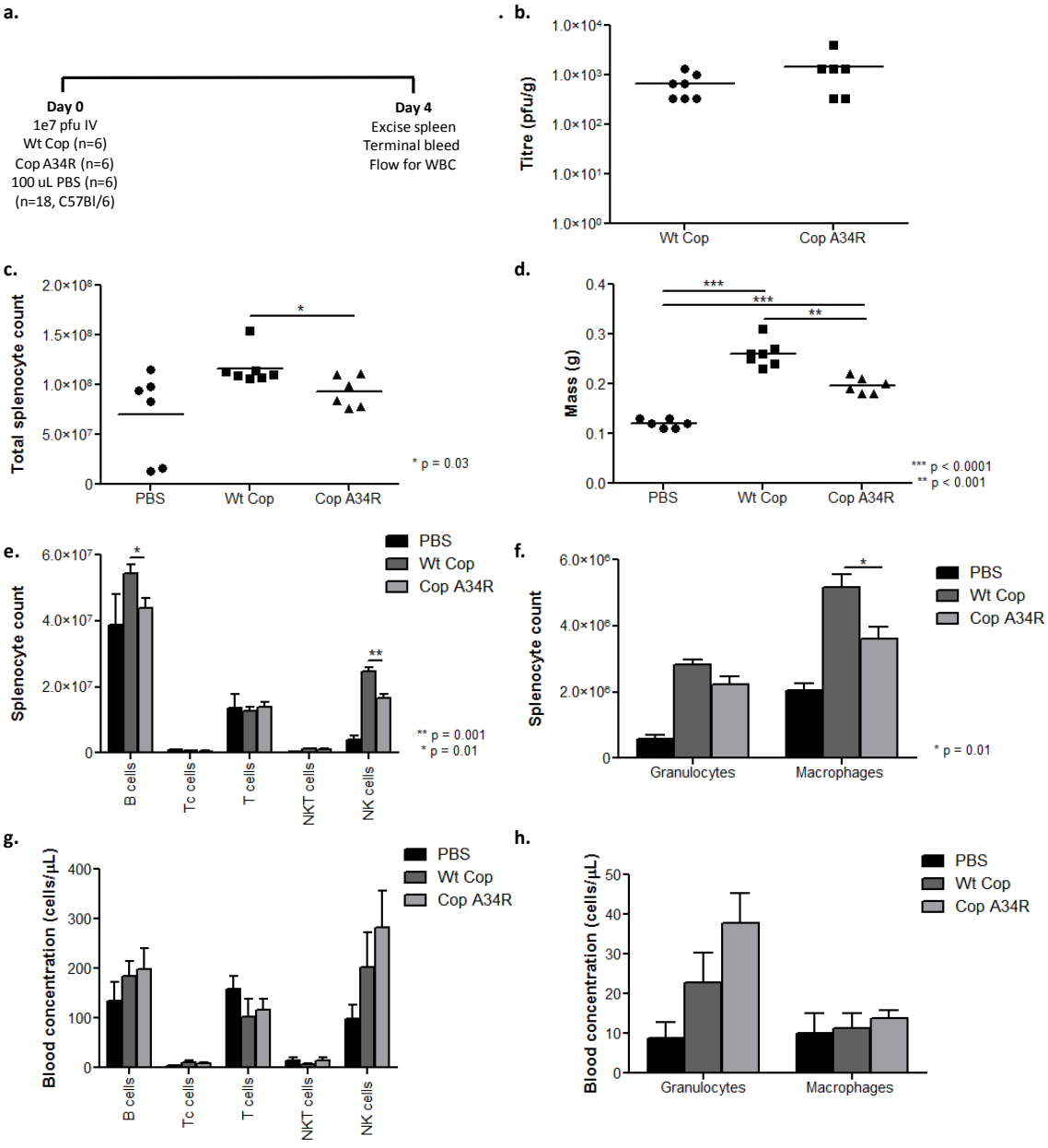
a.
Day 0
1e7 pfu IV
Wt Cop (n=6)
Cop A34R (n=6)
100 uL PBS (n=6)
(n=18, C57Bl/6)
Day 4
Excise spleen
Terminal bleed
Flow for WBC
b.
Titre (pfu/g)
1.0×10⁴
1.0×10³
1.0×10²
1.0×10¹
1.0×10⁰
Wt Cop
Cop A34R
c.
Total splenocyte count
2.0×10⁸
1.5×10⁸
1.0×10⁸
5.0×10⁷
0
*
* p = 0.03
PBS
Wt Cop
Cop A34R
d.
Mass (g)
0.4
0.3
0.2
0.1
0.0
***
***
**
*** p < 0.0001
** p < 0.001
PBS
Wt Cop
Cop A34R
e.
Splenocyte count
6.0×10⁷
4.0×10⁷
2.0×10⁷
0
*
**
** p = 0.001
* p = 0.01
PBS
Wt Cop
Cop A34R
B cells
Tc cells
T cells
NKT cells
NK cells
f.
Splenocyte count
6.0×10⁶
4.0×10⁶
2.0×10⁶
0
*
* p = 0.01
PBS
Wt Cop
Cop A34R
Granulocytes
Macrophages
g.
Blood concentration (cells/µL)
400
300
200
100
0
PBS
Wt Cop
Cop A34R
B cells
Tc cells
T cells
NKT cells
NK cells
h.
Blood concentration (cells/µL)
50
40
30
20
10
0
PBS
Wt Cop
Cop A34R
Granulocytes
Macrophages

Figure 3.20. Comet assay, VACV-LCMV-gpG2. a) The VACV recombinant, VACV-LCMV-gpG2 displays comet formation on BSC-40 and U2-OS cells when incubated with a liquid overlay. b) Sequence analysis demonstrated a spontaneous mutation to the *A34R* gene, bringing about the c) L151E substitution and thereby conferring the enhanced EEV releasing phenotype. d) Phylogenetic analysis of the *A34R* gene demonstrated a close relationship between VACV-LCMV-gpG2 and IHD-J. The maximum-likelihood method was utilized with the Tamura-Nei model of nucleotide substitution using Mega5 software.

a.

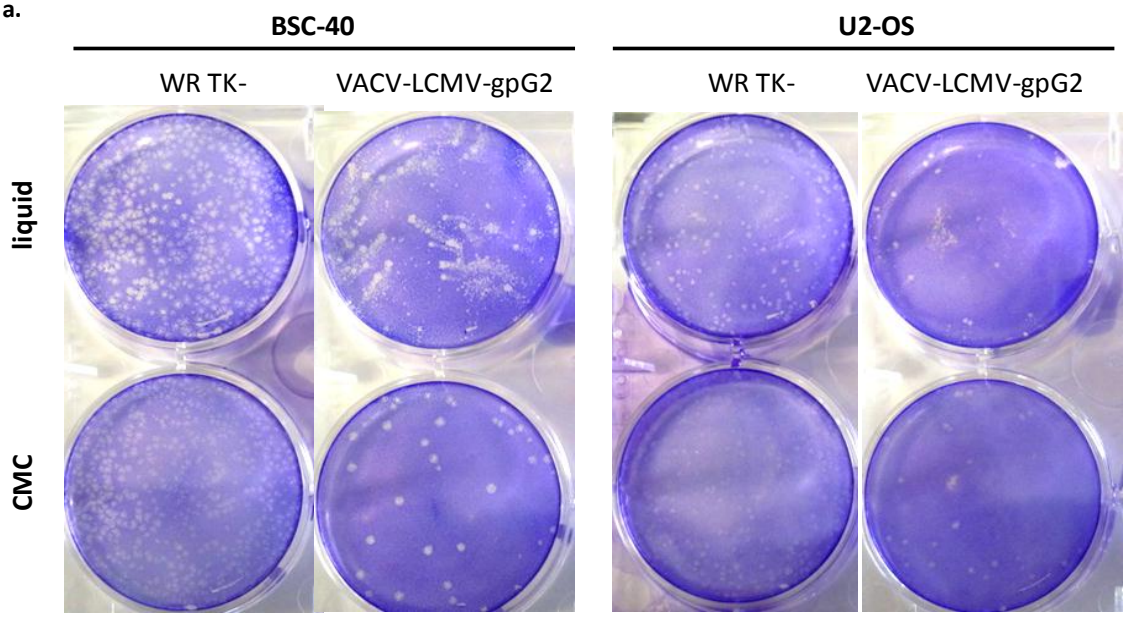

b.

```
                                                151
Wt Cop          TATACAAGTCTGGAAAACTGGTTAAAACAGTATGTAAAAGTAC
IHD-J           TATACAAGTCTGGAAAACTGGTTGAAACAGTATGTAAAAGTAC
Cop A34R        TATACAAGTCTGGAAAACTGGTTGAGACAGTATGTAAAAGTAC
VACV-LCMV-gpG2  TATACAAGTCTGGAAAACTGGTTGAAACAGTATGTAAAAGTAC
                                      * *
```

c.

```
                                                151
Wt Cop          LTNFKQLNSTTDAEACYIYKSGKLVKTVCKSTQSVLCVKKFYK
IHD-J           LTNFKQLNSTTDAEACYIYKSGKLVETVCKSTQSVLCVKKFYK
Cop A34R        LTNFKQLNSTTDAEACYIYKSGKLVETVCKSTQSVLCVKKFYK
VACV-LCMV-gpG2  LTNFKQLNSTTDAEACYIYKSGKLVETVCKSTQSVLCVKKFYK
                                              *
```

d.

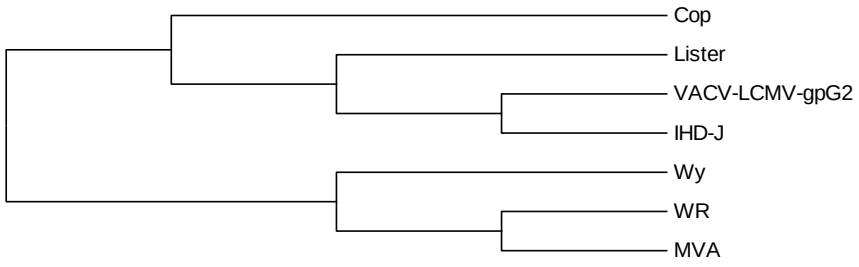

releasing phenotype (Fig. 3.20b, 3.20c). Intra-species phylogenetic analysis of the *A34R* gene demonstrated a close relationship between VACV-LCMV-gpG2 and IHD-J. The analysis also revealed a relative closeness of VACV-LCMV-gpG2 to wt Cop and Lister strains.

3.17 VIRUS RELEASE ENHANCEMENT FROM ABL TK OVER-EXPRESSING CELL LINE MDA-MB-231

MDA-MB-231human breast carcinoma cells have been previously shown to over-express active Abl TK (81). Virus release was significantly enhanced from this cell line in comparison with MCF-7 and HeLa cell lines, which have been shown to express lower levels of activated Abl TK (81) (Fig. 3.21a). Total virus production was decreased in this cell line, indicating potential growth attenuation as a result of enhanced release, likely due to an overall decrease in cell-to-cell spread (Fig. 3.21b).

3.18 VIRUS RELEASE ENHANCEMENT FROM ABL TK EXPRESSING TRANSFECTED CELL LINES

U2-OS and HeLa cells were transfected with v-Abl and with Bcr/Abl expression plasmids (Fig. 3.22). The YFP positive control was used as an indication of transfection efficiency. Virus release was then assessed 24 hours later and was shown to be enhanced in the Cop A34R infection group by v-Abl and Bcr/Abl expression (Fig. 3.22a, 3.22d). Total virus production was not significantly inhibited by the transfection, as demonstrated by comparison with untreated controls (Fig. 3.22b, 3.22e). Cell-to-cell spread was inhibited as a result of increased release, as demonstrated by smaller plaque size visualized by YFP expression (Fig. 3.22c, 3.22f).

Figure 3.21. Virus release assay in Abl TK over-expressing cell line MDA-MB-231. a) Virus released was significantly enhanced from the Abl TK over-expressing MDA-MB-231 cell line in comparison with the non-over-expressing MCF-7 and HeLa cell lines. b) Total virus production was decreased in this cell line indicating potential growth attenuation as a result of enhanced release. Error bars signify SEM; p-values were measured by unpaired, two-tailed T-test analysis.

a.

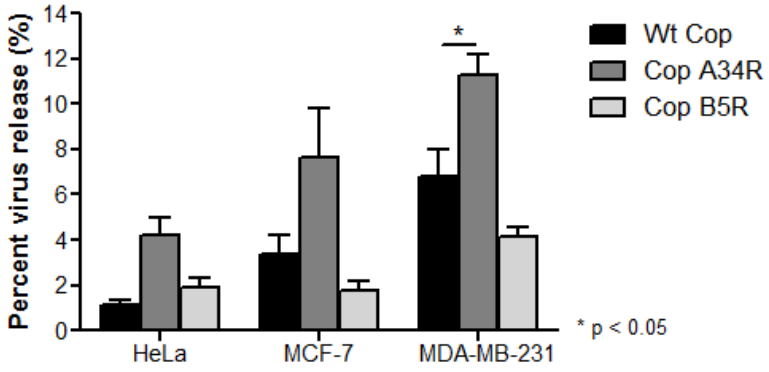
Percent virus release (%)
14
12
10
8
6
4
2
0
*
Wt Cop
Cop A34R
Cop B5R
* p < 0.05
HeLa
MCF-7
MDA-MB-231

b.

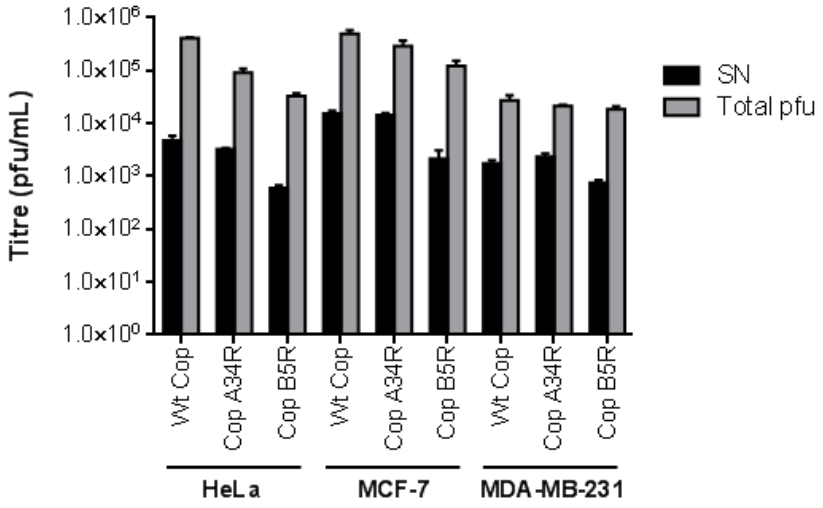
Titre (pfu/mL)
1.0x10^6
1.0x10^5
1.0x10^4
1.0x10^3
1.0x10^2
1.0x10^1
1.0x10^0
SN
Total pfu
Wt Cop
Cop A34R
Cop B5R
Wt Cop
Cop A34R
Cop B5R
Wt Cop
Cop A34R
Cop B5R
HeLa
MCF-7
MDA-MB-231

Figure 3.22. Virus release assay in Abl TK expressing transfected cell lines. a-c) U2-OS and d-f) HeLa cells were transfected with v-Abl or with Bcr/Abl expression plasmids. 24 hours later, the virus release assay was undertaken. a, d) Virus release was enhanced in the Cop A34R infection by v-Abl and Bcr/Abl expression. b, e) Total virus production was not significantly inhibited by the transfection, as demonstrated by comparison with untreated controls. c, f) Cell-to-cell spread was inhibited as a result of enhanced release as demonstrated by smaller plaque size visualized by YFP expression. The YFP positive control was used as an indication of transfection efficiency. Error bars signify SEM, p-values were measured by unpaired, two-tailed T-test analysis.

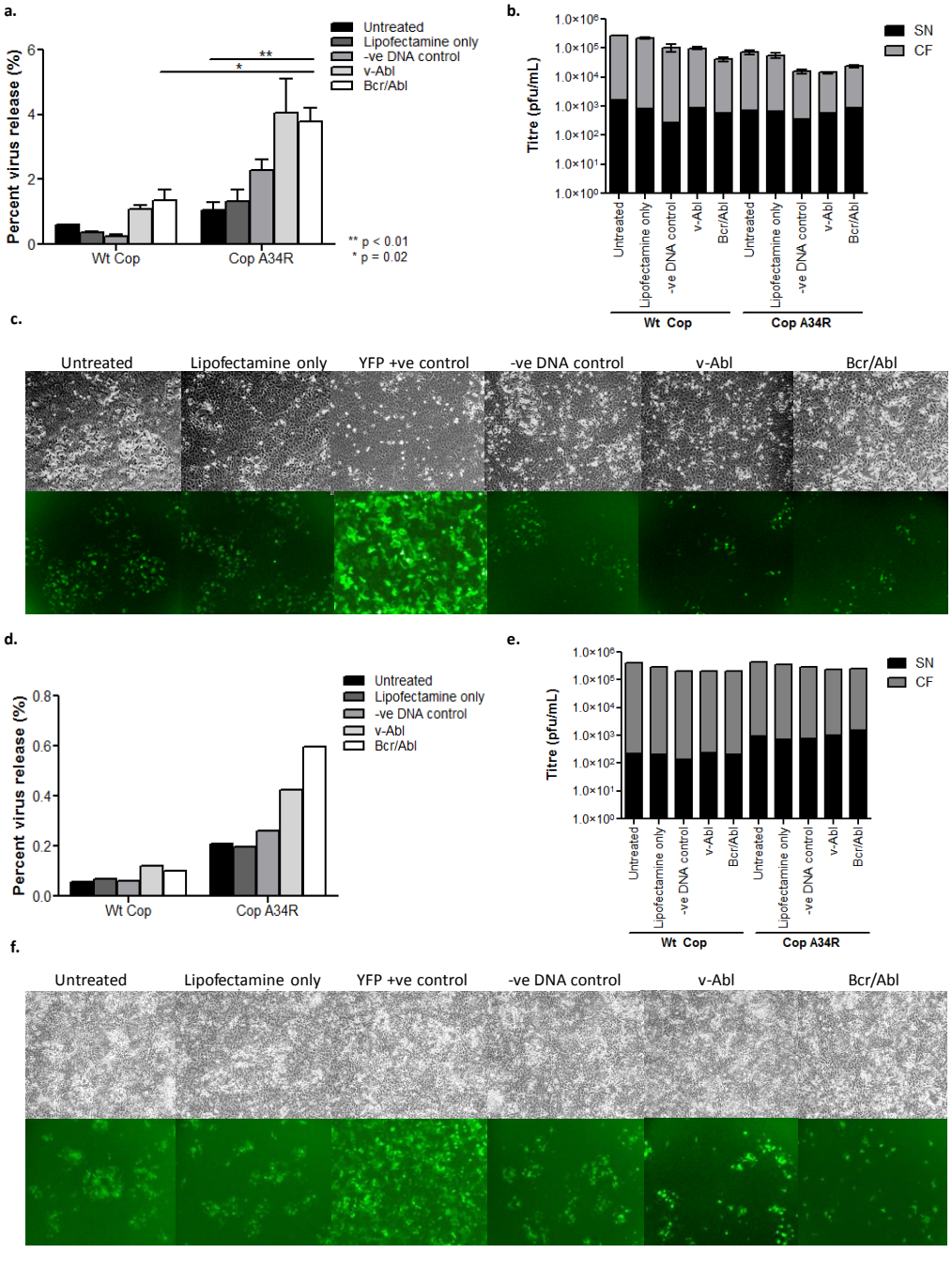
a.
Percent virus release (%)
Untreated
Lipofectamine only
-ve DNA control
v-Abl
Bcr/Abl
**
*
** p < 0.01
* p = 0.02
Wt Cop
Cop A34R
b.
Titre (pfu/mL)
SN
CF
Untreated
Lipofectamine only
-ve DNA control
v-Abl
Bcr/Abl
Wt Cop
Cop A34R
c.
Untreated
Lipofectamine only
YFP +ve control
-ve DNA control
v-Abl
Bcr/Abl
d.
Percent virus release (%)
Wt Cop
Cop A34R
e.
Titre (pfu/mL)
SN
CF
f.
Untreated
Lipofectamine only
YFP +ve control
-ve DNA control
v-Abl
Bcr/Abl

4. DISCUSSION

Enhancing mutations to EEV production during VACV replication were investigated as potential improvements to oncolytic efficiency. It was demonstrated that a mutation to the A34R envelope protein most significantly enhanced EEV release from the Cop VACV strain backbone. The Wy, WR and JX-594 backbones also displayed some enhancement to EEV release as a result of the A34R mutation, but release was significantly less efficient than that of the Cop backbone. In addition, intra-species phylogenetic analysis of the *A34R* gene revealed that the Cop strain is more closely related to the IHD-J strain than are Wy or WR. A mutation to the B5R envelope protein was also demonstrated to enhance EEV release *in vitro*, again to the greatest extent within the Cop backbone. The B5R mutation was less efficient in inducing enhanced viral spread than that of the A34R mutation. The A33R mutation was not observed to enhance EEV release. It was concluded that Cop A34R was the most effective EEV releasing combination.

Release from Cop A34R and Cop B5R was measured with the comet assay on cancer cell lines and both demonstrated enhanced viral spread when compared to the wt virus. Release was quantified with the virus release assay, wherein Cop A34R demonstrated the most significant enhancement in EEV production. Growth curves demonstrated that the Cop strain was the only of the four tested to not be significantly attenuated by the A34R mutation. Cop A34R infection was assessed *in vivo* in comparison with wt Cop in a biodistribution assay. Comparison of viral titres in various organs revealed no significant attenuation or enhancement to virulence, however Cop A34R seemed to reach or persist in the lungs and ovaries to a greater extent while the wt Cop infection was initially more widespread. In a lung metastasis cancer model, Cop A34R was shown to spread significantly more than the wt Cop or Cop B5R mutant, as demonstrated by a decreased number of metastases. This

decrease in lung tumour burden was also observed in the face of anti-Cop neutralizing antibodies. Viral spread *in vivo* was further shown to be enhanced in a preliminary, xenograft distant tumour model with a human cancer cell line.

The immunological profiles of the wt Cop and Cop A34R infections were variable. *In vitro,* Cop A34R EEV infection was limited by IFN action, resulting in a smaller plaque size in normal cells when compared with the wt Cop infection. *In vivo,* wt Cop induced a much more significant immune response than that of the EEV enhanced mutants, as measured by splenomegaly and flow cytometry of splenocytes. Following the analysis of neutralizing antibodies, the wt Cop infection was shown to result in a more diverse antibody production than that of Cop A34R. Finally, in a neutralizing anti-B5R antibody assay, Cop B5R EEV release was more highly neutralized than Cop A34R, which in contrast, seemed to be unexpectedly enhanced by the anti-B5R action.

In addition to the superior spreading capabilities observed by the artificially created A34R mutants, a recombinant VACV virus expressing an LCMV glycoprotein was shown to spontaneously produce significant EEV after years of serial passaging. After sequencing the *A34R* locus, VACV-LCMV-gpG2 was demonstrated to have spontaneously undergone the *A34R* L151E mutation, resulting in its enhanced spread *in vitro*. Phylogenetic analysis revealed that the *A34R* gene of VACV-LCMV-gpG2 was closely related to that of the IHD-J virus, which naturally encodes the A34R EEV enhancing mutation.

Abl TK action was also demonstrated to have an impact on EEV release. When naturally over-expressing activated Abl TK or when transfected with Abl TK expression plasmids, infected cells were shown to release significantly more virus than cancer cells that express normal Abl TK levels. This release was observed to be greater from the Cop A34R infection than that of wt Cop.

4.1 COP PROFICIENCY IN EEV RELEASE

The wt Cop VACV strain has been demonstrated to have a naturally enhanced potency when compared to wt Wy and wt WR, as demonstrated by heightened toxicity and quicker infection rates (41, 44). This enhanced virulence may partially explain the heightened efficiency in the spread and viral release of the Cop recombinants in comparison with the other strains. Furthermore, phylogenetic analysis revealed that the wt Cop *A34R* gene was more closely related to IHD-J than that of either other VACV strain. Therefore, there seems to be the potential that another locus within the gene predisposes the virus to a more enhanced viral release in response to the specific L151E mutation. Introducing the *A34R* gene into the Lister backbone may therefore be informative in relation to EEV release, as the phylogenetic analysis revealed it to be more closely related to Cop and IHD-J than are WR and Wy strains.

The potential impact of this theorized secondary locus may further explain the basis for the observation that the WR strain recombinants do not perform to the same extent as has been observed previously. Blasco *et al.* demonstrated that when the *A34R* gene of IHD-J is inserted into the *A34R* locus of WR, notated as WI, the highly enhanced EEV producing phenotype is conferred to this backbone (9, 43). The current study introduced only the specific point mutation into the *A34R* locus and the same levels of EEV production were not measured. It therefore seems likely another point in the gene may be required to attain the highest level of EEV release from the L151E mutation.

There are 5 nucleotide substitutions common to Cop and IHD-J that are not shared by the other strains, as well as one amino acid position common to Cop, IHD-J, Wy and VACV-LCMV-gpG2 (A34R N44) that is different from that of WR and MVA (A34R D44) (Fig. I.4). Mutagenic analysis of this site may demonstrate an impact on EEV release in

combination with the *A34R* L151E mutation.

In addition, Cop is the only backbone not attenuated by the A34R mutation. The growth inhibition observed within the other strains is thought to be due to a decrease in cell-to-cell spread, as a result of the enhanced release into the SN and lack of actin tail recruitment. The evolutionary closeness and sequence similarity of wt Cop to IHD-J may also account for this difference, as IHD-J growth has been demonstrated to be similar to that of other wt VACV strains (55). In addition, the overall growth kinetics of wt Cop infection are more rapid than that of wt WR and wt Wy (44), potentially compensating for the decrease in cell-to-cell spread. The basis for the enhanced potency of Cop in comparison with other VACV strains has yet to be investigated.

4.2 SUPERIOR PERFORMANCE OF THE A34R MUTATION IN EEV PRODUCTION

The *A34R* L151E mutation outperformed the EEV release levels and overall growth capabilities of the B5R P189S recombinants. The A34R mutation was naturally occurring in IHD-J strain, while the B5R mutation occurred under laboratory induced growth pressure, suggesting that the A34R mutation may function in a more intrinsic manner for spread while the B5R mutation was compensatory when necessary. Furthermore, it has been observed previously that IHD-J is more efficient than other VACV strains in the wrapping of IMV at the TGN site (56). It seems possible that the *A34R* L151E mutation affects not only release but overall CEV/EEV production by enhancing the enveloping process. The *B5R* P189S mutation seems likely to only affect release at the cell surface site, as shown by a complete lack of actin tail formation (38). This enhances the release process by reducing the interaction of CEV with the cell membrane and preventing its propulsion into neighbouring cells. The proportion of EEV liberated is thereby enhanced, but the total amount produced may not be affected. This may therefore explain the basis for the enhanced efficiency of the

A34R mutation in comet production and virus release when compared to the B5R recombinants.

The *A33R* c-terminus truncation did not result in enhanced EEV production in this study, as was observed previously by Katz *et al.* (37, 38). In the preceding studies, the mutation was induced by selective growth pressures brought on by the deletion of A36R. The envelope proteins A34R, A33R and B5R were then sequenced and the EEV enhanced phenotype was attributed to the c-terminus truncation observed in *A33R* (38). It seems possible that a secondary mutation had also occurred at another locus and was involved in the EEV releasing phenotype, but was not sequenced. A full genome sequencing of the original A33R mutant may reveal another mutation required to confer the EEV enhancing phenotype.

4.3 Immunological Implications of A34R and B5R Mutations

The anti-B5R antibody had an unexpected effect on wt Cop and Cop A34R plaque formation. This antibody effectively neutralized the comet formation of Cop B5R, as it bound the B5R epitope and neutralized viral spread and infection in the SN. In the Cop A34R as well as the wt Cop infections, the highest concentrations of the antibody seemed to enhance comet formation. This is theorized to be due to its interaction with B5R at the cell surface site. In binding the B5R epitope, the antibody may weaken the envelope protein's interaction with the cell surface, potentially allowing the virion to be released more easily. The potency of the Cop infection and the shrouding effect of the envelope may then allow some comet formation in the face of the neutralizing antibodies. In the case of Cop B5R, the interaction with the cell membrane at the B5R site is likely already weakened, due to the P189S mutation, therefore the antibody has no effect on enhancing release and neutralization is seen to a greater extent.

The IFN-β treatment revealed a neutralizing effect on EEV infection in normal cells. When untreated, Cop A34R infection was more widespread and diffuse than the wt Cop infection, however when the cells were treated with IFN-β 16 hours pre-infection, the effect of EEV spread was lost. The plaque size was also smaller in the Cop A34R infection, likely due to a diminished cell-to-cell spread, and the infection by the EEV particles appears to have been lost. It seems that the cell-to-cell spread is more efficient in infection than is EEV fusion in IFN treated cells. This indicates that EEV spread within normal tissues may be highly inhibited by the anti-viral IFN pathways, though spread is highly sustained in the investigated cancer cell lines. The impact of IFN-β on EEV infection will need to be quantified and assessed at physiological levels in normal and cancer cell lines in order to fully evaluate this effect, but it seems likely this correlation may confer a higher safety profile to the A34R mutant as well as explain aspects of its unique immunogenic profile.

In vivo, it was demonstrated several times that the wt Cop infection resulted in significant splenomegaly while the infection of the EEV enhanced mutants did not. It seems possible this may be a result of a combination of varying biological characteristics. Primarily, the recombinant viruses produce more EEV in the early infection stage, which are shrouded from the immune system by the cellular-derived envelope. In contrast, the release of IMV in the initial wt Cop infection is likely quicker, as a consequence of greater cell-to-cell infection or a quicker lysis due to greater IMV production, resulting in a more rapid immunogenic stimulation. The Cop A34R infection and cell lysis may be initially slower, as more IMV is likely to be wrapped in the TGN, and more of the progeny are then able to evade the immune system longer. The heightened immunoevasive capabilities of EEV may therefore partially explain the variable immunostimulatory profile observed.

Secondarily, it seems possible that the wt Cop is able to infect normal, IFN-

responsive tissues to a greater extent than the EEV mutants. This may result in a larger, more widespread initial infection by wt Cop, as demonstrated by the biodistribution assays. If the Cop A34R is more highly attenuated in normal tissues, due to IFN inhibition of EEV infection, the immune response will be blunted in comparison with the wt Cop infection. This may account for the variability in splenomegaly and immunostimulation profiles demonstrated in this study. Flow cytometry analysis revealed that the wt Cop infection results in a large recruitment of WBCs to the spleen, whereas the blood stream contained a higher WBC recruitment during the Cop A34R infection. It seems likely that the EEV virions are better able to spread out of the normal tissues into the blood where they initiate immune stimulation but infection is limited in the normal tissue, precluding the same splenocytic stimulation seen during the wt Cop infection.

The Cop A34R recombinant also seems to spread better in the face of neutralizing antibodies, as established by greater infection of lung metastases. Neutralizing antibody analysis demonstrated a diverse antibody profile brought about by the wt Cop infection when compared with Cop A34R in the vaccinated model at 6 dpi. It seems likely that the wt Cop infection produced more IMV early on, resulting in heightened antibody detection of the various IMV epitopes. EEV have fewer antigenic epitopes, potentially resulting in a more discrete antibody profile, as demonstrated by fewer bands in the neutralizing antibody western blot assay. The Cop B5R profile was intermediate between the wt Cop and Cop A34R suggesting it may be more immunogenic than Cop A34R. This may be due to the introduced alteration of B5R, the only immunogenic EEV antigen. Furthermore, in the unvaccinated mice, the wt Cop infection resulted in a measurable production of antibodies that was not detected by the Cop A34R infection and in only one case of the Cop B5R infection. This is indicative that the wt Cop infection is quicker in inducing antibody

production than are the EEV enhanced mutants. Further investigation and quantification of various neutralizing antibody titres in response to the Cop variant infections will need to be undertaken to fully characterize this relationship.

4.4 Potential of Cop and the *A34R* L151E Mutation in Cancer Treatment

The Cop backbone has proven to be exceptionally potent in cancer cell infection and destruction. The Cop A34R infection in cancer cell lines U2-OS and HeLa demonstrated enhanced EEV production and viral spread with little effect on viral growth or replication capabilities. The lack of attenuation of viral growth in cancer cells due to the mutation is suggestive of a potential use for the Cop backbone in cancer treatment, within an EEV enhanced oncolytic platform. Including the A34R mutation into an oncolytic candidate may elicit promising improvements to current standards.

The biodistribution assay revealed a higher sustained infection in the ovaries and an elevated titre of Cop A34R within the lungs when compared with the wt Cop infection. The infection of the ovaries is similar to infection at a tumour site, as ovaries replicate to a much higher degree than other tissue types and are believed to have leaky vasculature, making them a preferred site of infection for non-attenuated OVs. This higher infection level in the ovaries is indicative that the Cop A34R was better able to spread to a site of heightened cell-division and persist than was wt Cop. This data suggests that the A34R mutation may aid in enhancing viral spread and immunoevasion, allowing for sustained infection at distant sites.

The higher infection level in the lungs by Cop A34R on day 1 could be indicative of a heightened level of delivery during the initial infection. The primary site that the virus has a tendency to infect after IV delivery is the lungs, resulting in higher measured titres than other tissues in the biodistribution assays. The Cop A34R virus stock may have contained a higher level of EEV particles derived from the manufacturing process that enhanced the initial

delivery in its immunoevasive qualities. It was demonstrated that more than one freeze/thaw cycle is required to lyse all envelope membranes within a viral stock and allow for complete anti-IMV neutralization (Fig. III.1). It seems possible that EEV present in the initial IV dose allowed for an enhanced delivery, accounting for the higher viral titres within the lungs when compared with the wt Cop. This characteristic may therefore be favourable in its enhancement of initial dosing levels within an oncolytic therapy setting.

In the lung metastasis models, Cop A34R was able to decrease metastasis count to a much greater extent than wt Cop or Cop B5R. The heightened clearing of tumor burden is likely due to the enhanced spreading capability of the virus between metastasis sites. Although it is possible the viral delivery to the lungs is also enhanced due to EEV presence in the dose, one would predict that the delivery of Cop B5R to the lungs would be similar as EEV levels would be comparable. The Cop B5R treatment did not perform to the same extent as the Cop A34R treatment, indicating the impact of the enhanced delivery due to EEV alone cannot fully account for the decrease in lung met count. Enhanced spread between lung metastases was required for optimal tumour burden clearing.

In addition, the preliminary xenograft distant tumour model with the U-87 human glioblastoma cell line demonstrated enhanced intertumoural spread through the blood by Cop A34R when compared with the wt Cop infection. However, this model will need to be investigated on a larger scale to fully characterize the variability in distant viral spread from human cancer cells due to the EEV enhancing mutation.

Together, this study presents a promising enhancement to oncolytic VACV in the addition of the *A34R* L151E mutation and demonstrates the exceptional potential of the Cop backbone for use as an oncolytic candidate. The proficiency of infection, inter-metastasis spread and optimal delivery to the lungs may make this platform something to consider,

particularly for lung cancer treatment protocols.

4.5 Potential Enhancements to the Cop A34R Oncolytic Platform

The Cop A34R combination has proven to be the most efficient recombinant in EEV production, infection and growth. It was effective in clearing lung metastases, spreading between distant tumours as well as in the evasion of neutralizing antibodies and systemic immunostimulation when compared to the characteristics of wt Cop infection. It seems to infect normal tissues to a lesser extent due to IFN action, but retains its ability to spread effectively to rapidly-dividing cell sites. Together, this presents a very promising enhancement to the oncolytic platform, though the enhanced potency of the Cop backbone will need to be assessed on a safety level if it is to be used in human treatment.

In order to enhance the therapeutic safety profile and the tumour selectivity of the Cop backbone, a number of strategies may be undertaken for future oncolytic candidates. Primarily, the TK deletion can be assessed, as its use in JX-594 has demonstrated significant enhancement to infection selectivity for cancer cells. The VGF deletion may also be included to further enhance selectivity for rapidly dividing cells. The B18R truncation could enhance the safety profile by preventing the virus' anti-IFN mechanism, further inhibiting the growth of Cop A34R in normal tissues and targeting its infection in the tumour site. The impact of these attenuating mutations on overall EEV production will need to be assessed before utilization within this platform.

A safety switch could also potentially be included, in the addition of the HSV TK gene. If an uncontrolled infection were to occur in immunosuppressed individuals, treatment with acyclovir would halt viral growth and prevent any potential toxic implications of Cop replication. Finally, the inclusion of GM-CSF could enhance the patient's anti-tumour immunity and the addition of a pro-drug converting enzyme may aid in potentiating the

additive action of specific chemotherapeutics. Ultimately, a number of avenues can be taken to tailor the Cop A34R platform for optimal use in the treatment of human cancer.

4.6 VACV-LCMV-GP-G2

The VACV recombinant VACV-LCMV-gp-G2 was demonstrated to spontaneously take on the *A34R* L141E mutation. It seems likely that the large, bulky glycoprotein was affecting the movement of CEV/EEV during infection, creating a selective growth pressure. The virus may have mutated in response to this, allowing enhanced release to compensate for the presence of the glycoprotein. The spontaneous addition of *A34R* L151E demonstrates the virus' biological predisposition to enhancing spread from this site. This further supports the potential of this mutation on a biological level. Full genome sequencing should be undertaken to confirm the utilized backbone strain before direct comparison with experimental WR A34R.

4.7 THE IMPACT OF ABL TK ON VIRUS RELEASE

It was demonstrated in this study that the effects of Abl TK action may influence virus release and over-expression can result in the enhancement of egress into the SN. This relationship may be exploited in the treatment of Abl TK over-expressing cancers, such as invasive breast carcinomas. Spread between metastases may be further improved with the enhancement of EEV production by Abl TK action. This relationship may further be utilized on a virus manufacturing level. If significantly more virus could be released into the SN during viral replication, the isolation and purification of virus from the CF may not be required. This improvement could streamline the manufacturing process, allowing for the development of quicker and lower-cost protocols. Utilizing or creating an optimal cell line that over-expresses Abl TK in combination with infection by an EEV enhanced recombinant virus could therefore pose an important improvement for manufacturing purposes.

5. Concluding Remarks

The Cop A34R EEV enhanced mutant proved to be superior to wt VACV as well as other EEV enhanced recombinants in viral spread and immunoevasion. It was characterized as the only recombinant not to be attenuated by the introduced mutation. Furthermore, enhanced spread and viral release were observed in comparison with wt Cop during infection in various cancer cell lines. Cop A34R demonstrated an enhanced initial delivery to the tumour site and improved spread within a biodistribution model as well as elicited a significant decrease in tumour burden in a lung metastases model when compared with wt Cop. Cop A34R infection was limited by the addition of IFN to normal cells and a more discrete neutralizing antibody profile was observed from treated mice than that of the wt Cop infection. The EEV enhanced mutant was also able to spread and decrease tumour burden within the lungs in the face of neutralizing anti-VACV antibodies.

The Cop A34R platform may therefore represent a significant improvement to current oncolytic candidates in the enhancement of viral spread, delivery and immunoevasion. Safety measures will need to be evaluated in their ability to enhance virus selectivity to cancer cells in addition to their impact on EEV production. Generating future clinical products within the Cop A34R backbone may aid in the overcoming of current hurdles to oncolytic therapies.

REFERENCES

1. 2012. Canadian Cancer Statistics 2012. Canadian Cancer Society.

2. 2012. JX-929: Jennerex First-in-Class Targeted & Armed Poxviruses: Combined Virotherapy and Immunotherapy. Jennerex Biotherapeutics Inc. [Online.]

3. **Alcamí, A., J. A. Symons, and G. L. Smith.** 2000. The vaccinia virus soluble alpha/beta interferon (IFN) receptor binds to the cell surface and protects cells from the antiviral effects of IFN. Journal of Virology **74:**11230-11239.

4. **Aldaz-Carroll, L., J. C. Whitbeck, M. Ponce de Leon, H. Lou, L. Hirao, S. N. Isaacs, B. Moss, R. J. Eisenberg, and G. H. Cohen.** 2005. Epitope-mapping studies define two major neutralization sites on the vaccinia virus extracellular envelope virus glycoprotein B5R. Journal of Virology **79:**6260-6271.

5. **Appleyard, G., A. J. Hapel, and E. A. Boulter.** 1971. An Antigenic Difference between Intracellular and Extracellular Rabbitpox Virus. Journal of General Virology **13:**9-17.

6. **Behbehani, A. M.** 1983. The Smallpox Story: Life and Death of an Old Disease. Microbiological Reviews **47:**455-509.

7. **Bell, E., M. Shamim, J. C. Whitbeck, G. Sfyroera, J. D. Lambris, and S. N. Isaacs.** 2004. Antibodies against the extracellular enveloped protein virus B5R protein are mainly responsible for the EEV neutralizing capacity of vaccinia immune globulin. Virology **325:**425-431.

8. **Blasco, R., and B. Moss.** 1991. Extracellular vaccinia virus formation and cell-to-cell virus transmission are prevented by deletion of the gene encoding the 37,000-Dalton outer envelope protein. Journal of Virology **65:**5910-5920.

9. **Blasco, R., J. R. Sisler, and B. Moss.** 1993. Dissociated of progeny vaccinia virus from the cell membrane is regulated by a viral envelope glycoprotein: effect of a point mutation in the lectin homology domain of the A34R gene. Journal of Virology **67:**3319-3325.

10. **Breitbach, C. J., J. Burke, D. Jonker, J. Stephenson, A. R. Haas, L. Q. M. Chow, J. Nieva, T.-H. Hwang, A. Moon, R. Patt, A. Pelusio, F. L. Boeuf, J. Burns, L. Evgin, N. D. Silva, S. Cvancic, T. Robertson, J.-E. Je, Y.-S. Lee, K. Parato, J.-S. Diallo, A. Fenster, M. Daneshmand, J. C. Bell, and D. H. Kirn.** 2011. Intravenous delivery of a multi-mechanistic cancer-targeted oncolytic poxvirus in humans. Nature **477:**99-102.

11. **Breitbach, C. J., J. M. Paterson, C. G. Lemay, T. J. Falls, A. McGuire, K. A. Parato, D. F. Stojdl, M. Daneshmand, K. Speth, D. Kirn, J. A. McCart, H. Atkins, and J. C. Bell.** 2007. Targeted Inflammation During Oncolytic Virus Therapy Severely Compromises Tumor Blood Flow. Molecular Therapy **15:**1686-1693.

12. **Buller, R. M., G. L. Smith, K. Cremer, A. L. Notkins, and B. Moss.** 1985. Decreased virulence of recombinant vaccinia virus expression vectors is associated with a thymidine kinase-negative phenotype. Nature Medicine **317:**813-815.

13. **Buller, R. M. L., S. Chakrabarti, J.A. Cooper, D. R. Twardzik, and B. Moss.** 1988. Deletion of the vaccinia virus growth factor gene reduces virus virulence. Journal of Virology **62:**866-874.

14. **Cahill, D. P., K. W. Kinzler, B. Vogelstein, and C. Lengauer.** 1999. Genetic instability and darwinian selection in tumours. Trends in Cell Biology **9:**M57-M60.

15. **Chalikonda, S., M. H. Kivlen, M. E. O'Malley, X. D. E. Dong, J. A. McCart, M. C. Gorry, X. Y. Yin, C. K. Brown, H. J. Zeh, Z. S. Guo, and D. L. Bartlett.** 2008. Oncolytic virotherapy for ovarian carcinomatosis using a replication-selective vaccinia virus armed with a yeast cytosine deaminase gene. Cancer Gene Therapy **15:**115-125.

16. **Chin, L., W. C. Hahn, G. Getz, and M. Meyerson.** 2011. Making sense of cancer genomic data. Genes and Development **25:**534-555.

17. **Chiocca, E. A.** 2002. Oncolytic Viruses. Nature Reviews: Cancer **2:**939-950.

18. **Clercq, E. D.** 2002. Cidofovir in the treatment of poxvirus infections. Antiviral Research **55:**1-13.

19. **Colamonici, O. R., P. Domanski, S. M. Sweitzer, A. Larner, and R. M. Buller.** 1995. Vaccinia virus B18R gene encodes a type I interferon-binding protein that blocks interferon alpha transmembrane signaling. The Journal of Biological Chemistry **270:**15974-15978.

20. **Cundy, K. C., Z. H. Li, M. J. Hitchcock, and W. A. Lee.** 1996. Pharmacokinetics of cidofovir in monkeys. Evidence for a prolonged elimination phase representing phosphorylated drug. Drug Metabolism and Disposition **24:**738-744.

21. **Dranoff, G.** 2002. GM-CSF-based cancer vaccines. Immunological Reviews **188:**147-154.

22. **Dranoff, G., E. Jaffee, A. Lazenby, P. Golumbek, H. Levitsky, and K. Brose.** 1993. Vaccination with irradiated tumor cells engineered to secrete murine granulocyte-macrophage colony-stimulating factor stimulates potent, specific, and long-lasting anti-tumor immunity. PNAS USA **90:**3539-3543.

23. **Dranoff, G., and R. C. Mulligan.** 1994. Activities of granulocyte-macrophage colony-stimulating factor revealed by gene transfer and gene knockout studies. Stem Cells **12:**173-182.

24. **Duke-Cohan, J. S., K. Wollenick, E. A. Witten, M. S. Seaman, L. R. Baden, R. Dolin, and E. L. Reinherz.** 2009. The heterogeneity of human antibody responses to vaccinia virus revealed through use of focused protein arrays. Vaccine **27:**1154-1165.

25. **Duncan, S. A., and G. L. Smith.** 1992. Identification and characterization of an extracellular envelope glycoproteins affecting vaccinia virus egress. Journal of Virology **66:**1610-1621.

26. **Elion, G. B.** 1982. Mechanism of action and selectivity of acyclovir. The American Journal of Medicine **73:**7-13.

27. **Engelstad, M., and G. L. Smith.** 1993. The vaccinia virus 42-kDa envelope protein is required for the envelopment and egress of extracellular virus and for virus virulence. Virology **194:**627-637.

28. **Foloppe, J., J. Kintz, N. Futin, A. Findeli, P. Cordier, Y. Schlesinger, C. Hoffmann, C. Tosch, J. M. Balloul, and P. Erbs.** 2008. Targeted delivery of a suicide gene to human colorectal tumors by a conditionally replicating vaccinia virus. Gene Therapy **20:**1361-1371.

29. **Fyfe, J. A., P. M. Keller, P. A. Furman, R. L. Miller, and G. B. Elion.** 1978. Thymidine Kinase from Herpes Simplex Virus Phosphorylates the New Antiviral Compound, 9-(2-Hydroxyethoxymethyl)guanine. The Journal of Biological Chemistry **253:**8721-8727.

30. **Guo, Z. S., S. H. Thorne, and D. L. Bartlett.** 2008. Oncolytic virotherapy: Molecular targets in tumour selective replication and carrier cell-mediated delivery of oncolytic viruses. Biochimica et Biophysica Acta - Reviews on Cancer **1785:**217-231.

31. **Guse, K., V. Cerullo, and A. Hemminki.** 2011. Oncolytic vaccinia virus for the treatment of cancer. Expert Opinion on Biological Therapy **11:**595-608.

32. **Held-Warmkessel, J.** 2011. Complications. Nursing 2011**:**31-37.

33. **Hengstschläger, M., M. Knöfler, E. W. Müllner, E. Ogris, E. Wintersberger, and E. Wawra.** 1994. Different regulation of thymidine kinase during the cell cycle of normal versus DNA tumor virus-transformed cells. The Journal of Biological Chemistry **269:**13836-13842.

34. **Hernandez-Alcoceba, R.** 2011. Recent advances in oncolytic virus design. Clinical and Translational Oncology **13:**229-239.

35. **Husain, M., and B. Moss.** 2001. Vaccinia Virus F13L Protein with a Conserved Phospholipase Catalytic Motif Induces Colocalization of the B5R Envelope Glycoprotein in Post-Golgi Vesicles. Journal of Virology **75:**7528-7542.

36. **Jacobs, B. L., J. O. Langland, K. V. Kiblera, K. L. Denzlera, S. D. Whitea, S. A. Holecheka, ShukmeiWonga, T. Huynha, and C. R. Baskin.** 2009. Vaccinia virus vaccines: Past, present and future. Antiviral Research **84:**1-13.

37. **Katz, E., B. M. Ward, A. Weisberg, and B. Moss.** 2003. Mutations in the Vaccinia Virus A33R and B5R Envelope Proteins that Enhance Release of Extracellular Virions and Eliminate Formation of Actin Containing Microbilli without Preventing Tyrosin Phsophorylation of the A36R Protein. Journal of Virology **77:**12266-12275.

38. **Katz, E., E. J. Wolffe, and B. Moss.** 2002. Identification of Second-Site Mutations That Enhance Release and Spread of Vaccinia Virus. Journal of Virology **86:**11637-11644.

39. **Kim, J. H., J. Y. Oh, B. H. Park, D. E. Lee, J. S. Kim, H. E. Park, M. S. Roh, J. E. Je, J. H. Yoon, S. H. Thorne, D. Kirn, and T. H. Hwang.** 2006. Systemic Armed Oncolytic and Immunologic Therapy for Cancer with JX-594, a Targeted Poxvirus Expressing GM-CSF. Molecular Therapy **14:**361-370.

40. **Kirn, D., R. L. Martuza, and J. Zwiebel.** 2001. Replication-selective virotherapy for cancer: Biological principles, risk management and future directions. Nature Medicine **7:**781-787.

41. **Kirn, D. H., and S. H. Thorne.** 2009. Targeted and armed oncolytic poxviruses: a novel multi-mechanistic therapeutic class for cancer. Nature Reviews: Cancer **9:**64-71.

42. **Kirn, D. H., Y. Wang, F. L. Boeuf, J. Bell, and S. H. Thorne.** 2007. Targeting of Interferon-Beta to Produce a Specific, Multi-Mechanistic Oncolytic Vaccinia Virus. PLoS Medicine **4:**2001-2012.

43. **Kirn, D. H., Y. Wang, W. Liang, C. H. Contag, and S. H. Thorne.** 2008. Enhancing Poxvirus Oncolytic Effects through Increased Spread and Immune Evasion. Cancer Research **68:**2071-2075.

44. **Kretzschmar, M., J. Wallinga, P. Teunis, S. Xing, and R. Mikolajczyk.** 2006. Frequency of Adverse Events after Vaccination with Different Vaccinia Strains. PLoS Medicine **3:**1341-1351.

45. **Lee, J.-H., M.-S. Roh, Y.-K. Lee, M.-K. Kim, J.-Y. Han, B.-H. Park, P. Trown, D. H. Kirn, and T.-H. Hwang.** 2010. Oncolytic and immunostimulatory efficacy of a targeted oncolytic poxvirus expressing human GM-CSF following intravenous administration in a rabbit tumor model. Cancer Gene Therapy **17:**73-79.

46. **Liu, T.-C., T. Hwang, B.-H. Park, J. Bell, and D. H. Kirn.** 2008. The Targeted Oncolytic Poxvirus JX-594 Demonstrates Antitumoral, Antivascular, and Anti-HBV Activities in Patients With Hepatocellular Carcinoma. Molecular Therapy **16:**1637-1642.

47. **Liu, T.-C., and D. Kirn.** 2007. Systemic Efficacy with Oncolytic Virus Therapeutics: Clinical Proof-of-Concept and Future Directions. Cancer Research **67:**429-432.

48. **Lohr, L.** 2008. Chemotherapy-induced nausea and vomiting. Cancer Journal **14:**85-93.

49. **MacTavish, H., J.-S. Diallo, B. Huang, M. Stanford, F. L. Boeuf, N. D. Silva, J. Cox, J. G. Simmons, T. Guimond, T. Falls, J. A. McCart, H. Atkins, C. Breitbach, D. Kirn, S. Thorne, and J. C. Bell.** 2010. Enhancement of Vaccinia Virus Based Oncolysis with Histone Deacetylase Inhibitors. PLoS ONE **5:**1-9.

50. **Mathew, E., C. M. Sanderson, M. Hollinshead, and G. L. Smith.** 1998. The Extracellular Domain of Vaccinia Virus Protein B5R Affects Plaque Phenotype, Extracellular Enveloped Virus Release, and Intracellular Actin Tail Formation. Journal of Virology **72:**2429-2438.

51. **McCart, J. A., M. Puhlmann, J. Lee, Y. Hu, S. K. Libutti, H. R. Alexander, and D. L. Bartlett.** 2000. Complex interactions between the replicating oncolytic effect and the enzyme/prodrug effect of vaccinia-mediated tumor regression. Gene Therapy **7:**1217-1223.

52. **McCart, J. A., J. M. Ward, J. Lee, Y. Hu, H. R. Alexander, S. K. Libutti, B. Moss, and D. L. Bartlett.** 2001. Systemic Cancer Therapy with a Tumor-selective Vaccinia Virus Mutant Lacking Thymidine Kinase and Vaccinia Growth Factor Genes. Cancer Research **61:**8751-8757.

53. **McFadden, G.** 2005. Gleevec casts a pox on poxviruses. Nature Medicine **11:**711-712.

54. **McFadden, G.** 2005. Poxvirus Tropism. Nature Reviews: Microbiology **3:**201-213.

55. **McIntosh, A. A., and G. L. Smith.** 1996. Vaccinia Virus Glycoprotein A34R is Required for Infectivity of Extracellular Enveloped Virus. Journal of Virology **70:**272-281.

56. **Meiser, A., D. Boulanger, G. Sutter, and J. K. Locker.** 2003. Comparison of virus production in chicken embryo fibroblasts infected with the WR, IHD-J and MVA strains of vaccinia virus: IHD-J is most efficient in trans-Golgi network wrapping and extracellular enveloped virus release. Journal of General Virology **84:**1383-1392.

57. **Miller, J. D., R. G. v. d. Most, R. S. Akondy, J. T. Glidewell, S. Albott, D. Masopust, K. Murali-Krishna, P. L. Mahar, S. Edupuganti, S. Lalor, S. Germon, C. D. Rio, M. J. Mulligan, S. I. Staprans, J. D. Altman, M. B. Feinberg, and R. Ahmed.** 2008. Human Effector and Memory CD8+ T Cell Responses to Smallpox and Yellow Fever Vaccines. Immunity **28:**710-722.

58. **Morokata, T., J. Ishikawa, K. Ida, and T. Yamada.** 1999. C57BL/6 mice are more susceptible to antigen-induced pulmonary eosinophilia than BALB/c mice, irrespective of systemic T helper 1/T helper 2 responses. Immunology **98:**345-351.

59. **Moss, B.** 2006. Poxvirus entry and membrane fusion. Virology **344:**48-54.

60. **Newsome, T. P., I. Weisswange, F. Frishknecht, and M. Way.** 2006. Abl collaborates with Src family kinases to stimulate actin-based motility of vaccinia virus. Cellular Microbiology **8:**233-241.

61. **Panicali, D., and E. Paoletti.** 1982. Construction of poxviruses as cloning vectors: Insertion of the thymidine kinase gene from herpes simplex virus into the DNA of infectious vaccinia virus. PNAS USA **79:**4927-4937.

62. **Parato, K. A., D. Senger, P. A. J. Forsyth, and J. C. Bell.** 2005. Recent progress in the battle between oncolytic viruses and tumours. Nature Reviews: Cancer **5:**965-976.

63. **Payne, L. G.** 1980. Significance of Extracellular Enveloped Viris in the in vitro and in vivo Dissemination of Vaccinia. Journal of General Virology **50:**89-100.

64. **Prichard, M. N., K. A. Keith, M. P. Johnson, E. A. Harden, A. McBrayer, M. Luo, S. Qiu, D. Chattopadhyay, X. Fan, P. F. Torrence, and E. R. Kern.** 2007. Selective Phosphorylation of Antiviral Drugs by Vaccinia Virus Thymidine Kinase. Antimicrobial Agents and Chemotherapy **51:**1795-1803.

65. **Puhlmann, M., C. K. Brown, M. Gnant, J. Huang, S. K. Libutti, H. R. Alexander, and D. L. Bartlett.** 2000. Vaccinia as a vector for tumor-directed gene therapy: Biodistribution of a thymidine kinase-deleted mutant. Cancer Gene Therapy **7:**66-73.

66. **Pütz, M. M., C. M. Midgley, M. Law, and G. L. Smith.** 2006. Quantification of antibody responses against multiple antigens of the two infectious forms of Vaccinia virus provides a benchmark for smallpox vaccination. Nature Medicine **12:**1310-1315.

67. **Raguz, S., and E. Yague.** 2008. Resistance to chemotherapy: new treatments and novel insights into an old problem. British Jounral of Cancer **99:**387-391.

68. **Reeves, P. M., B. Bommarius, S. Lebeis, S. McNulty, J. Christensen, A. Swimm, A. Chahroudi, R. Chavan, M. B. Feinberg, D. Veach, W. Bornmann, M. Sherman, and D. Kalman.** 2005. Disabling poxvirus pathogenesis by inhibition of Abl-family tyrosine kinases. Nature Medicine **11:**731-739.

69. **Roberts, K. L., and G. L. Smith.** 2008. Vaccinia virus morphogenesis and dissemination. Trends in Microbiology **16:**472-479.

70. **Roper, R. L., E. J. Wolffe, A. Weisberg, and B. Moss.** 1998. The Envelope Protein Encoded by the A33R Gene Is Required for Formation of Actin-Containing Microvilli and Efficient Cell-to-Cell Spread of Vaccinia Virus. Journal of Virology **72:**4192-4204.

71. **Rubartelli, A., and M. T. Lotza.** 2007. Inside, outside, upside down: damage-associated molecular-pattern molecules (DAMPs) and redox. Trends in Immunology **28:**429-436.

72. **Sanderson, C. M., F. Frischknecht, M. Way, M. Hollinshead, and G. L. Smith.** 1998. Roles of vaccinia virus EEV-specific proteins in intracellular actin tail formation and low pH-induced cell-cell fusion. Journal of General Virology **79:**1415-1425.

73. **Seet, B. T., J. B. Johnston, H. Everett, C. Cameron, J. Spyula, S. H. Nazarian, A. Lucas, and G. McFadden.** 2003. Poxviruses and Immune Evasion. Annual Review of Immunology **21:**377-423.

74. **Shanafelt, A. B., K. E. Johnson, and R. A. Kastelein.** 1991. Identification of critical amino acid residues in human and mouse granulocyte-macrophage colony-stimulating factor and their involvement in species specificity. The Journal of Biological Chemistry **266:**13804-13810.

75. **Shen, Y., and J. Nemunaitis.** 2004. Fighting Cancer with Vaccinia Virus: Teaching New Tricks to an Old Dog. Molecular Therapy **11:**181-195.

76. **Shida, H.** 1986. Nucleotide sequence of the vaccinia virus hemaglutinin gene. Virology **150:**451-462.

77. **Smith, G. L.** 1999. Vaccinia virus immune evasion. Immunology Letters **65:**55-62.

78. **Smith, G. L., and B. Moss.** 1983. Infectious poxvirus vectors have capacity for at least 25 000 base pairs of foreign DNA. Gene **25:**21-28.

79. **Smith, G. L., and A. Vanderplasschen.** 1998. Extracellular enveloped vaccinia virus: entry, egress and evasion. Plenum Press, New York.

80. **Smith, G. L., A. Vanderplasschen, and M. Law.** 2002. The formation and function of extracellular enveloped vaccinia virus. Journal of General Virology **83:**2915-1931.

81. **Srinivasan, D., and R. Plattner.** 2006. Activation of Abl tyrosine kinases promotes invasion of aggressive breast cancer cells. Cancer Research **66:**5648-5655.

82. **Tamura, K., D. Peterson, N. Peterson, G. Strecher, M. Nei, and S. Kumar.** 2011. MEGA5: Molecular Evolutionary Genetics Analysis using Maximum Likelihood, Evolutionary Distance, and Maximum Parsimony Methods. Molecular Biology and Evolution **28:**2731-2739.

83. **Thorne, S. H., T.-H. H. Hwang, W. E. O'Gorman, D. L. Bartlett, S. Sei, F. Kanji, C. Brown, J. Werier, J.-H. Cho, D.-E. Lee, Y. Wang, J. Bell, and D. H. Kirn.** 2007. Rational strain selection and engineering creates a broad-spectrum, systemically effective oncolytic poxvirus, JX-963. The Journal of Clinical Investigation **117:**3350-3358.

84. **Tucker, W. E.** 1982. Preclinical toxicology profile of acyclovir: An overview. The American Journal of Medicine **73:**27-30.

85. **Tzahar, E., J. D.Moyer, H. Waterman, E. G.Barbacci, J. Bao, G. Levkowitz, M. Shelly, S. Strano, R. Pinkas-Kramarski, J. H.Pierce, G. C.Andrews, and Y. Yarden.** 1998. Pathogenic poxviruses reveal viral strategies to exploit the ErbB signaling network. The EMBO Journal **17:**5948-5963.

86. **Vaha-Koskela, M. J. V., J. E. Heikkila, and A. E. Hinkkanen.** 2007. Oncolytic viruses in cancer therapy. Cancer Letters **254:**178-216.

87. **Vanderplasschen, A., M. Hollinshead, and G. L. Smith.** 1997. Antibodies against vaccinia virus do not neutralize extracellular enveloped virus but prevent virus release from infected cells and comet formation. Journal of General Virology **78:**2041-2048.

88. **Vanderplasschen, A., E. Mathew, M. Hollinshead, R. B. Sim, and G. L. Smith.** 1998. Extracellular enveloped vaccinia virus is resistant to complement because of incorporation of host complement control proteins into its envelope. PNAS USA **95:**7544-7549.

89. **Vanderplasschen, A., E. Mathew, M. Hollinshead, R. B. Sim, and G. L. Smith.** 1998. Intracellular and extracellular vaccinia virions enter cells by different mechanisms. Journal of General Virology **79:**877-887.

90. **Vijaysri, S., G. Jentarra, M. C. Heck, A. A. Mercer, C. J. McInnes, and B. L. Jacobs.** 2008. Vaccinia viruses with mutations in the E3L gene as potential replication-competent, attenuated vaccines: intra-nasal vaccination. Vaccine **26:**664-676.

91. **Ward, B. M., A. S. Weisberg, and B. Moss.** 2003. Mapping and Functional Analysis of Interaction Sites within the Cytoplasmic Domains of the Vaccinia Virus A33R and A36R Envelope Proteins. Journal of Virology **77:**4113.

92. **Whitton, J. L., J. R. Gebhard, H. Lewicki, A. Tishon, and M. B. Oldstone.** 1988. Molecuclar definition of a major cytotoxic T-lymphocyte epitope in the glycoprotein of lymphocytic choriomeningitis virus. Journal of Virology **62:**687-695.

93. **Willey, J. M., L. M. Sherwood, and C. J. Woolverton.** 2008. Microbiology, 7 ed. McGraw-Hill, New York.

94. **Wittek, R.** 2006. Vaccinia immune globulin: current policies, preparedness, and product safety and efficacy. International Journal of Infectious Disease **10:**193-201.

95. **Wolffe, E. J., E. Katz, A. Weisberg, and B. Moss.** 1997. The A34R Glycoprotein Gene is Required for Induction of Specialized Actin Tail-Containing Microvilli and Efficient Cell-to-Cell Transmission of Vaccinia Virus. Journal of Virology **71:**3904-3915.

96. **Zhu, J., J. Martinez, X. Huang, and Y. Yang.** 2007. Innate immunity against vaccinia virus is mediated by TLR2 and requires TLR-independent production of IFN-β Blood **109:**619-625.

CONTRIBUTIONS OF COLLABORATORS

Laura Evgin, Dr. Fabrice Le Boeuf and Dr. Jiahu Wang designed and created the recombinant plasmids for the insertion of *A34R* L151E, *B5R* P189S and *A33R* c-term truncation mutations into wt VACV.

Dr. Chris Storbeck created the Cop A34R recombinant.

Theresa Falls and Christiano Tanese de Souza performed all *in vivo* injections.

Laura Evgin aided in performing the western blot of Fig. 3.16b.

Kieran Woulfe aided in preparing the samples for the biodistribution of Fig. 3.1.

APPENDIX I

Figure I.1. *A34R* L151E recombinant sequencing. Sequencing results from A34R recombinants in comparison with the wt VACV backbone sequence. a) Nucleotide and b) protein analysis revealed the A34R L151E mutation was conferred to all four backbones.

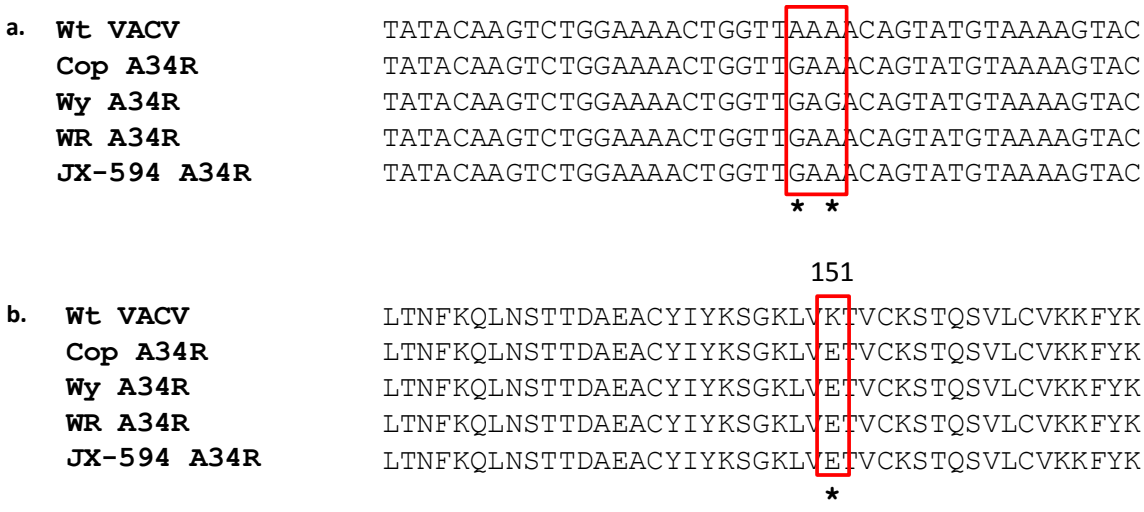
a.
Wt VACV TATACAAGTCTGGAAAACTGGTTAAAACAGTATGTAAAAGTAC
Cop A34R TATACAAGTCTGGAAAACTGGTTGAAACAGTATGTAAAAGTAC
Wy A34R TATACAAGTCTGGAAAACTGGTTGAGACAGTATGTAAAAGTAC
WR A34R TATACAAGTCTGGAAAACTGGTTGAAACAGTATGTAAAAGTAC
JX-594 A34R TATACAAGTCTGGAAAACTGGTTGAAACAGTATGTAAAAGTAC
* *
151
b.
Wt VACV LTNFKQLNSTTDAEACYIYKSGKLVKTVCKSTQSVLCVKKFYK
Cop A34R LTNFKQLNSTTDAEACYIYKSGKLVETVCKSTQSVLCVKKFYK
Wy A34R LTNFKQLNSTTDAEACYIYKSGKLVETVCKSTQSVLCVKKFYK
WR A34R LTNFKQLNSTTDAEACYIYKSGKLVETVCKSTQSVLCVKKFYK
JX-594 A34R LTNFKQLNSTTDAEACYIYKSGKLVETVCKSTQSVLCVKKFYK
*

Figure I.2. *B5R* P189S recombinant sequencing. Sequencing results from B5R recombinants, in comparison with the wt VACV backbone sequence. a) Nucleotide and b) protein analysis revealed the B5R P189S mutation was conferred to all four backbones.


a.
Wt VACV TCATGTCAACAAAAATGTGATATGCCGTCTCTATCTAATGGAT
Cop B5R TCATGTCAACAAAAATGTGATATGTCTTCTCTATCTAATGGAT
Wy B5R TCATGTCAACAAAAATGTGATATGTCTTCTCTATCTAATGGAT
WR B5R TCATGTCAACAAAAATGTGATATGTCTTCTCTATCTAATGGAT
JX-594 B5R TCATGTCAACAAAAATGTGATATGTCTTCTCTATCTAATGGAT
* *
189
b.
Wt VACV GASYISCTANSWNVIPSCQQKCDMPSLSNGLISGSTFSIGGVI
Cop B5R GASYISCTANSWNVIPSCQQKCDMSSLSNGLISGSTFSIGGVI
Wy B5R GASYISCTANSWNVIPSCQQKCDMSSLSNGLISGSTFSIGGVI
WR B5R GASYISCTANSWNVIPSCQQKCDMSSLSNGLISGSTFSIGGVI
JX-594 B5R GASYISCTANSWNVIPSCQQKCDMSSLSNGLISGSTFSIGGVI
*

Figure I.3. *A33R* c-terminus truncation recombinant sequencing. Sequencing results from A33R recombinants in comparison with the wt VACV backbone sequence. a) Nucleotide and b) protein analysis revealed the A33R c-term truncation was conferred to the Cop and Wy backbones.

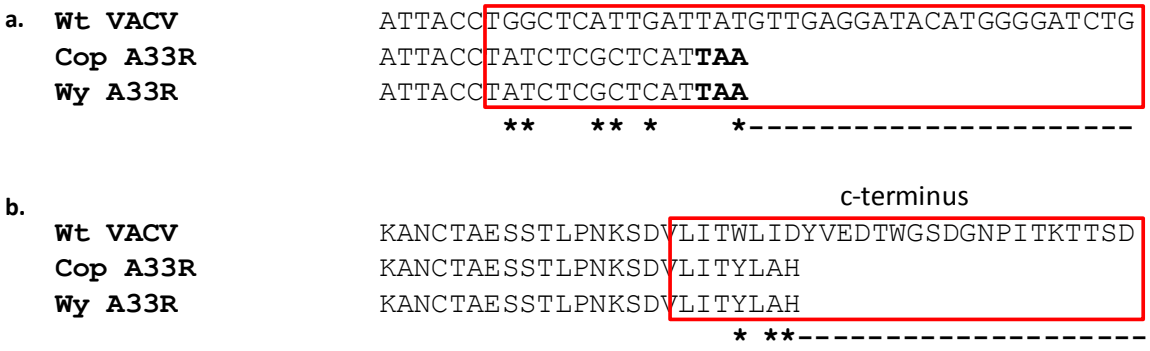
a.
Wt VACV ATTACCTGGCTCATTGATTATGTTGAGGATACATGGGGATCTG
Cop A33R ATTACCTATCTCGCTCATTAA
Wy A33R ATTACCTATCTCGCTCATTAA
** ** * *----------
b.
c-terminus
Wt VACV KANCTAESSTLPNKSDVLITWLIDYVEDTWGSDGNPITKTTSD
Cop A33R KANCTAESSTLPNKSDVLITYLAH
Wy A33R KANCTAESSTLPNKSDVLITYLAH
* **----------

Figure I.4. A34R protein sequence analysis; various strains. Sequence comparison of the *A34R* gene from the various VACV strains, demonstrating an amino acid substitution at position 44. Wt Cop, Wy, IHD-J and VACV-LCMV-gp-G2 encode asparagine (N) at this site while WR and MVA encode aspartic acid (D).

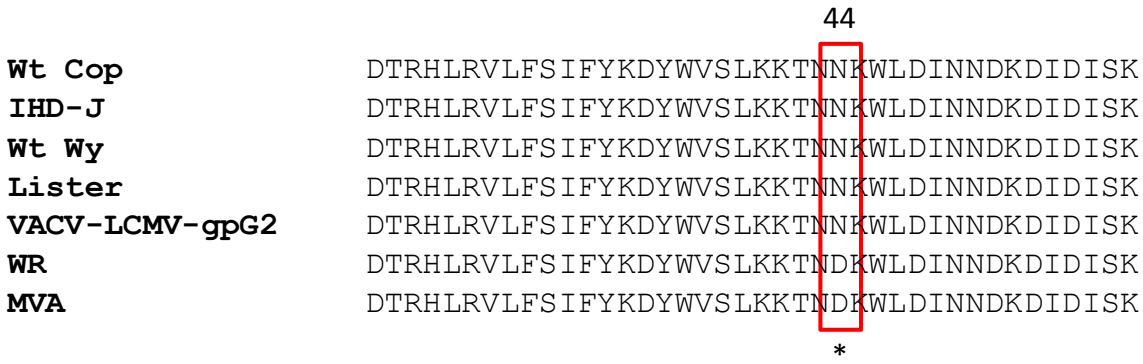
44
Wt Cop DTRHLRVLFSIFYKDYWVSLKKTNNKWLDINNDKDIDISK
IHD-J DTRHLRVLFSIFYKDYWVSLKKTNNKWLDINNDKDIDISK
Wt Wy DTRHLRVLFSIFYKDYWVSLKKTNNKWLDINNDKDIDISK
Lister DTRHLRVLFSIFYKDYWVSLKKTNNKWLDINNDKDIDISK
VACV-LCMV-gpG2 DTRHLRVLFSIFYKDYWVSLKKTNNKWLDINNDKDIDISK
WR DTRHLRVLFSIFYKDYWVSLKKTNDKWLDINNDKDIDISK
MVA DTRHLRVLFSIFYKDYWVSLKKTNDKWLDINNDKDIDISK
*

APPENDIX II

Figure II.1. Supplemental comet assay on U2-OS cells, 90 hpi. Comet formation was assessed on U2-OS at 90 hpi. Comet formation is visible by Cop A34R.

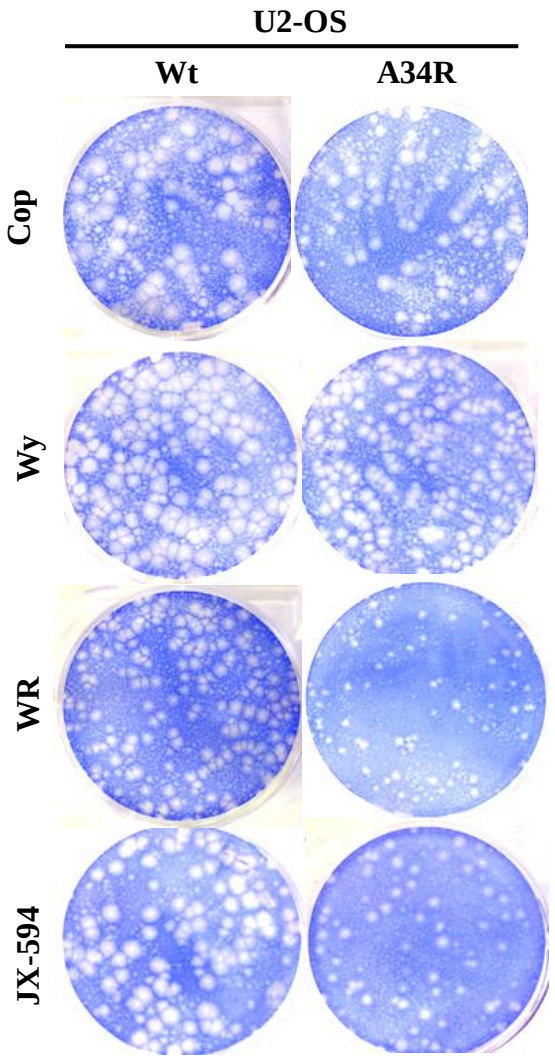
U2-OS
Wt
A34R
Cop
Wy
WR
JX-594

APPENDIX III

Figure III.1. EEV freeze/thaw analysis. L1R neutralization of IMV revealed the proportion of EEV membranes remaining after subsequent freeze/thaw cycles. More than one cycle is required to lyse all EEV membranes within a viral stock.

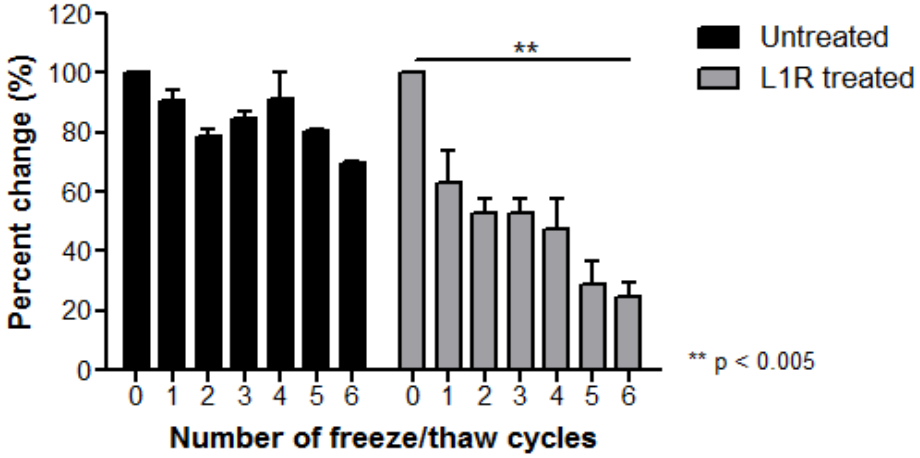
120
100
80
60
40
20
0
Percent change (%)
**
Untreated
L1R treated
** p < 0.005
0 1 2 3 4 5 6 0 1 2 3 4 5 6
Number of freeze/thaw cycles

AIMÉE N. LAPORTE

EDUCATION

2010 – 2012 **M.Sc. Biochemistry**
Collaborative program in Human and Molecular Genetics
Department of Biochemistry, Microbiology and Immunology
University of Ottawa, Ottawa, Ontario.
Thesis: *Enhancing the oncolytic efficiency of vaccinia virus by mutagenic augmentation of EEV production*
Supervisor: Dr. John C. Bell

2006 – 2010 **B.Sc.(Hons.) Life Sciences**
Subject of Specialization in Cancer Research
Department of Pathology and Molecular Medicine
Queen's University, Kingston, Ontario.
Thesis (2009-2010): *Examining the role of the leukemic oncoprotein E2A-PBX1 in apoptosis and lineage reassignment of pre-B cells*
Supervisor: Dr. David P. LeBrun

RESEARCH EXPERIENCE

2010 – 2012 **Centre for Innovative Cancer Research**,
Ottawa Hospital Research Institute, *Ottawa, Ontario*
- Graduate work, Department of Biochemistry, University of Ottawa
- Developed novel oncolytic viruses for cancer therapy

2009 – 2010 **Queen's University Cancer Research Institute,** *Kingston, Ontario*
- Undergraduate honour's work, Department of Pathology and Molecular Medicine, Queen's University
- Investigated the role of a chromosomal translocation in the linage assignment of leukocyte pre-cursors

2009 **University of Guelph,** *Guelph, Ontario*
- Undergraduate NSERC USRA, Department of Pathobiology, Ontario Veterinary College, University of Guelph
- Undertook the genomic sequencing and mutagenic analysis of the oncogenic retrovirus ENTV with Dr. Sarah K. Wootton

2008 **Royal Military College of Canada,** *Kingston, Ontario*
- Undergraduate NSERC USRA, Department of Chemistry and Chemical Engineering, Royal Military College of Canada
- Investigated the anti-apoptotic properties of select human cardiac genes utilizing recombinant yeast cells with Dr. Michael T. Greenwood

AWARDS & SCHOLARSHIPS

2012	**Ontario Graduate Scholarship (OGS)** (Declined) *University of Ottawa, Ottawa, Ontario*
2012	**Biochemistry, Immunology and Microbiology Symposium, 1st place** ($100) Oral seminar *University of Ottawa, Ottawa, Ontario*
2011 – 2012	**Ontario Graduate Scholarship (OGS)** ($15 000) *University of Ottawa, Ottawa, Ontario*
2010 – 2012	**Excellence Admission Scholarship** ($15 000) *University of Ottawa, Ottawa, Ontario*
2010 – 2011	**Ontario Graduate Scholarship (OGS)** ($15 000) *University of Ottawa, Ottawa, Ontario*
2009	**Student Leadership and Research Program Symposium, 1st place** ($100) Poster presentation *University of Guelph, Guelph, Ontario*
2009	**NSERC Undergraduate Student Research Award (USRA)** ($5 600) *University of Guelph, Guelph, Ontario*
2008	**NSERC Undergraduate Student Research Award (USRA)** ($5 600) *Royal Military College of Canada, Kingston, Ontario*
2006 – 2010	**Dean's Honour List** *Queen's University, Kingston, Ontario*
2006 – 2010	**Queen Elizabeth II Aiming for the Top** ($13 500) *Queen's University, Kingston, Ontario*
2006	**Queen's University Excellence Scholarship** ($2 500) *Queen's University, Kingston, Ontario*

REFEREED PUBLICATIONS

Drew Williams, Grant Norman, Chamel Khoury, Naomi Metcalfe, Jennie Briard, **Aimee Laporte**, Sara Sheibani, Craig Mandato and Michael T. Greenwood. (2011) Evidence for a second messenger function of dUTP during Bax mediated apoptosis of yeast and mammalian cells. *Biochemica et Biophysia Acta – Molecular Cell Research*. 1813(2):315-321.

Scott R. Walsh, Nicolle M. Linnerth-Petrik, **Aimee N. Laporte**, Paula I. Menzies, Robert A. Foster, Sarah K. Wootton. (2010). Full-length genome sequence analysis of enzootic nasal tumor virus reveals an unusually high degree of genetic stability. *Virus Research.* 151:74-87.

PATENTS AND INTELLECTUAL PROPERTY RIGHTS

Patent filed March 2012: *Recombinant Orf Virus*. John Bell, Julia Rintoul, **Aimee Nicole Laporte**, Monica Komar. PAT 6738W-90 US.

PUBLISHED ABSTRACTS

Aimée N. Laporte, Chris Storbeck, Laura Evgin, Fabrice Le Boeuf, John C. Bell. (2012). Enhancing the Oncolytic Efficiency of Vaccinia Virus by Mutagenic Augmentation of EEV Production. XIX International Poxvirus, Asfarvirus and Iridovirus Conference. Salamanca, 2012. Vectors, Vaccines and Antivirals. P8-18, pp 272.

Aimée N. Laporte & Sarah K. Wootton. (2009). Mutational analysis of the transforming domain of the enzootic nasal tumour virus envelope protein. *Studies by Undergraduate Researchers at Guelph*. 3(1):67-68.

CONFERENCES & PRESENTATIONS

Aimée N. Laporte, Chris Storbeck, Laura Evgin, Fabrice Le Boeuf, John C. Bell. Enhancing the Oncolytic Efficiency of Vaccinia Virus by Mutagenic Augmentation of EEV Production. *XIX International Poxvirus, Asfarvirus and Iridovirus Conference.* Salamanca, Spain. June 24-28, 2012. [International conference] ***(Poster presented by A.N. Laporte)***

Aimée N. Laporte, Chris Storbeck, Laura Evgin, Fabrice Le Boeuf, John C. Bell. Enhancing the Oncolytic Efficiency of Vaccinia Virus by Mutagenic Augmentation of EEV Production. *Department of Biochemistry, Microbiology and Immunology Research Symposium.* University of Ottawa. Ottawa, ON. Feb 22, 2012. [Institutional symposium] ***(Invited talk by A.N. Laporte, award: 1st place)***

Aimée N. Laporte, Chris Storbeck, Laura Evgin, Fabrice Le Boeuf, John C. Bell. Enhancing the Oncolytic Efficiency of Vaccinia Virus by Mutagenic Augmentation of EEV Production. *The Canadian Cancer Research Conference*. Toronto, ON. November 27-30, 2011. [International conference] ***(Poster presented by A.N. Laporte)***

Aimée N. Laporte, Julia Rintoul and John C. Bell. Enhancing the Oncolytic Efficiency of Orf Virus by Recombination with the E3L Gene of Vaccinia Virus. *Department of Biochemistry, Microbiology and Immunology Research Day.* University of Ottawa, Ottawa, ON. May 19, 2011. [Institutional conference] ***(Poster presented by A.N. Laporte)***

Aimée N. Laporte, Julia Rintoul and John C. Bell. Enhancing the Oncolytic Efficiency of Orf Virus by Recombination with the E3L Gene of Vaccinia Virus. *The 6th International Conference on Oncolytic Viruses as Cancer Therapeutics.* Las Vegas, NV. March 16-19, 2011. [International conference] ***(Poster presented by A.N. Laporte)***

Aimée N. Laporte, Julia Rintoul and John C. Bell. Enhancing the Oncolytic Efficiency of Orf Virus by Recombination with the E3L Gene of Vaccinia Virus. *10th Annual OHRI Research Day.* Ottawa, ON. November 18, 2010. [Institutional conference] ***(Poster presented by A.N. Laporte)***

Aimée N. Laporte, Mark Woodcroft and David LeBrun. Examining the role of the leukemic oncoprotein E2A-PBX1 in apoptosis and lineage reassignment of pre-B cells. *Department of Life Sciences Annual Undergraduate Poster Day.* Queen's University, Kingston, ON. March 30, 2010. [Institutional symposium] ***(Poster presented by A.N. Laporte)***

Scott R. Walsh, **Aimee N. Laporte**, Nicolle M. Linnerth, Paula I. Menzies, Robert A. Foster, Sarah K. Wootton. Phylogenetic Characterization of Enzootic Nasal Tumor Virus (ENTV) Infecting Canadian Sheep. *1st Annual Sheep Research Day: Ontario Sheep Marketing Agency*. Cambridge, ON. November 27, 2009. [National conference] ***(Invited talk by S.K. Wootton)***

Michael T. Greenwood, Drew Williams, Chamel Khoury, Naomi Metcalfe, **Aimee Laporte** and Craig Mandato. Using yeast as a model cardiac cell in order to identify and characterize novel anti-apoptotic sequences. *27th International Specialized Symposium on Yeasts (ISSY). Pasteur's legacy: Yeasts for health and biotechnologies.* Institut Pasteur, Paris, France, August 26-29, 2009. [International conference] ***(Invited talk by M.T. Greenwood)***

Aimée N. Laporte, Scott R. Walsh and Sarah K. Wootton. Genomic sequencing of sheep enzootic nasal tumour virus isolates and mutagenic analysis of the transforming domain of the ENTV envelope protein. *SLRP 6th annual Scientific Poster Competition.* University of Guelph, Guelph, Ontario. August 11-12, 2009. [Institutional symposium] ***(Poster presented by A.N. Laporte; Award: 1st place)***

ADDITIONAL TRAINING

2012	**Standard First Aid, CPR C and AED Certification** *City of Ottawa Paramedic Service, Ottawa, Ontario*
2012	**WHMIS for Workers Training course** *Ottawa Hospital Research Institute, Ottawa, Ontario*
2012	**Radiation Safety Training course** *Ottawa Hospital Research Institute, Ottawa, Ontario*
2010	**National Institutional Animal User Training (NIAUT)** *University of Ottawa, Ottawa, Ontario*
2009	**Summer Leadership and Research Program (SLRP)** *University of Guelph, Guelph, Ontario*

VOLUNTEER EXPERIENCE

2011 – 2012	**Ride the Rideau,** *Ottawa, Ontario*
2010 – 2012	**Let's Talk Science,** *Ottawa, Ontario*
2009 – 2012	**Canadian Cancer Society,** *Guelph/Ottawa, Ontario*
2008 – 2009	**Queen's Project Red,** *Kingston, Ontario*
2008 – 2009	**St. Mary's of the Lake Hospital (Providence Care),** *Kingston, Ontario*
2007 – 2010	**Queen's Health Outreach**, *Kingston, Ontario*